TIDAL STREAM DEVICES: RELIABILITY PREDICTION MODELS DURING THEIR CONCEPTUAL & DEVELOPMENT PHASES

DELORM, TATIANA, MOLINA

TIDAL STREAM DEVICES:
RELIABILITY PREDICTION MODELS
DURING THEIR CONCEPTUAL & DEVELOPMENT PHASES

by

Tatiana Molina Delorm

Thesis presented for the degree of
Doctor of Philosophy

Energy Group
School of Engineering and
Computing Sciences
Durham University
United Kingdom
2014

Dedicated to

my family

ABSTRACT

Title of Document:	TIDAL STREAM DEVICES: RELIABILITY PREDICTION MODELS DURING THEIR CONCEPTUAL & DEVELOPMENT PHASES
	Tatiana Molina Delorm , Doctor of Philosophy, 2014
Directed By:	Emeritus Professor Peter J. Tavner, Energy Group School of Engineering and Computing Sciences Durham University, United Kingdom

Tidal Stream Devices (TSDs) are relatively new renewable energy converters. To date only a few prototypes, primarily horizontal-axis turbine designs, are operational; therefore, little reliability data has accumulated. Pressure to develop reliable sources of renewable electric power is encouraging investors to consider the technology for development. There are a variety of engineering solutions under consideration, including floating tethered, submerged tethered, ducted sea-bed bottom-mounted and sea-bed pile-mounted turbines, but in the absence of in-service reliability data it is difficult to critically evaluate comparative technologies. Developing reliability models for TSDs could reduce long-term risks and costs for investors and developers, encouraging more feasible and economically viable options.

This research develops robust reliability models for comparison, defining TSD reliability block diagrams (RBD) in a rigorous way, using surrogate reliability data from similarly-rated wind turbines (WTs) and other relevant marine and electrical industries.

The purpose of the research is not to derive individual TSD failure rates but to provide a means of comparison of the relative reliabilities of various devices. Analysis of TSD sub-assemblies from the major types of TSDs used today is

performed to identify criticality, to improve controllability and maintainability. The models show that TSDs can be expected to have lower reliability than WTs of comparable size and that failure rates increase with complexity. The models also demonstrate that controls and drive train sub-assemblies, such as the gearbox, generator and converter, are critical to device reliability.

The proposed developed models provide clear identification of required changes to the proposed TSD system designs, to raise availability, including duplication of critical systems, use of components developed for harsh environments and migration of equipment onshore, wherever practicable.

Author's Publications

This methodology for the prediction and comparison of TSD reliability modelling was first published by the author of this Thesis in 2009-2011 as Assembly posters, SuperGen UK Centre for Marine Energy Research, see Delorm and Tavner (2009, 2010, 2011b); and this work was developed further in the author's two co-written papers as Delorm et al. (2011) and Delorm and Tavner (2011a) This body of work is listed below and included in Chapter 9: References.

Published papers:

- Delorm, T. M., Zappala, D. and Tavner, P. J. 2011. Tidal stream device reliability comparison models. Proceedings of the Institution of Mechanical Engineers, Part O: Journal of Risk and Reliability. February 2012, 226(1): 6-17.

- Delorm, T.M and Tavner, P. J. 2011a. Reliability methodology for evaluating tidal stream devices. 11th International Conference on Applications of Statistics and Probability in Civil Engineering – ICASP 11, Zurich, 1-4 August, 2011. Faber, Kohler & Nishijima (eds), Taylor & Francis Group. London.

Published assembly posters:

- Delorm, T. M. and Tavner, P. J. 2011b. Reliability Prediction Models for Tidal Stream Devices. SuperGen UK Centre for Marine Energy Research Annual Assembly 2011. URL: http://www.supergen-marine.org.uk/

- Delorm, T. M. and Tavner, P. J. 2010. Tidal Stream and Ocean Current Energy Converter Reliability. SuperGen UK Centre for Marine Energy Research Annual Assembly 2010. URL: http://www.supergen-marine.org.uk/

- Delorm, T. M. and Tavner, P. J. 2009. Tidal Stream and Ocean Current Energy Converter Reliability. SuperGen UK Centre for Marine Energy Research Annual Assembly 2009. URL: http://www.supergen-marine.org.uk/

Declaration

The work in this Thesis is based on research carried out in the Energy Group of the School of Engineering and Computing Sciences, Durham University, United Kingdom. No part of this Thesis has been submitted elsewhere for any other degree or qualification. The Thesis content presents my own work unless referenced to the contrary in the text.

Acknowledgments

The work in this Thesis was sponsored by an award from the EPSRC Supergen Marine programme in Work Stream 8.

This Thesis has been written with the invaluable help of many people that I would like to thank:

- Firstly my supervisors, Emeritus Prof. Peter J. Tavner and Dr. Robert Dominy for their guidance and effort in making this emerging field of research possible
- Prof. Dimitri Val of Heriot-Watt University, for his availability and collaboration in this Thesis
- Dr. David Nicholls, Reliability Information Analysis Center (RIAC), for his guidance in systems reliability
- Ned H. Criscimagna, Criscimagna Consulting LLC, for his additional guidance in systems reliability modelling and prediction
- Prof. Peter Fraenkel, Fraenkel-Wright Ltd, Visiting Professor at University of Edinburgh and Graeme Mackie, Oceanflow Development Ltd, for sharing their expert knowledge in tidal stream technology development and constant support
- Dr. Francis Franklin, Newcastle University, for his availability and assistance with mathematical models
- Dr. Tod Caldwell, Department of Energy (DOE), USA, for his assistance in physical science
- Ko Okazaki, for his assistance with Thesis graphics

Finally, special thanks to William Burgess, Terri Edwards, Tamara Juswigg Dikhanov and Victoria Vladimirovna Molina for their English language support and to Dr. Arthur W. Winston, Co-founder and Director-Emeritus, The Gordon Institute, Tufts University, for his inspiration.

Table of Contents

List of Figures

List of Tables

Nomenclature

b	TSD a sub-system study branch for reliability prediction
C_m	multiplier representing uncertainties associated with a modification method
$COVc_m$	coefficient of variation for a given C_m
FRE	failure rate estimate
FRE_{con}	conservative failure rate estimate without adjustment
FRE_{env}	environmentally adjusted failure rate estimate
$F(t)$	failure function
$f(t)$	instantaneous probability of failure
g	gravitational constant, m/s^2
H	pressure head of the fluid, metres
$h(t)$	hazard rate
i	a component in a TSD
j	number of components with the same λ
K_n	turbine selection coefficient
$\lambda(t)$	failure intensity or hazard function
λ	failure rate, failure intensity when hazard function is constant with time
λ_{ob}	obtained failure rate
λ_i	*i-th* sub-assembly failure rate
$\lambda_i^{(B)}$	*i-th* sub-assembly failure rate in branch B
λ_{i_FREcon}	*i-th* sub-assembly failure rate conservative without environmental adjustment
λ_{i_FREenv}	*i-th* sub-assembly failure rate environmentally adjusted

λ_{Gi_min}	minimum surrogate *i-th* sub-assembly failure rate
λ_{Gi_max}	maximum surrogate *i-th* sub-assembly failure rate
λ_b	uninterrupted electrical assembly single branch total failure rate
λ_{dt}	drive train single branch total failure rate
$\lambda_i^{(b)}$	predicted failure rate, λ, for *i-th* sub-assembly in branch *b*
$\lambda_{0.05}$	prior distribution failure rate, 5% confidence limit
$\lambda_{0.95}$	prior distribution failure rate, 95% confidence limit
λ_{tot}	total predicted failure rate series/parallel network
λ_{tot_Np}	total predicted failure rate parallel network single branch
λ_{tot_Ns}	total predicted failure rate series network
λ_U	single branch total failure rate support structure
λ_{wi}	wind turbine failure rate per year
N_{tot}	total number of device sub-assemblies
N	turbine speed, rev/s
N_b	number of sub-assemblies in series in one branch *b* of an assembly
N_s	number of sub-assemblies in series with none in parallel
N_p	number of sub-assemblies in series within an identical parallel branch
P	turbine power output, Watts
π_{Ei}	environmental adjustment factor
π_{Tbi}	ocean turbulence adjustment factor
π_{Cbi}	corrosion adjustment factor
π_{Hi}	human adjustment factor
π_{Qi}	quality adjustment factor
$R(t)$	reliability survivor function, hazard function not constant with time
$R(\lambda,t)$	reliability survivor function, hazard function λ constant with time

$R_i(t)$	reliability survivor function of the i-th sub-assembly
R_a	model uncertainty analytical data
R_r	model uncertainty real life data
ρ	fluid density, kg/m^3
t	predicted device total operating time offshore, for determining λ, years
T	period of the tidal cycle, h
u	tidal velocity, m/s
u_r	rated tidal stream velocity, m/s
u_{peak}	peak sea surface velocity, m/s
$u_{sp,}$ u_{np}	spring and neap tidal stream velocity, m/s
u_{max}	maximum tidal stream velocity, m/s
X_{mod}	model uncertainty modifier

Abbreviations

AC	Alternating Current
ADCP	Acoustic Doppler Current Profiler
AIEE	American Institute of Electrical Engineers
AR	Atlantis Resources
DACS	Data Analysis Center for Software
DC	Direct Current
EPRI	Electrical Power Research Institute
FBD	Functional Block Diagram
FCCC	UN Framework Convention on Climate Change
FMEA	Failure Modes & Effects Analysis
FTA	Fault-Tree Analysis
GB	Ground Benign: Protected Environment
GF	Ground Fixed: Severe Environment
GHG	Greenhouse Gas
GM	Ground Mobile Environment
HV	High Voltage
IEEE	Institution of Electrical and Electronic Engineers, USA
IP	Intellectual Property
ISET	Institut für Solare Energieversorgungstechnik, Kassel, Germany
LV	Low Voltage
LWK	Landwirtschaftskammer Schleswig-Holstein, source of wind turbine reliability data
MCT	Marine Current Turbines
MEC	Marine Energy Converters

MIL-HDBK	Military Handbook
MTBF	Mean Time Between Failure
NOAA	National Oceanic and Atmospheric Administration
NOS	National Ocean Service
NPRD	Non-electronic Parts Reliability Data
NS	Naval Sheltered: Normal Environment
NU	Naval Unsheltered: Severe Environment
OREDA	Offshore Reliability Data
PCRPT	Parts Count Reliability Prediction Technique
PDF	Probability Distribution Function
RDS-PP	Reference Designation System for Power Plants
PSD	Portfolio of Surrogate Data
RB	Reliability Block
RBD	Reliability Block Diagram
RIAC	Reliability Information Analysis Center
RMP	Reliability Modelling and Prediction
SCADA	Supervisory control and data acquisition
SRTT	Scotrenewables Tidal Turbine
TDRM	Time-Dependent Reliability Model
TISEC	Tidal in Stream Energy Conversion
TSD	Tidal Stream Device
VGB	German Power Standards Company Nomenclature, as follows:
	AA Grid Connection Subsystem
	AAG10 Umbilical electrical cable
	AB Corrosion Protection Subsystem, Corrosion control

B	LV DC	Uninterrupted electrical assembly
	MSA12 QB001	LV load-break switch
	BUU10	Converter AC/DC
	BUU11 LV	Supply 400V circuit breaker
	BUV10	Battery
	BU LV	DC cables
CA	Control and Management Subsystem	
	CA10	Programmable controller
	CA11	Process automation & SCADA
	MDY10	Turbine controller
	XAA30	HVAC controller
DT	Drive train	
MD	Turbine Subsystem	
	MDA10	Rotor blades
	MDA20	Hub
	MDC10UP001	Pitch bearings
	MDC10	Pitch systems
	MDK10	Main shaft
	MDK10 UP001	Main bearing
	MDK40	Couplings
	MDK11	Shaft seal
	MDK20	Gearbox
	MDV10	Lubrication & cooling system
MK	Generator Subsystem	
	MDK30	Brakes

	MKA10	Generator
	MKY10	Converter, AC/AC
	MKY11	Converter controller
	MKC10	Generator circuit-breaker
MS	Electrical Subsystem	
	MST10	Transformer, including cooling
	MSA10	Generator transmission cable
	MSC10	Main circuit-breaker
	MSC10QA001	Isolator switch

U Structure, Nacelle/Foundation/Moorings

XA Ancillary Subsystem assembly

	XAA10	Ventilation
	XAA20	Heat exchanger, water cooled

WEC Wave Energy Converter

WMEP Wissenschaftlichen Mess-und Evaluierungsprogramm, source of wind turbine reliability data

WT Wind Turbine

1. Introduction

1.1 Renewable Energy & Technology

A stranger once said to the tides in the bay
How strange you should live in this indolent way;
You crawl up the strand then crawl down again
Why can't you be useful and helpful to men?
For the past thousand years you have been just the same,
Such an idle existence! It's really a shame!

Grace Helen Mowat (1928)

Grace Helen Mowat's fable of attempting to harvest the natural energy from the tides is more relevant now than when she wrote it in 1928 at the Bay of Fundy, Nova Scotia. Mowat's stranger, an engineer fresh out of college, knew the energy in tides is an inexhaustible source of energy, but inconsiderately went forward to build a barrage dam that was wrecked by the tide:

Down, down, went the dam and the sea-wall besides,
And the engineer fell with the wreck of the tides.
And the waves washed his pockets as clean as could be
And carried his plan and his gold out to sea.

The moral of the fable is:

These facts tell us plainly to look on all sides
Before we are tempted to tamper with tides;
And when we are strangers, wherever we go,
There's always a side that we still do not know;
And if we too suddenly start to reform
Our plans and our gold may be lost in the storm!

Rendered into the language of engineering, predicting the reliability of a tidal stream device (TSD) is essential for harnessing the tidal force cost-effectively.

In the 21st century, efforts are being made to move towards a form of tidal energy device that will harness the free-flowing tidal stream and ocean current without the high cost and potential risks of a dam or barrage. Tidal stream power technology has gained prominence because of its simplicity, the ability to harvest energy directly from tidal currents, and the ecologically non-intrusive nature of the system.

TSD is an emergent technology. The systems are all under development and consequently there is no bank of information about their operating reliability. To date, at least 79 different tidal or ocean current technologies have been identified by the U.S. Department of Energy in its Marine and Hydrokinetic Technology Database (DOE 2011), including a majority of horizontal-axis devices (approximately 53) and vertical-axis turbines (approximately 26).

Few of these technologies are likely to be economically viable on a large scale of operation. How can those be identified? What are the problems of evaluation? This Thesis will argue that, as other forms of power-generating technology are well-developed, so the technological problems of extracting energy from the tides should be solvable. It will explore reliability models of horizontal axis TSDs as these are the most common form of tidal energy conversion technologies proposed today and also because their design is comparable with wind turbine technologies, for which a considerable body of reliability data is available.

1.2 Contribution of Research

The experience of reliability in the wind power industry, gained by Durham University in the UK EPSRC SuperGen Wind Consortium, is to be applied to the emerging tidal energy objectives of the UK EPSRC SuperGen Marine Consortium. This research extrapolates wind and other industry experience to predict TSD reliability and proposes a methodology for comparing TSD types at the early stage of

design, when historical reliability data are lacking. The models developed are based on a classical, simple method and can be adapted to many different designs.

In essence, the objective is to view and predict TSD reliability as a probability that a system will survive for a specified period of time. The system is considered non-repairable during this operational time and all sub-assemblies are independent. Surrogate failure rate data such as component failure rates from the existing WT and other industry databases are applied to tidal systems, and a methodology and models to assess TSD reliability during their conceptual and development phases are proposed, in order to identify the most reliable architecture.

Powerful graphic TSD models have been created, based on structures defined in *Guideline, Reference Designation System for Power Plants* by VGB (2007) for WTs. The research deploys the Reliability Modelling and Prediction (RMP) method presented in RIAC & DACS (2005) in assessing five horizontal-axis TSDs with different arrangements of sea-bed grounding and operational sea environments.

The author has made an original contribution by consistently applying an appropriate methodology that has not, until this time, been used in a fully-informed fashion. The originality of this methodology lies in the consistent use of the most relevant surrogate failure rate data originating from European onshore WT databases, petrochemical industry databases, generic databases and IEEE surveys, which are presented as Portfolio of Surrogate Data (PSD) in Chapter 4.4 and Appendix 3 of this Thesis.

The resulting Thesis of theory and evidence allows the author to analyse further the comparison of TSD sub-assemblies and sub-systems, and to make the reliability comparisons with other renewable energy extraction devices, by highlighting predictions of the most unreliable sub-assemblies under the conditions of a tidal

environment, and to identify candidates for improvements. These predictions should be taken into consideration for improvements in reliability of devices and sub-assemblies in their early design stage.

1.3 SuperGen Marine Energy Research Consortium

SuperGen is the flagship initiative of the UK Engineering and Physical Sciences Research Council (EPSRC) in Sustainable Power Generation and Supply. SuperGen researchers work in a multi-disciplinary Consortia involving universities and industry, focused on specific programmes of work to advance sustainable power generation. The first Consortia were launched in November 2003 and since then a total of ten Consortia have been supported with a total budget of £25 million.

The SuperGen Marine Energy Research Consortium focuses on exploiting energy from the seas around the UK coast. It brings together experts from seven British universities: Edinburgh, Strathclyde, Heriot-Watt, Lancaster, Robert Gordon and Durham, working with participants from twenty national and international marine energy and electrical supply companies.

The aim of the SuperGen Marine Energy Research Consortium is to increase knowledge of the extraction of energy from the sea to reduce investment risk and uncertainty. The vision of the Consortium is that through its own efforts and extensive collaboration with others, methodologies will be established to facilitate the progress of new concepts and devices, so that marine energy will take its proper place in the national energy portfolio as quickly as possible.

The work reported in this Thesis was led by Edinburgh University and funded as a Doctoral Training Award as part of the Reliability Work Stream 8 of the SuperGen Marine Energy Research Consortium. The leader of Work Stream 8 was Professor Dmitri Val of Heriot-Watt University, Edinburgh.

1.4 Structure of the Thesis

This Thesis is organized as follows:

- **Chapter 1** provides an overview of the current state of TSD development in the context of renewable energy research
- **Chapter 2** reviews the literature about the past and current situation in the field of reliability prediction for ocean energy devices.
- **Chapter 3** presents generic TSD taxonomies.
- **Chapter 4** presents reliability prediction modelling concepts, explains the TSD reliability prediction methodology chosen and developed, and establishes a portfolio of surrogate data for reliability analysis and device comparison.
- **Chapter 5** presents and analyses the reliability prediction models proposed in Chapter 4 for five different types of offshore horizontal-axis tidal turbines of generic manufacture rated at 1.0-1.2 MW.
- **Chapter 6** proposes a theory for validating proposed models based on recent wind turbine (WT) and wave energy converter (WEC) reliability studies; analyses the reliability prediction of TSD assemblies, sub-assemblies and components; presents comparison of TSD devices with SeaGen early performance reliability data; presents results and discusses applications of reliability models for comparison.
- **Chapter 7** presents conclusions drawn from this research.
- **Chapter 8** gives recommendations for further research.
- **Appendices 1-5** contain additional information related to TSD technology, comparative results derived from proposed reliability modelling methodology, and the published and submitted papers of this author.

2. Ocean Energy, Tidal Technology & Reliability

2.1 Why Re-Evaluate Tidal Energy Technology?

Ocean renewable energy technologies, specifically TSDs, provide one method of satisfying increasing global energy demand, while at the same time reducing greenhouse gas (GHG) which is a priority under the UN Framework Convention on Climate Change (FCCC), according to Watson et al., eds. (1996). This new-generation technology is clean and more environmentally friendly to the natural world than large-scale tidal barrage power plants with conventional turbines. These conventional turbines extract the potential energy from ocean tides and convert it to electrical power, but they require massive civil engineering construction in order to create high water heads for effective energy extraction, according to Gorlov (2001).

Traditional tidal barrage construction is costly and time-consuming, a large tract of land is lost to other uses, and a large volume of ocean water is processed. All of this means that the barrage technology is difficult to commercialise, according to the Department of Trade and Industry Report, DTI (2010). Figure 2.1 illustrates La Rance, a barrage-type power plant in France. General characteristics of this plant are presented in Table 2.2 included in Section 2.3.

Figure 2.1 Tidal power plant, barrage type, at La Rance, France

Source: De Laleu (2009)

TSDs have many advantages over the barrage type tidal power plant pictured above. Gorlov (2001) argued that tidal energy is one of the best candidates for the "approaching revolution" in replacing traditional energy sources with new renewables. New generation tidal energy devices can be made available worldwide through the development and use of new artificial and environmentally-friendly low-carbon energy converters such as the vertical turbines shown in Figure 2.2. This type of machine may be used for both multi-megawatt tidal power farms and mini-power stations generating only a few kilowatts. Such mini-power stations can be of great utility to small communities, and might even be used by individual households or facilities located on shorelines, straits, or remote islands.

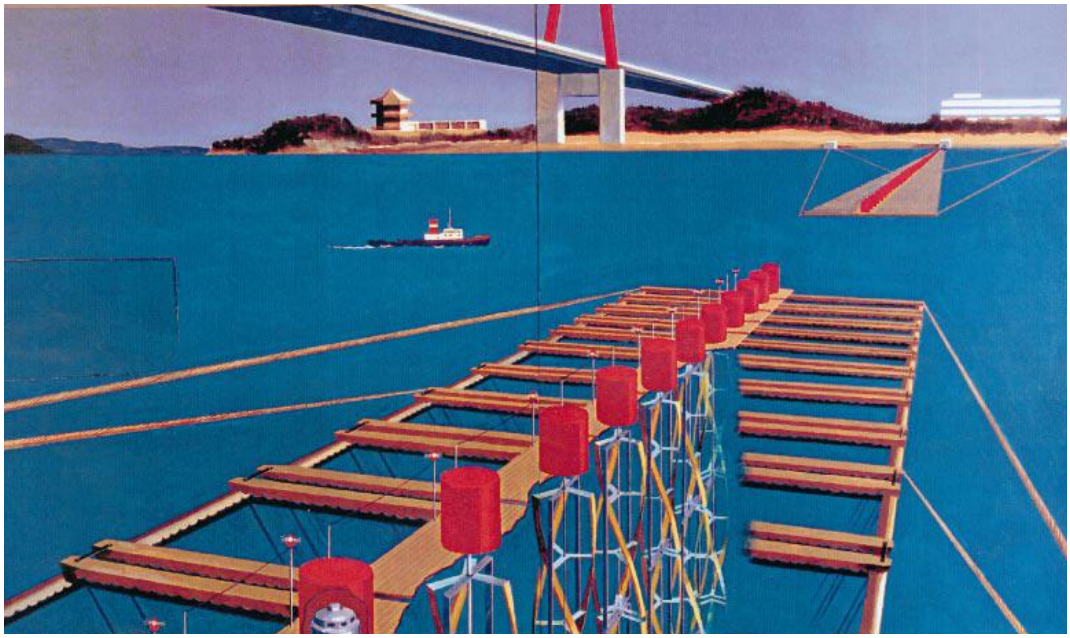

Figure 2.2 New generation of floating tidal power plant with vertical turbines.

Source: Gorlov (2001)

In 2001 a UK Government White Paper, Cabinet Office (2001), projected a UK contribution to the global effort to overcome the problem of climate change with a strategy based on developing renewable sources of energy: wind, solar, biomass, wave and tidal energy The Government set a target of securing 20% of the UK energy supply from renewable sources by 2020.

This 2001White Paper states that the UK can greatly benefit from renewable energy sourced from waves and tidal flow because it is an island in tidal seas with considerable tidal range enhancement. These sources could provide as much as 15-20% of the country's electricity supply.

According to the DTI (2003), the UK is at the forefront of research into wave and tidal technologies, and the Government is supporting industry development of prototype technologies in projects off the Western Isles and Devon coasts. The DTI

“UK renewable” timeline shows the key dates and critical path to accomplish the 20% target goal by 2020. On this timeline, TSDs become available in 2010-2015.

Recent reports by Black &Veatch Ltd. (2004), (2005) suggest that the UK tidal stream power could feasibly represent as much as 5% of UK electricity demand. Although there are still uncertainties in the resource estimate, this suggests that tidal stream power can make a significant contribution to renewable energy in the UK.

2.2 Tidal Current Resources, UK & Europe

TSDs require sufficient tidal currents resources, which are strongest around coastal headlands or in narrow straits. The most reliable tidal resource data of the UK coast, including tidal flows, tidal range and annual tidal power estimates, are published in BERR (2008), *Atlas of UK Marine Renewable Energy Resources.* An example of mean spring tidal peak flows around mainland Britain can be seen in Figure 2.3.

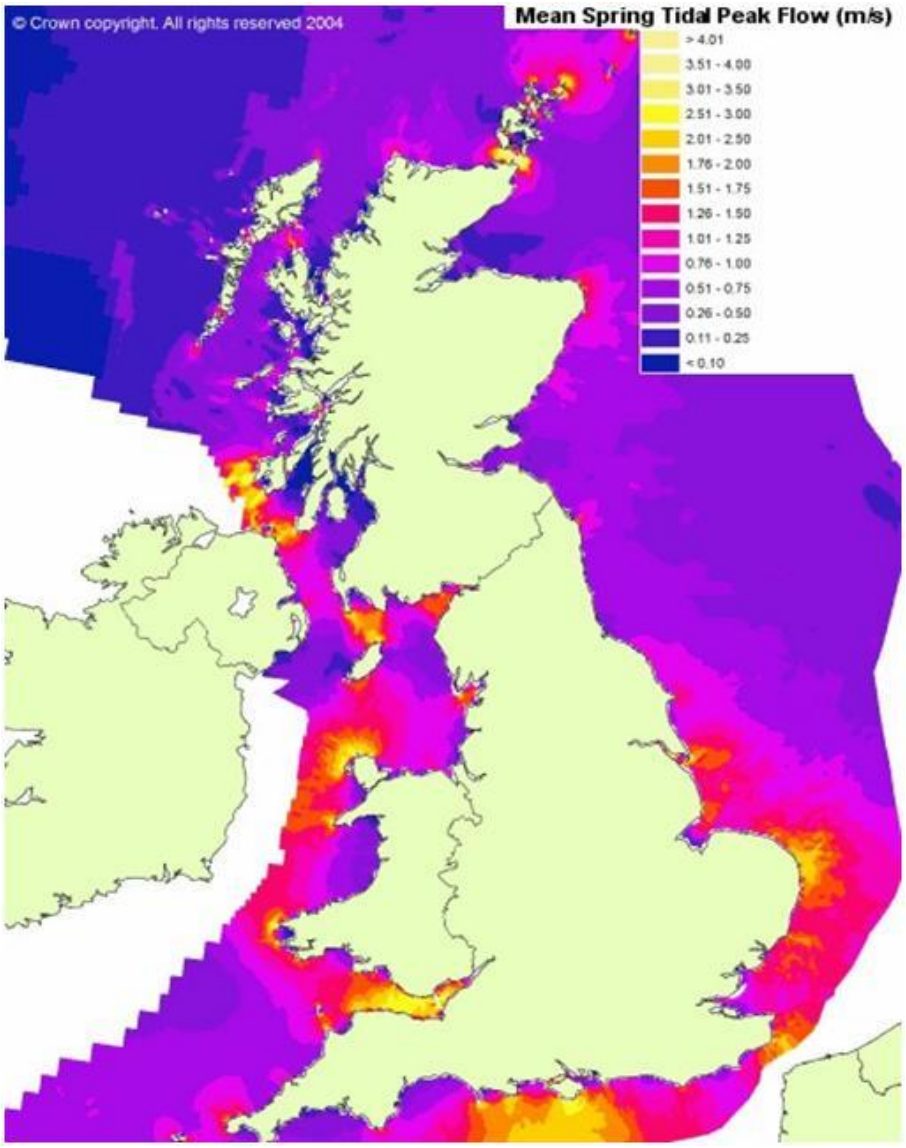

Figure 2.3 Mean spring tidal peak flows (m/s) around the UK Coast

Source: adapted from BERR (2008)

This illustration demonstrates the importance of TSD positioning in order to maximize the potential of tidal power.

Fraenkel and Musgrove (1979) analysed potential tidal resources around the UK; their study, summarized in Table 2.1.

Table 2.1 Potential UK Tidal Current Resources

	Irish Sea, North Channel	**Pentland Firth**	**English Channel**	**Orkneys/ Shetland Channel**	**Alderney Race**
Width (km)	18.0	5.0	98.0	80.0	15.0
Mean Depth (m)	110.0	75.0	55.0	100.0	18.0
Peak Velocity Spring Tides, u_{max} (m/s)	2.4	5.2	1.7	1.1	4.0
Daily Average Power Spring Tides (GW)	5.7	9.7	5.3	2.7	2.8
Annual Average Power Neap Tides (GW)	1.0	1.7	0.9	0.4	0.2
Annual Average Power (GW)	3.6	6.1	3.3	1.7	1.6

Source: adapted from Fraenkel and Musgrove (1979)

The report by Black & Veatch Ltd. (2005) found that about 20% of the UK's tidal resource is at 30–40m depth, with a mean velocity of 2.5–4.5 m/s. These sites could be most suitable for commercial development. Approximately 50% of the resource is at sites deeper than 40m with a mean tidal velocity of more than 3.5 m/s, which is suitable for development. The Black & Veatch report discusses uncertainty in the data, but detailed site analysis and modelling can reduce these uncertainties.

Blunden and Bahaj (2006) quoted the European Commission electronic database of tidal stream energy resources around Europe, including UK sites. Their report estimated the Europe-wide potential power output at 12.5 GW with UK sites contributing 8.9 GW. Forty-two sites were identified in the UK; total potential UK annual energy output was estimated at 30.9 TWh with a peak stream velocity u_{max}

more than 1.5m/s, compared to the UK annual electricity energy demand of about 360 TWh. This is equivalent to approximately 8.5% of demand, greater than the 5% of demand reported by Black & Veatch Ltd. (2005), which is understandable given that this resource is in the initial stages of research.

2.3 Tidal Stream Technology Development

The concept of harvesting ocean energy emerged as a discipline in the 1970s and the technologies have now matured enough to be implemented, it is argued by Boyle (2004). However, the problems of reliability of new technologies in TSDs need to be overcome. Gorlov (2001) notes that in the 20th century, the four most significant large-scale applications of tidal energy for generation of electricity with bulb turbines were barrage-type and were built in France-1967, Russia-1968, Canada-1984 and China-1985. The technology is well described by Gorlov (2001) and Boyle (2004), Table 2.2 demonstrating the general characteristics of the four conventional tidal power plants.

Table 2.2 Largest Barrage Type Tidal Power Plants

Country	Site	Installed power (MW)	Basin area (km^2)	Mean tide (m)	Year of installation	Operation status
France	**La Rance**	240	22	8.55	1967	operating
Russia	**Kislaya Guba**	0.4	1.1	2.3	1968	operating
Canada	**Annapolis**	18	15	6.4	1984	operating
China	**Jiangxia**	3.9	1.4	5.08	1985	operating

Source: adapted from Gorlov (2001)

Tidal bulb turbines, installed in barrages on the Rance River in France and in Kislaya Bay in northern Russia, have 30 years of operating history, according to Usachev et

al. (2007). Figure 2.4 illustrates a model of a bulb turbine, which is a type of barrage turbine.

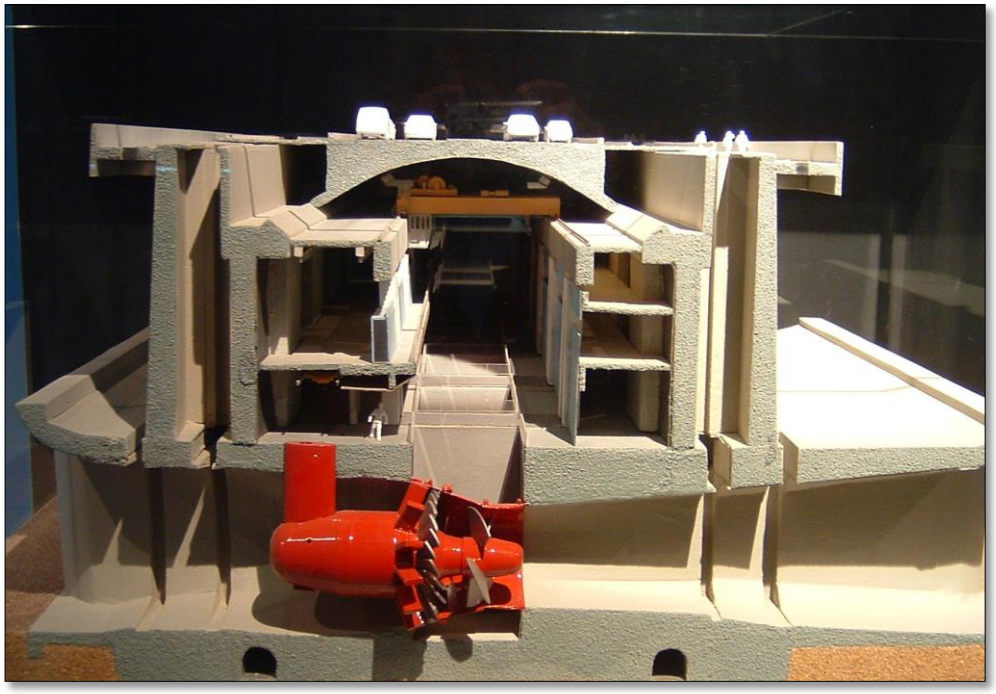

Figure 2.4 Bulb turbine

Source: De Laleu (2009)

In all barrage types, water passes through the barrage during the ebb and flood tides. Water passes through the turbines during the flood tide and can generate power. However, water is also impounded by the sluice gates during ebb tide and is allowed to flow out through the turbines later in the tidal cycle, generating power during an extended period in the ebb tide.

The Rance River turbines, installed in France in 1967, had mechanical problems in 1975, but overall the plant has proved successful, with 90% annual operational availability from 240 MW installed capacity and an annual energy production of 600 GWh, indicating a capacity factor of 28.5%.

The Kislaya Bay plant, located in Russia, is described by Usachev et al. (2007). It entered service as long ago as 1968. It was originally employed with a horizontal-axis bulb turbine manufactured by the French company Alstom, generating 400 kW. When the service life of that turbine ended after 40 years of operation, it was replaced with a new vertical-axis turbine, which proved more efficient, designed by the engineering firm *Gidroproekt*.

The successful operation of these two plants proves that tidal energy converters can be reliable and have great potential for further long-term development. The other two plants in Gorlov's list are much newer and were still operating in 2001 according to his report.

Unlike a tidal barrage, TSDs can be constructed on a modular basis and installed incrementally. For a full list of known TSD types, see Appendix 2.

There are a number of classifications of TSDs. Boyle (2004) for example defined the types of TSDs, examples of which are shown in Figures 2.5, as follows:

- Vertical axis turbine design;
- Venturi type design, a hydraulically tapped ducted system;
- 'Polo' turbine design;
- Horizontal axis propeller design, on which the research in this Thesis has focused: see Chapter 3 and 5.

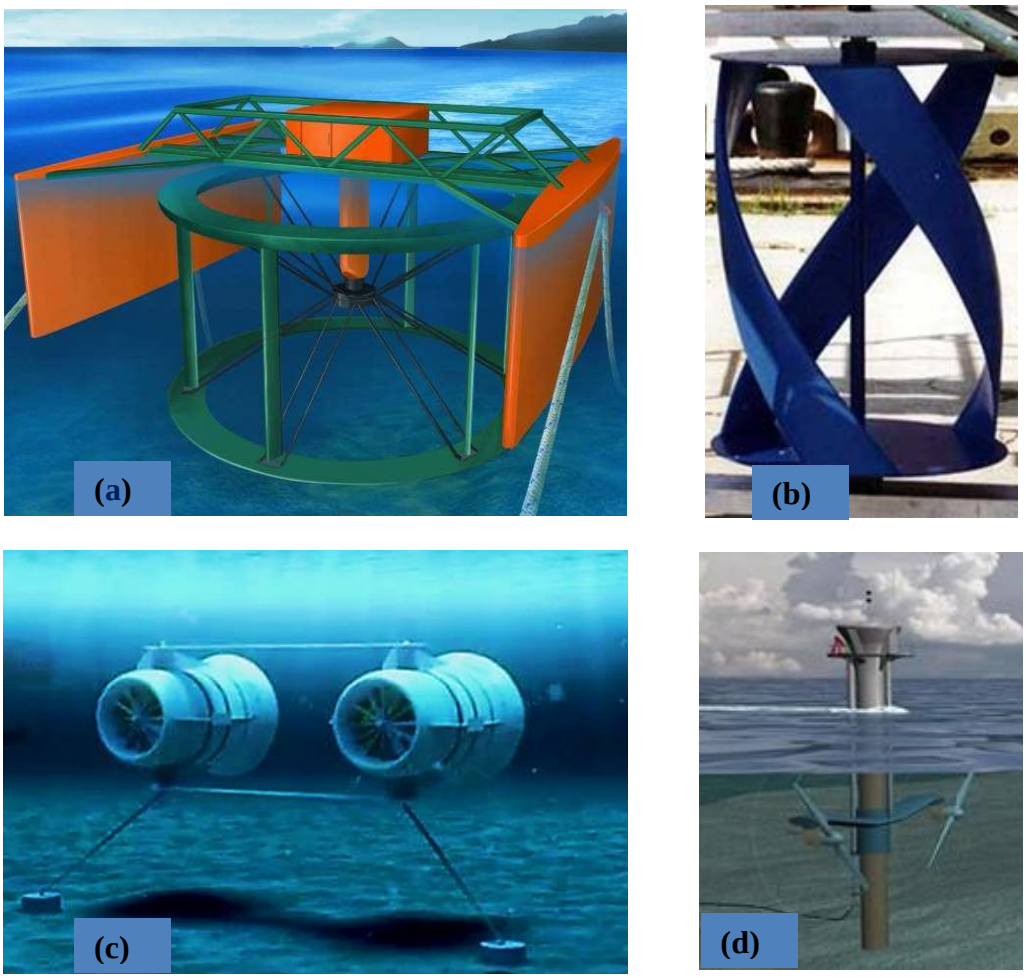

Figure 2.5 Example of TSD turbines

(a) 'Polo' turbine, taken from Val (2010)

(b) Gorlov's vertical axis turbine, Gorlov (2001)

(c) Venturi effect design, EET SeaUrchin (2012)

(d) MCT SeaGen, Fraenkel (2007)

The US Department of Energy classifies prospective tidal stream technology somewhat differently, using a nomenclature based on tidal current flow and the attitude of the turbine; e.g. axial-flow turbine, cross-flow turbine and reciprocating Figure 2.6 below is adapted from DOE (2011).

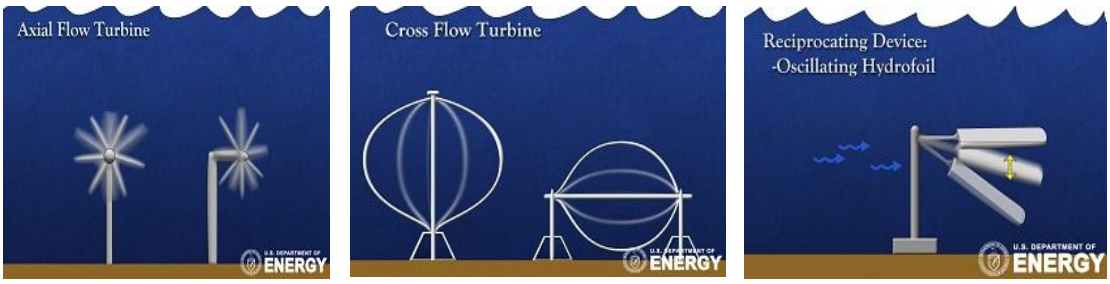

Figure 2.6 Classification of TSDs by technology types and applications

Source: adapted from DOE (2011)

There are also other ways technology types can be classified and each turbine type can be sub-classified, as shown in Figure 2.7.

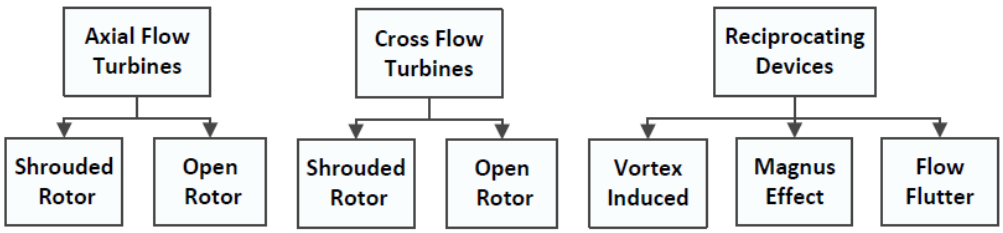

Figure 2.7 Classification of TSDs by principles of operation

Source: adapted from IPCC (2011)

Numerous defined sub-classifications can be found in EPRI (2004) and Hardisty (2009). These numerical device classifications confirm the many tidal energy conversion technologies currently under consideration.

Mackie (2009) argues that the type of device, following Douglas et al. (1995), depends on a turbine selection coefficient, *Kn*, also known as a specific speed, which varies according to the prospective tidal site. Table 2.3 shows the effect of this coefficient on decision-making regarding turbine type, based on device power optimization.

$$Kn = \frac{N\sqrt{P}}{\frac{\rho}{2}\mathrm{g}H^{5/4}}$$

Equation 2.1

where

N is a turbine speed (revs/sec)
P is the power output (Watts)
ρ is the fluid density (kg/m^3)
H is the pressure head of the fluid (m)
g is gravitational constant, m/s^2

Table 2.3 Example of Turbine Selection Against *Kn* Coefficient

***Kn* range**	**Optimum turbine type**
2.0-2.5	Axial flow (horizontal)
0.4-2.0	Francis (horizontal, guided vanes)
< 0.4	Pelton (vertical turbine)

Source: Mackie (2009)

In addition to the coefficient, *Kn*, other factors such as the requirement to generate power with bi-directional flow of ebb and flood, would affect the form of axial horizontal or vertical impulse turbine design.

The majority of TSDs in existence or in development today are axial flow turbines, also called horizontal axis devices. According to Mackie (2008b) horizontal axis devices can be further sub-categorised by their sea-bed fixing options and the position of the turbine in the water column. Figure 2.8 illustrates generic horizontal axis tidal turbines with different sea-bed fixing options currently being considered by the marine renewables industry.

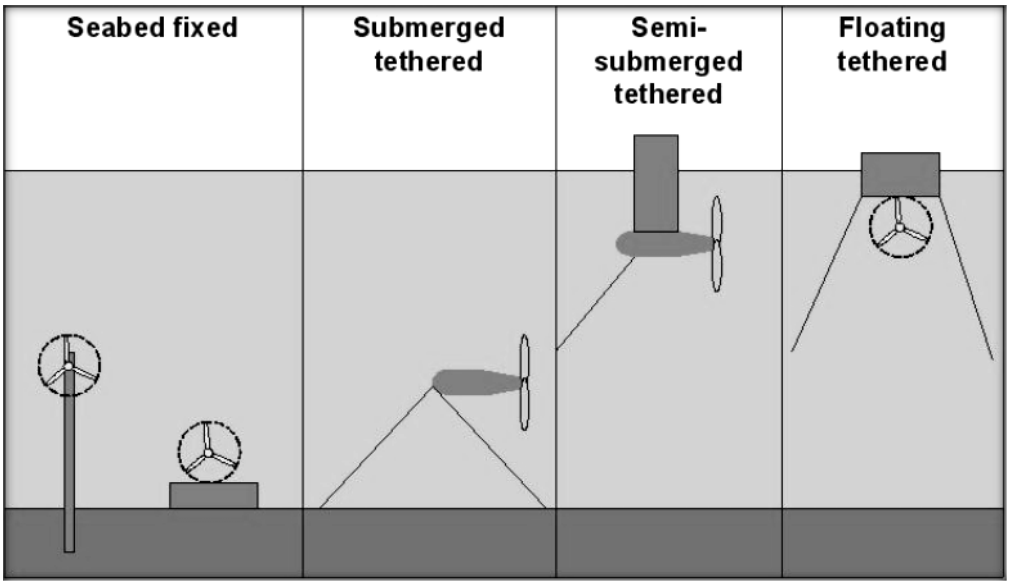

Figure 2.8 Types of horizontal axis TSDs

Source: Mackie (2008)

2.4 Overview of Uncertainties: Tide and Power Fluctuations

2.4.1 *Tide Prediction and Fluctuation*

The design of a tidal device becomes complex and therefore potentially less reliable in tidal stream or ocean currents where flow rate is variable and flow direction reversible. This is so in tidal ebb and flood conditions and when the turbine is some distance from the seabed, although such devices benefit from higher flow rates because they are outside bottom fluid boundary layers (Mackie 2008b). It is argued

by Sulter (2012) that turbulence is stronger near the seabed. When turbine rotors are 50m or more below the surface, they - in particular their blades - will be affected by sea-bed turbulence. If so, such devices must be designed with a high level of reliability for operation in that specific environment.

There are three tidal flow types, which influence TSD power capacity and reliability:

- Semi-diurnal, with two high peaks and two low peaks within a 24 hour period, usually at equal heights to each other;
- Diurnal tides, one high peak and one low peak during a 24 hour period;
- Mixed tides, successive high and low peaks with different heights.

The most recent glossary related to tides and currents are presented in NOAA (2000).

Most of the UK coastline has predominantly semi-diurnal tides. Other parts of the world have predominantly diurnal or mixed semi-diurnal tides. Topographical factors, such as the variation of the ocean floor, influence tidal flow when tides enter a basin, creating a complex predominant tidal-type distribution, therefore increasing or decreasing turbine capacity, as stated in EPRI (2006b). These natural changes in tidal flow distribution are one of several environmental effects that are crucial for system reliability. Accumulated data of these flow changes at selected sites must be taken into consideration in device design.

The methodology for calculating tidal flow involves complex equations, including as many as 40 parameters for each site, and the actual tidal data reflect fluctuations caused by daily site meteorological conditions. This methodology can be applied to create numerical tidal and current flow prediction.

Software based on harmonic analysis is available online:

- Windows WXTide32 (2013), worldwide tides;
- Nobeltec Navigation Tides & Currents (2011), also worldwide;
- US National Oceanic and Atmospheric Administration (NOAA), NOAA/NOS (2013), US sites only.

Figure 2.9 provides an example of NOAA daily tide prediction fluctuation from 12 am January 11th to 12 am January 13th 2013 for the Anchorage station, Alaska, USA.

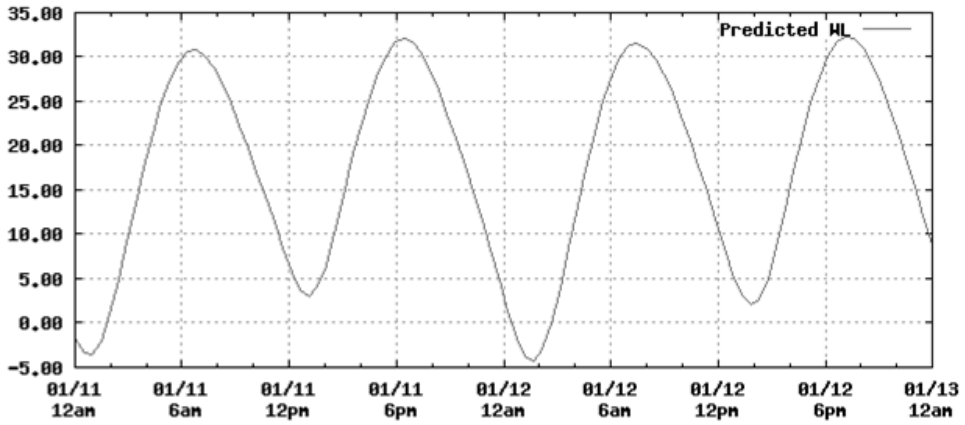

Figure 2.9 Variation of high and low tides at Cairn Point (AK) USA

y-axis = tidal fluctuation by height feet, high low and low high tide

x-axis = date/month and time

Source: NOAA (2013)

A simplified mathematical model for tidal flow can be computed where the only one input required is the peak, spring tidal flow velocity, u_{sp}, or the low, neap tidal flow velocity, u_{np}. A simple equation for tidal flow velocity following a cyclic pattern is presented in ESRU (2013):

$$u(t)=u_{max}\sin(\omega t);\ \omega=2\pi/T$$

Equation 2.1

Where: u_{max} is the peak surface current velocity, ω is the angular velocity of the tide, and T is the period of the tidal cycle, typically 12h 25 min or 745 minutes.

A tidal site, Cairn Point near Anchorage, Alaska, was studied by the EPRI (2006a) for possible installation of TSDs. The change of angle between ebb and flood tides was found to be 167^{o}. This differs from the theoretical prediction of bi-directional tides where the tidal change of angle would be 180^{o}. Turbine design would be affected by a departing flow diverging from the mean axis by at least 6.5^{o}. EPRI also found that variation of tidal current velocity to be among *the greatest unknown*, affecting design, installation and reliability prediction of tidal turbine array deployment. The study found that the tidal environment was promising; however, the main question was not answered as to which technology was the most promising for that region.

Tidal velocity turbulence is another matter requiring investigation. An Acoustic Doppler Current Profiler (ADCP) obtained experimental data from the Firth of Forth which were analysed by Okorie (2012). These data show that the tidal fluctuations are affected by wind and wave interaction, seabed and coast geography and roughness, channel walls, as well as the gravitational pull of the sun and moon. Okorie's main conclusion is that these tidal ebb and flows are very turbulent, Figures 2.10-2.12, and they affect the current so that it does not follow as simple a pattern as predicted by Equation 2.1.

Figure 2.10 is a scatter plot showing velocity samples from a 14-day survey during spring and neap tides, using the ADCP set in 10 meter-deep water. East-west and north-south velocity vectors are shown. The current does not move in a predictable direction, although the scatter shows a SW-NE trend.

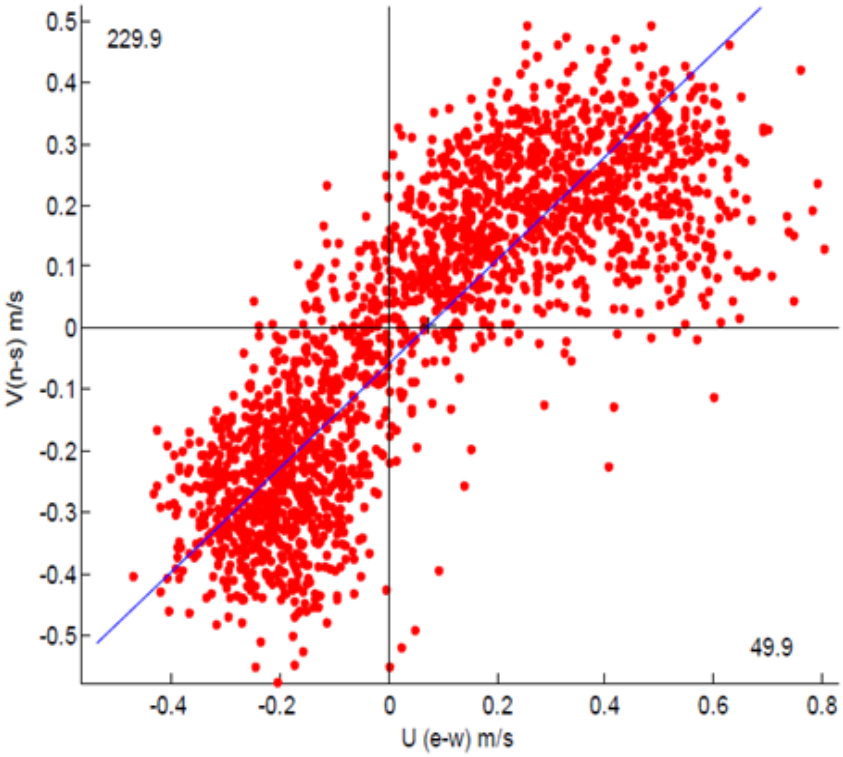

Figure 2.10 ADCP horizontal velocity scatter plot for neap and spring tides

Source: Okorie et al. (2011)

Figure 2.11 shows the trajectory of individual fluid particles recorded by this ADCP. The left side of the figure shows the average velocity by depth. The paths of fluid particles are chaotic and the velocity varies. Data samples taken at different times showed dissimilar results, reflecting the diversity of flow and velocity in natural environments. Vorticity, which is the circular or spiral motion of fluid, is apparent at the bottom-left, where the paths curl inward, signifying the predisposition of water to rotate. Figure 2.11 shows that the overall effect is orderly, even if it does not comply with preconceptions about tidal flow.

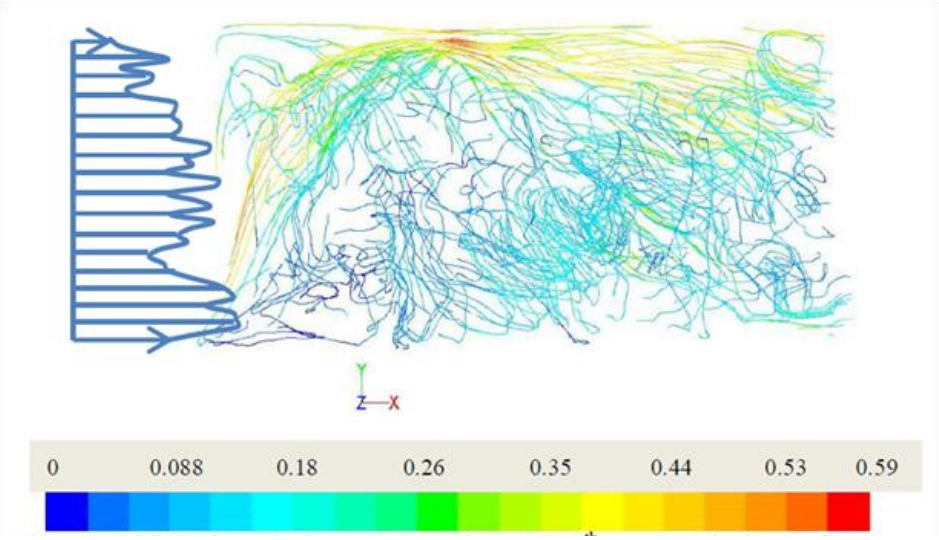

Figure 2.11 ADCP velocity profile in m/s with depth, showing particle trajectories.

Source: Okorie et al. (2011)

Figure 2.12 shows significant vortices, indicating the presence of strong turbulent flow in the natural tidal environment.

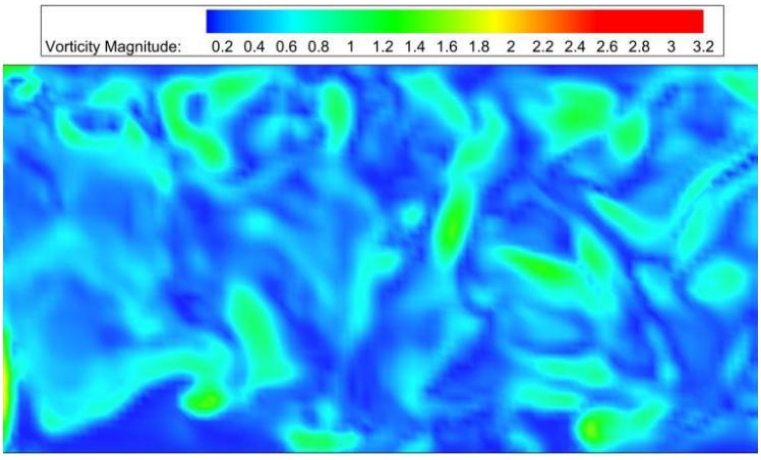

Figure 2.12 Vorticity field as shown by ADCP velocity profile data

Source: Okorie et al. (2011)

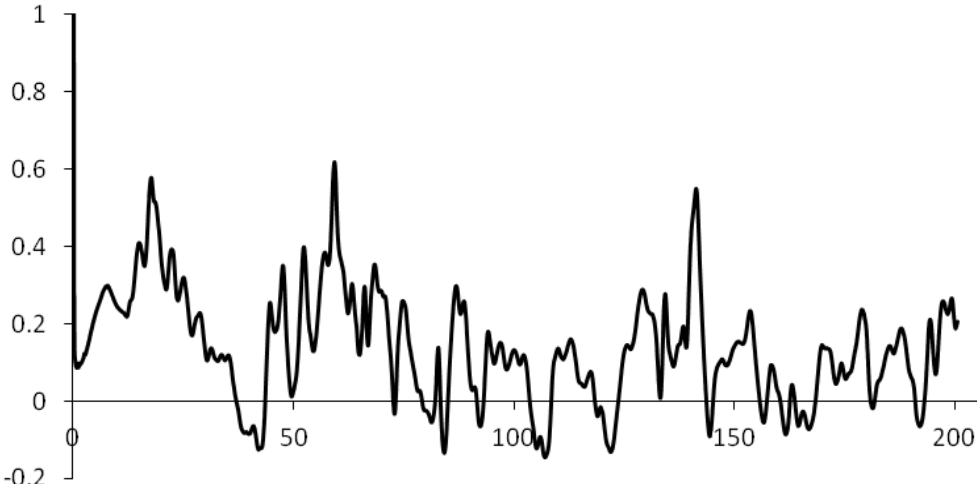

Figure 2.13 Drag coefficient against flow time from velocity data simulation

x-axis = flow time (t), y-axis = drag coefficient

Source: Okorie et al. (2011)

ADCP data shows that the drag coefficient arising at this site has negative values: see Figure 2.13 above. These aspects come together to produce a classic flow effect on TSDs affecting their reliability. While the drag force on the TSD can be calculated theoretically, the flow characteristics which affect the drag coefficient are not fully understood. Okorie's study excluded consideration of the experimental 'noise'. Richard et al. (2012) showed that ADCP produces 'Doppler noise'. Further investigation is needed to account for this factor in the natural environment.

Judging from NOAA databases, tidal ebb and flow conditions could differ due to geographical issues at specific sites. Judging from the ADCP measurements, tidal flow conditions are very turbulent. From a reliability point of view, further investigation of tidal flow variation and turbulence effect on TSDs at each prospective deployment site should improve reliability model calculations and reduce TSD reliability model uncertainty.

2.4.2 *Power Estimation and Fluctuation*

Estimating the extractable power from a TSD depends on several factors, making prediction a challenging task. These factors are:

- Flow velocity distribution;
- TSD size and efficiency;
- Geographical location.

Methodologies for power flow and device performance calculation are presented in EPRI (2006a, 2006b). EPRI (2006a) presents a study of 1MW MCT turbine performance at Cairn Point, AK, USA. Table 2.4 illustrates for this location the velocity fluctuation, passing through rotor cross sectional area of the device, and the effect on flow power and predicted power extraction.

Table 2.4 MCT Device Study Performance at Cairn Point,AK, USA

Flow Velocity (m/s)	% Cases	% Load	Power Flux (kW/m^2)	Flow Power (kW)	Extracted Power (kW)	PTO Efficiency	Electric Power (kW)
0.09	7.07%	0.0%	0.00	0	0	9.38%	0
0.27	8.28%	0.3%	0.01	5	0	16.13%	0
0.45	8.28%	1.3%	0.05	24	0	36.54%	0
0.63	8.74%	3.7%	0.13	66	0	62.66%	0
0.82	9.58%	7.9%	0.28	141	64	79.18%	50
1.00	10.54%	14.4%	0.51	258	116	84.58%	98
1.18	9.17%	23.7%	0.84	425	191	86.30%	165
1.36	8.51%	36.4%	1.28	654	294	87.95%	259
1.54	7.64%	53.1%	1.87	951	428	90.12%	386
1.72	6.01%	74.1%	2.61	1328	598	92.94%	555
1.90	4.27%	100.0%	3.52	1793	807	94.08%	759
2.08	3.09%	100.0%	4.63	2356	807	94.08%	759
2.26	2.42%	100.0%	5.95	3026	807	94.08%	759
2.45	1.98%	100.0%	7.49	3811	807	94.08%	759
2.63	1.53%	100.0%	9.28	4723	807	94.08%	759
2.81	1.11%	100.0%	11.33	5769	807	94.08%	759
2.99	0.87%	100.0%	13.67	6959	807	94.08%	759
3.17	0.46%	100.0%	16.31	8302	807	94.08%	759
3.35	0.30%	100.0%	19.27	9808	807	94.08%	759
3.53	0.11%	100.0%	22.57	11487	807	94.08%	759
Average 1.13			1.72	873	260		238

Source: EPRI (2006a)

Figure 2.14 shows predicted power fluctuations: fluid power and turbine extracted power for MCT device based on Table 2.4.

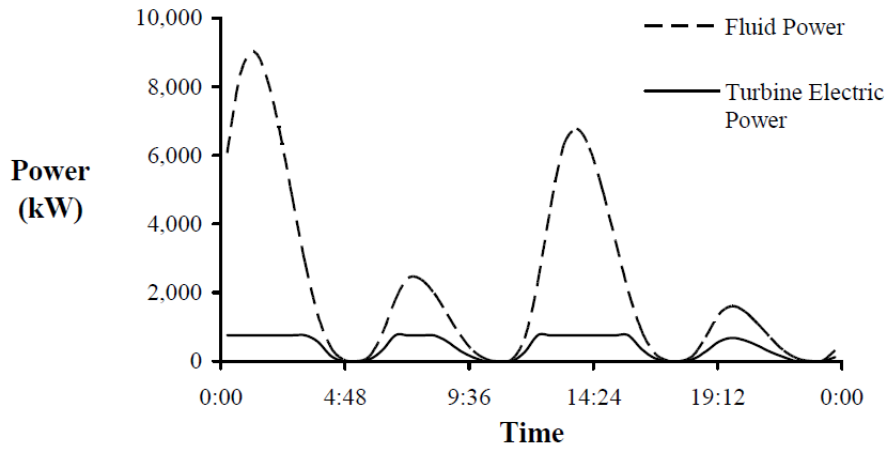

Figure 2.14 Variation of daily flow & power from 1MW MCT at Cairn Point

Source: EPRI (2006a)

TSDs require selected tidal site analyses to minimize output power fluctuation. EPRI (2006a) studies show that average tidal and current velocities and power fluctuations are dependent on one another and this affects TSD design. The rated speed of tidal turbines will be affected by the maximum velocity fluctuation at the installation site.

2.5 Problems with Reliability Assessment

The prediction of tidal energy extraction requires a systems reliability analysis and risk assessment. In early 2009 when this Thesis began, the author's search of the literature found only a handful of tidal device reliability papers: Wolfram (2006), Mermiris and Hifi (2008), Flinn and Ferreira (2008), Val (2009) and two extensive studies on wave power device reliability, by Y-ARD Ltd. (1980) and AME Ltd. (1992).)

The assessment and testing of marine energy converters started from consideration of the problem of system reliability; specifically, the sources of unreliable machine component performance and total system unavailability in new technologies such as wave-energy converters and TSDs.

Wolfram (2006) addressed the reliability and availability factors in a viability assessment of any potential wave or tidal stream device and critiqued the methodology proposed by Y-ARD Ltd. (1980), later adapted by AME Ltd. (1992). These studies performed a Failure Modes, Effects and Criticality Analysis (FMECA) for each of three wave-power devices, estimating failure rates for the novel elements. Wolfram remarked that both of the above-mentioned studies used random failure rate modelling from the components without considering common cause or common failures or possible cascade-type failures. Sensitivity studies were not undertaken, wherein estimated failure rates were varied for novel components. As with any new technology, there was no specific historical performance operating data to assess

device reliability and availability in a particular environment and a particular operating condition. These could include, for example:

- External water pressure admitting corrosive salt water to the system, deforming structures in ways that inhibit movement;
- Linear and rotational cyclic motions and accelerations;
- Inaccessibility, preventing monitoring of function and impeding maintenance.

Wolfram argued that in order to compare different devices there must be a framework for reliability and availability assessment. He called for building a database of failure distributions based on the failure mode of each component under specific environments. He proposed arranging devices in 'farms', with arrays of up to a hundred or more converters, producing 2-3000 MW of electrical energy. The result would be multiple generating devices, not all working at peak efficiency at a given moment, but overall still producing significant energy. Wolfram proposed a method of simulation modelling to predict the availability of this type of energy converter, using discrete event simulation. Such modelling would allow for seasonal variations in downtime, time-to-failure and time-to-repair or replacement distribution factors.

Following Wolfram, Flinn and Bittencourt-Ferreira (2008) presented a methodology for estimating wave and tidal stream device reliability in the absence of operational data, an expedient. They set a framework for a reliability estimation method, which is shown in the flow chart of Figure 2.15.

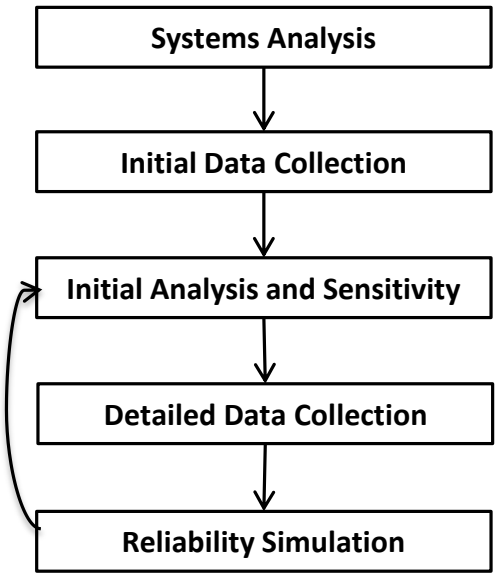

Figure 2.15 Framework for a reliability estimation method.

Source: adapted from Flinn and Bittencourt-Ferreira (2008)

The first step is in-depth learning about the new technologies and the method of dealing with operational reliability problems. Component and sub-system reliability data from offshore and wind energy sources may be applicable; Flinn and Bittencourt-Ferreira proposed initiating data collection using the OREDA (Offshore Reliability Database 1984-2009). Uncertainties were predicted in applying these data to the offshore environment.

Val (2009) pointed out the way in which reliability results affect cost and budgets, critically projecting from the operational data of WTs, summarized in Table 2.5, based on a proposal by Tavner et al. (2005).

Table 2.5 Annual Failure Rates for WT Sub-Systems

Subsystem	Tavner et al. (2007)		Ribrant (2006)		
	Germany	Denmark	Sweden	Finland	Germany
Rotor	0.223	0.035	0.052*	0.210*	0.230*
Pitch control	0.097	0.001			
Main shaft & bearings	0.024	0.011	0.004	0.000	0.050
Gearbox	0.101	0.040	0.045	0.150	0.120
Generator	0.120	0.002	0.021	0.080	0.050
Mechanical brake	0.039	0.014	0.005	0.004	0.100
Electrical controls	0.224	0.050	0.050	0.100	0.260
Hydraulics	0.110	0.031	0.061	0.360	0.210
Electrical system	0.341	0.019	0.067	0.110	0.490

*Includes the pitch control mechanism

Source: Val (2009)

Val argued that, under the environmental conditions in which tidal turbines operate, TSDs must be designed to be more reliable than onshore WT and be able to operate year-round. Based on joint studies under the SuperGen Marine Consortium, in which the author of this Thesis participated, Val proposed a simple reliability model of the reliability of such a system, Figure 2.16.

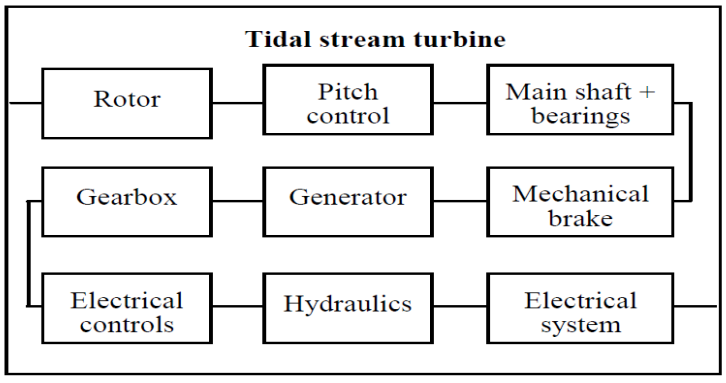

Figure 2.16 Reliability block diagram of generic TSDs

Source: taken from Val (2009)

Thies et al. (2009) analyzed the application of a traditional reliability method based on an exponential distribution failure probability implying constant failure rate data for sub-assemblies using a reliability block diagram and surrogate data from Y-ARD (1980), OREDA (1984-2002) and other sources to a notional WEC configuration. However, Thies et al. also argued that the paucity of failure rate data would lead to results with a high level of uncertainty. They therefore proposed component testing, which is live testing of device components in testing facilities for failure mode analysis, rather than applying the traditional reliability methods to WECs.

Two more papers related to component testing as another method of reliability analysis, with identification of failure modes of each component, were presented by Thies et al. in 2010 and 2011. In these papers, the simple and quick classical modelling method, known as the Parts Count Reliability Prediction Technique (PCRPT) in MIL-HDBK 217F (1991), was not applied to the device analysis. Surrogate data, from sources such as MIL-HDBK 217F, NPRD-95 and IEEE, were not used in these papers and neither was a comparison between different WECs proposed.

Iliev and Val (2011) presented a method of assessing failure rates of mechanical components of a power train, such as a main shaft and a main bearing. The method is based on a non-conventional reliability prediction or Bayesian approach, which facilitates the combination of generic failure rate data from similar sub-assemblies of other industries with new information from observing the performance of the components in operating tidal stream turbines. Specifics of this approach are the application of ‘influence’ factors, which are treated as random variables, and the prior distribution of component failure rates is obtained by Monte Carlo simulation. The posterior distribution of component failure rates

is estimated when new information about the component performance in an operating tidal turbine becomes available.

Later, Thies et al (2012) tested this method for a marine dynamic reliability power/umbilical cable to reduce uncertainties in reliability prediction data. Their proposed use of the Bayesian approach can achieve a higher confidence result, due to better assessment, stemming from new reliability data of prototype operation and commercial installation. For a full explanation of the Bayesian approach, see Chapter 4.3.2 and Appendix 3.

The author has treated the Bayesian method as complementary to her research. The approaches of Iliev and Val and of Thies et al. are more sophisticated, relying on software applications and may be more costly. Their models include uncertainties in reliability predictions. They are not suitable for straightforward for reliability comparisons, though these methods could potentially provide a reliability prediction model verification for this author's Thesis in the future. Iliev and Val (2011) noted that the Bayesian method could be used when an operating tidal turbine becomes available.

Flinn and Bittencourt-Ferreira (2011) predicted that industry-leading prototypes would be deployed and that accurate assessment of these systems would be essential. This would be the time for demonstrating the reliability of ocean energy devices. They also addressed the problems of marine energy devices (MEC) in general, and reliability assessment benefits, concluding that work is needed to improve assessment of the reliability and availability of all stages of device development. They proposed that a new model can be structured so that reliability data from operation of prototypes and commercial installation is fed back into the assessment in order to improve confidence in the result. However,

uncertainty is likely to remain significant until mature design concepts operate, and monitoring allows a database of failures to be built.

Flinn and Bittencourt-Ferreira also proposed running component lifecycle testing to produce failure mode and failure rate data for the components in their likely operating conditions as a solution to the problem of reducing uncertainties. Another solution is to use surrogate data from other industries, such as the oil and gas data collected for the OREDA project. They acknowledge that the OREDA data is not from the same operational environment therefore to allow comparison of results, the consistent assessment of uncertainty is required. However, it is also the case that factors such as experience, novelty, complexity and misfit will contribute to the uncertainty induced by application of data from other industries:

Flinn and Bittencourt-Ferreira therefore proposed to develop a 'model uncertainty' using a modifier for reducing uncertainties

$$X_{mod}=R_r/R_a$$

Equation 2.2

where

X_{mod} is the modifier.

R_r - real life data

R_a – analytical data

This model requires extensive testing of the components under specific wave or tidal environments in order to apply a sufficient collection of data to derive a failure rate distribution. The data were compared with other sources and the level of modification identified. Thus, reliability testing is essential for a first indication of data modification. Reliability results from prototype testing that is extensive will be used to update the input data and thus reduce uncertainty. They proposed, graphically, an assessment process and a way to reduce uncertainty, Figure 2.17.

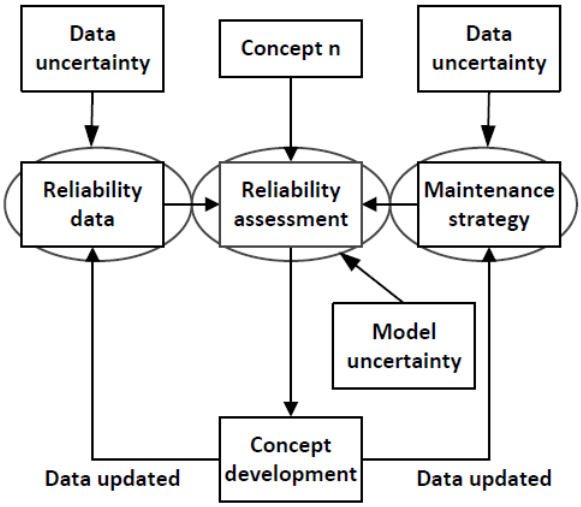

Figure 2.17 Iterative approach to reliability assessment

Source: Flinn and Bittencourt-Ferreira (2011)

As with the Bayesian approach, this method of assessment could also be used as a complement to the author's proposed reliability prediction model. The Flinn and Bittencourt-Ferreira (2011) method requires advanced system analysis of device reliability rather than the simple and quick classical reliability prediction approach that this author applies to predict the most reliable architecture.

2.6 Potentially Valuable Methodologies

2.6.1 *Y-ARD Methodology for Wave Device Reliability Analysis*

The Y-ARD Ltd Report (1980) presented extensive studies on reliability of wave energy devices based on a methodology in accordance with Ministry of Defence Naval Weapon Specification No. 10 (NWS10), 'Development Documentation System for Weapon Systems and Equipment.' The studies were in two phases. Phase 1 concerned initial assessment of each of three device designs and identified sources of unreliability within the device; Phase 2 concerned reliability and maintainability

analyses during conceptual design. During Phase 2, the method of quantitative analysis was assessed and applied with the reliability data available. The Y-ARD methodology established the following steps:

- A study boundary with all equipment and auxiliary systems directly contributing to power production was included.
- A functional block diagram for each device, presenting a logical functional analysis, providing the basis in which quantitative assessments of a device was undertaken.
- A study time base, e.g., one year of operation, with the assumption that plant availability will be the same for each year and seasonal variations were applied.
- Failure rates for individual components, sub-assemblies, assemblies and equipment of a single device, all calculated for a period of useful life in which random failures occur at a constant rate.
- The principle that individual equipment failure rates require adjustment factors to make them representative for a specific application.
- Calculated annual failure rates for main equipment and auxiliary systems. Standard reliability formulas were used to calculate values for each system in series and series-parallel configurations, providing analysis of system reliability characteristics.

2.6.2 *Latest Methodology for Systems Reliability Analyses*

In 1989 the US Department of Defense published the principles of reliability prediction of electronic equipments and their systems at different design and development stages in MIL-HDBK 217, which was developed from 1989 to 1992, updated to version MIL-HDBK-217F, Notice 2 in 1995, Nicholls (2006).

In this Thesis, the general principles and definitions for system reliability analysis have been applied and used with formulae based on the *System Reliability Toolkit* of RIAC&DACS (2005) and *Reliability Modeling* of RIAC (2010), which both include key mathematical concepts. The latter also summarises key data from the MIL-HDBK217F. These concepts will be discussed in Chapter 4 of this Thesis.

2.7 Surrogate Data Sources - Pros & Cons

Reliability data are vital to developing reliability requirements for a new technology. System reliability prediction analysis requires failure rate data on all the components. However, when no historical information is available, surrogate data can be used, as stated in RIAC & DACS (2005).

Rausand and Hoyland (2004) demonstrated that several types of data are required to model and analyze the reliability of a device, such as technical, operational, environmental and maintenance data. Technical data means the reliability data supplied by equipment manufacturers. Operational and environmental data are needed for analysis and modelling. Maintenance data are crucial for procedures, quality resources, maintenance duration in order to identify total system availability. In 2004 operational, environmental and maintenance reliability data were not available in published sources, the exception being OREDA (2002). The author of this Thesis found that the IEEE Gold Book (1997) presents electrical equipment reliability data with annual failure rates and operational availability data, as do the European onshore WT databases discussed below.

Val (2009) proposed using data on failure rates from OREDA, NPRD-95 and wind-turbine industry statistical data, though data could also be collected from a wider range of applications.

The valuable part of the proposed surrogate reliability data sources is that they represent the phase of equipment useful life, where failure rates are close to constant. According to OREDA, all failure rate estimates are based on the assumption that the failure rate is constant and independent of time, using $\lambda(t) = \lambda$, as for other databases.

The application of these data gives rise to uncertainties regarding TSDs, since the cited sub-assembly data are from manned installations where maintenance is carried out when required. Therefore the surrogate data will have a higher level of uncertainty and will not be specifically applicable in tidal environments. Adjustment of these surrogate data to tidal environments will be discussed in Chapter 5.

Information on human error is not included in any of the above databases. However, component failure may be caused by human error, therefore the OREDA project includes human error in its failure rate estimates (OREDA 2002).

2.8 Summary

Experts acknowledge that estimations of TSD reliability and availability are very difficult because of the novelty of this technology. The uncertainties of system reliability estimation are a disincentive for investors and developers. Preceding research to this Thesis showed that the reliability of sub-systems and systems starts with the realization that a sequential failure process exists. However, the modelling of this process has not been fully tested. Models thus far are sophisticated, and some require prior (or base) failure rate data, which are difficult to obtain and computationally expensive. The authors surveyed in this chapter do not present the well-defined reliability model that is necessary for simple cost effective reliability prediction analyses. They express concern that data is not yet available for tidal turbine's prediction analysis; they agree that architectures and core technologies of tidal and WTs are similar and that reliability data for WTs is available from the

WMEP and LWK databases. They all treat the possibility of analysing systems using data from offshore industries; however, the main question of the relevance of these failure rate data to tidal stream generator technology has not yet been answered.

This study will therefore attempt:

- To apply the component failure rates from WT databases and other existing databases to create a robust system reliability model for tidal energy converters;
- To apply methodologies in the RIAC & DACS (2005), VGB PowerTech (2007) and Y-ARD Ltd (1980) to assess the reliability of different types of architecture of tidal energy converters;
- To develop a new methodology for TSD to assess the reliability of tidal energy converters for the most reliable architecture.

3. TSD Taxonomies, Systems & Sub-systems

3.1 TSD Taxonomies

The general taxonomy of tidal stream energy converters is the basis for reliability prediction models and the methodology for evaluating TSD designs during their conceptual and development phases.

Tidal stream and wind power conversion turbines both extract kinetic energy from a moving fluid, water and air respectively. Today, wind power turbine technology is well developed and wind farms have been moving to offshore sites. The similarities between tidal and wind power turbine design underline why the tidal stream design concept is expected to be similar to wind power design concepts. The tidal nacelle can have several sub-assemblies: a rotor, a generator, a gearbox, inverter converter drives, transformer, which are similar to a WT nacelle.

Figure 3.1 illustrates horizontal-axis turbine TSD sub-assemblies. Notice the similarity to WT nacelles shown in Figure 3.2.

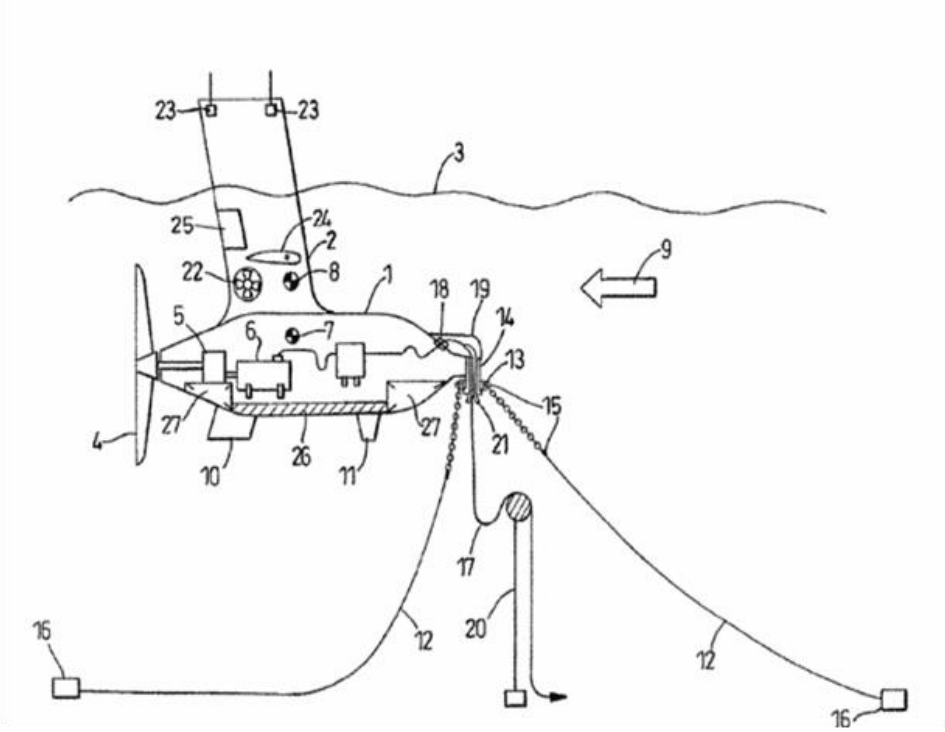

Figure 3.1 TSD with horizontal axis turbine and moored design

Source: GB Patent 2422978 (Mackie 2008a)

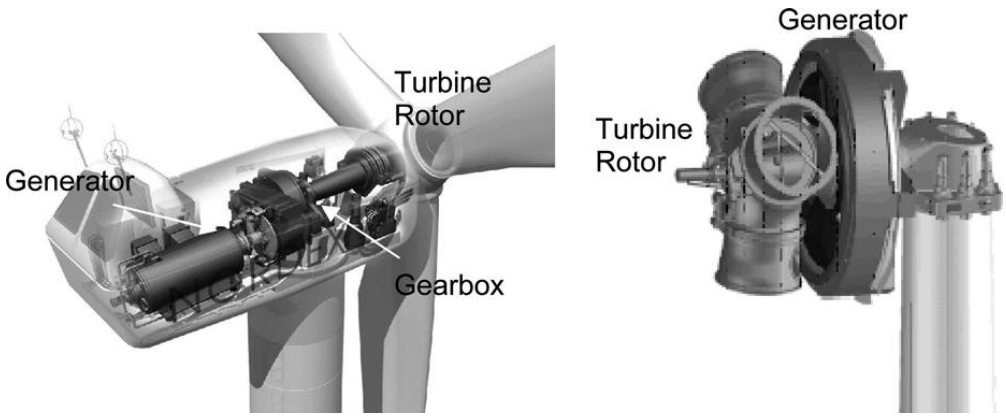

Figure 3.2 Typical drive train arrangements of WT sub-assemblies

Source: Spinato et al. (2009)

The GB Patent 2422978 (Mackie 2008a) describes the taxonomy of the Evopod technology of Ocean Flow Technology TSD, shown in Fig 3.1 as follows:

A floating, semi-submerged, tethered device that supports the horizontal axis turbine and power generation equipment for extracting kinetic energy from a tidal stream or ocean current. A submerged body (1) is supported by surface piercing struts (2) of small water plane area. The device is tethered to the seabed by a spread of mooring lines (12) that are deployed both into and away from the direction of the tidal current. A horizontal axis turbine (4) harnesses energy from the water flow and drives a generator housed within the body. A horizontal strut hydrofoil (24) corrects the trim of the device when subject to carrying loads from the mooring system and can also be used to dampen pitch motion. Radar flaps in the struts (25) can be used to counteract roll motion. Power is exported from the device to the seabed by an umbilical (17). A thruster (22) can be used to constrain the rotation of the device about its mooring system to prevent excessive twist building up between the mooring lines and the power export umbilical.

Regarding the mooring, the patent says:

The device is moored such that it is free to yaw (weathervane) into the predominant current direction which allows the use of simple fixed pitch downstream turbine. The semi-submerged nacelle has surface piercing struts so that there is sufficient reserve of buoyancy to resist vertical component of drag force reacted by the moorings. […] The device is moored off to a geo-fixed spread moored midwater buoy that is sufficiently immersed to avoid the worst of wave action and has positive buoyancy to help support the weight of the catenary mooring lines.

Based upon such TSD design concepts obtained from the work of Mackie (2008a), Fraenkel (2007a, b), the University of Southampton (2008) and Ainsworth (2006) the author is able to establish a general taxonomy of tidal stream energy converters as described in Table 3.1. Classification of TSD systems and sub-systems has been done according to the international RDS-PP Wind Turbine Guideline, VGB-B 116 D2, published in VGB PowerTech (2007). This decision was made because of the similarity of WT and TSD taxonomies, Figures 3.1 and 3.2.

Table 3.1 Established Classification of TSD According to VGB PowerTech (2007)

SUB-SYSTEM	SUB-ASSEMBLY	CODE
DRIVE TRAIN (DT) (TURBINE – MD & GENERATOR -MK)	Rotor blades	**MDA10**
	Hub	**MDA20**
	Pitch bearings	**MDC10UP001**
	Pitch systems	**MDC10**
	Main shaft	**MDK10**
	Main bearing	**MDK10 UP001**
	Couplings	**MDK40**
	Shaft seal	**MDK11**
	Gearbox	**MDK20**
	Lubrication & cooling system	**MDV10**
	Brakes	**MDK30**
ELECTRICAL SYSTEM (MS)	Generator	**MKA10**
	Converter, AC/AC	**MKY10**
	Converter controller	**MKY11**
	Generator circuit-breaker	**MKC10**
	Transformer, including cooling	**MST10**
	Generator transmission cable	**MSA10**
	Main circuit-breaker	**MSC10**
	Isolator switch	**MSC12 QA001**
	LV load-break switch	**MSA12 QB001**
LV DC UNINTERRUPTABLE ELECTRICAL SUPPLY (B)	Converter AC/DC	**BUU10**
	LV Supply 400V circuit breaker	**BUU11**
	Battery	**BUV10**
	LV DC cables	**BU**
GRID CONNECTION (AA)	Umbilical electrical cable,	**AAG10**
ANCILLARY SYSTEM (XA)	Ventilation	**XAA10**
	Heat exchanger, water cooled	**XAA20**
CONTROL & MANAGEMENT (CA)	Programmable controller	**CA10**
	Process automation & SCADA	**CA11**
	Turbine controller	**MDY10**
	HVAC Controller	**XAA30**
CORROSION PROTECTION (AB)	Corrosion control system	**AB**
STRUCTURE (U)	Nacelle/Foundation/Moorings	**U**

Sub-systems vary considerably between TSDs and may not be present in every device and there can be a number of overlapping systems due to individual designs.

3.2 TSD Generic Sub-Systems, Assemblies & Sub-Assemblies

Due to the novelty of tidal stream technology, there is not yet a universal agreement about the layout of the TSD system, sub-systems and components. The following provides a generic description of major sub-systems and sub-assemblies.

3.2.1 *Drive Train*

A drive train consists of two sub-systems: the turbine and the generator. The turbine has rotor blades, blade yaw and pitch systems, seals, shaft, bearings, brakes and gearbox. The generator sub-system consists of the generator itself, inverter modules and circuit breakers.

Most TSD designs use a turbine which delivers torque through its shaft axis to a rotating generator. The mechanical energy of the turbine is thus converted by a transmission system and a generator into electrical energy, which is then converted to grid-compatible form and is fed into the electrical grid. A typical TSD arrangement is illustrated in Figures 3.1.

3.2.2 *Rotor Blades*

Rotor blade performance is essential to successful TSD technology, the loads on the rotor acting as the starting point for turbine design. These rotor blades generate lift, which forces the drive shaft to travel faster than the tidal flow velocity and drag, which generates a thrust load on the turbine module and structure. The lift makes for efficient power development. The turbine may have fixed-geometry blades, so that the tidal flow can move only one way, or the blades of the turbine may allow

operation in a bi-directional tidal regime by use of variable pitch rotor blades or rotation of the nacelle, allowing the turbine to extract energy more efficiently at varying velocities and from both ebb and flood tides. However, a turbine can also be bi-directional without being variable-speed. Variable speed allows a more efficient extraction of tidal energy and allows a turbine to reverse flow while retaining the same sense of rotation, facilitating bi-directional operation.

A tidal turbine must be designed with appropriate blade geometry, transmission and generators suitable for the tidal environment, in order to successfully recover energy from a flow stream. According to Mackie (2008), the blade geometry for floating devices must be coordinated with the device structure for the correct drag force to be applied to the mooring system. It is essential to have load control systems to prevent blades from stalling, as this can cause rapid fall-off of lift force and sudden changes in torque and thrust, which will lower reliability.

3.2.3 *Gearboxes*

The gearbox is a transmission device to increase the drive-shaft speed of rotation to satisfy specific generator requirements, determined by the generation frequency and grid connection specifications. The turbine first develops low-speed, high-torque power, which a gearbox converts into high-speed, low-torque power needed for electrical generation. The gearbox ratio facilitates this conversion and may have a single or multiple stages between the turbine-shaft and generator. A lubrication system is required to prevent premature gear and bearing degradation. A brake may be included to stop energy production in an emergency and hold the turbine stationary during maintenance

3.2.4 *Generators*

A TSD could have a synchronous or an asynchronous (induction) generator. The synchronous generator rotates synchronously with grid frequency generating electricity. The asynchronous generator rotates above the grid synchronous speed at a slip speed determined by the load. Choosing the generator is dependent on a number of factors. If using direct-drive, a gearbox will be unnecessary, reducing the number of system components, the generator would most likely be synchronous and because of its low speed will be large and heavy. Using a gearbox increases the number of system components, but a higher speed, smaller and lighter generator can be used, with the option of being either synchronous or asynchronous. The cooling medium may be air using a fan, or water using a pump, thus requiring additional parts and a control system. The cooling system could be classed as a stand-alone ancillary system (XA).

Mackie (2008b) argued that a typical tidal stream site with fluid flows:

- maximum neap tide flow velocity, about 2 m/s;
- maximum spring tide flow velocity, about 4 m/s;
- extreme storm surge tide, about 5 m/s

is a different environment than that in which a WT operates, at fluid flows of 3-25 m/s because the density of air is approximately 1/800 that of water. With tidal velocity limited to $\leq$ 6 m/s, turbines do not have a top shut-down velocity. Two solutions to adjust the power of the tidal turbine are:

- using adjustable pitch turbine blades, reducing blade loads and output torque;
- selecting a generator and transmission components with high rated power.

3.2.5 *Power Converters*

A TSD would not be connected directly to the power grid. A converter would convert the frequency of AC produced by the generator to the grid frequency, 50 or 60 Hz. The converter consists of three parts, a generator-side inverter which converts the generator energy to DC, a DC link capacitor, and a grid-side inverter which converts DC to AC grid frequency. The converter allows the generator to operate at variable frequency, thereby making it possible to vary turbine speed, which could maximise turbine power extraction.

3.2.6 *Electrical Systems*

The electricity produced by a TSD generator is high-current, low-voltage (LV). To minimize dissipation due to heat loss in the TSD-to-shore transmission, the LV is changed by a step-up transformer to the grid voltage, for example 11 kV, 50 Hz AC. This transformer requires a cooling system, a circuit breaker to protect the power circuits against damage from short circuit faults and an isolator switch to interrupt power circuits for maintenance.

3.2.7 *LV DC Uninterrupted Electrical Supply Systems*

Some TSDs with a fixed-pitch turbine start generating as soon as water flow is sufficient; others must draw power from the grid to start the turbine. Electricity is also needed to power braking, communication and lubrication systems. The TSD needs a means of supplying these secondary systems in the event of a grid fault. This back-up power is usually provided by an on-board LV battery, which can draw charging current from the grid. A double battery could provide back-up power in case of a battery failure. Therefore, an LV DC electrical system supply is usually required to charge the back-up batteries.

3.2.8 *Grid Connection Systems*

Export of power is a key issue for developers, otherwise how could power be supplied at appropriate transmission voltages through fixed cables? It is planned to transmit TSD-produced electricity to shore via sea-bed cable. Two different approaches can be taken depending on the sea-bed grounding type of the TSD. Fixed TSDs can be connected through the TSD structure to an export power cable on the sea-bed, as is done for offshore WTs. Floating TSDs need a flexible umbilical cable to the sea-bed cable. The umbilical cable must respond reliably to floating device mooring system excursions and be capable of disconnection. The power transmission cable, the only fixed link to shore, is also used to carry communication lines, usually fibre-optic. Renewable energy devices are generally designed to be fully autonomous but the ability to communicate with them is important for control, particularly to instruct shutdown, and for routine monitoring.

3.2.9 *Control & Management System*

As in a WT, the TSD control system monitors the total device to determine that it is operating correctly, within specified limits for each mechanical component. The critical parameters are:

- Tidal flow;
- Rotor speed;
- Blade position and adjustment;
- Blade-pitch activation on start and when the turbine is close to the rated power;
- Brake operation.

The control system also monitors the functioning of the lubrication and cooling systems, the mechanical brake hydraulics, hydraulic pressure level, temperatures, surface wear and rate of corrosion. The control can remotely stop the TSD when needed for safety, inspection, maintenance or emergency reasons.

3.2.10 *Support Structures*

Depending on the sea environment, the TSD could have a moored floating platform, or moorings fixed to the sea-bed, or on piles positioned appropriately for the turbine location in the water. Support struts, foundation structure or mooring systems must resist the drag load from the turbine and nacelle. Turbines supported on a monopile will put a high bending moment on the pile. Pile diameter depends on the height of the turbine above the seabed and the piling condition of the seabed. A floating tethered turbine concept using catenary mooring systems is under study. Only a few support structure solutions have being tested for TSDs to date, for example:

- Monopile support structure, see Fraenkel (2007a,b);
- Mooring support structure, see Mackie (2008b);
- Gravity-based structure, see Corcoran (2009).

3.3 Different TSD Concepts

3.3.1 *General*

Tavner et al. (2007) analysed the reliability of maintained, onshore WT by using historic data from the Windstats survey, a European database of WT reliability and availability. His study concluded that WT design configuration affects reliability. As illustrated in Section 3.2, the general configuration of a TSD being similar to a WT; its mechanical and electrical system configuration must play a crucial role not only in energy production but in reliability and availability.

The TSD design concept can be more flexible than that for a WT; it is not limited by the demands of being mounted on a tower but by the challenging ocean environment, sea-bed grounding and consequent energy production scenarios.

Different concepts were reported in DTI (2007) and analysed with respect to an aggressive marine environment, operation, and maintenance strategy.

3.3.2 *Mechanical & Electrical Configurations*

Four different mechanical and electrical configurations were considered, as illustrated in Figures 3.5-3.8, and are currently under consideration by ocean energy device developers: see the examples of TSDs in Section 3.5 and Appendix 4.

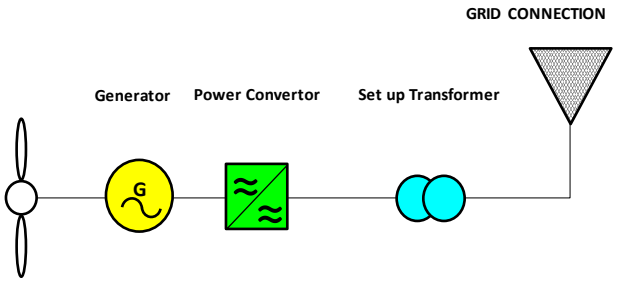

Figure 3.3 Single turbine, generator, converter, step-up transformer & AC link

Source: DTI (2007)

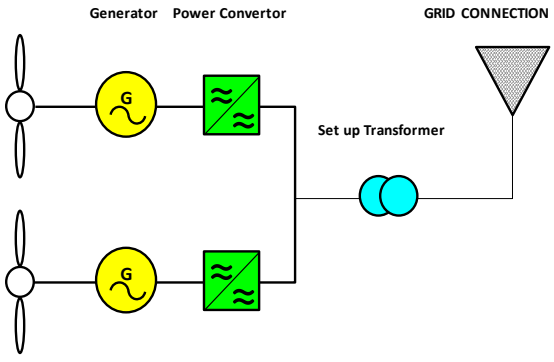

Figure 3.4 Multiple turbines, generators & converters, step-up transformer & AC link

Source: DTI (2007)

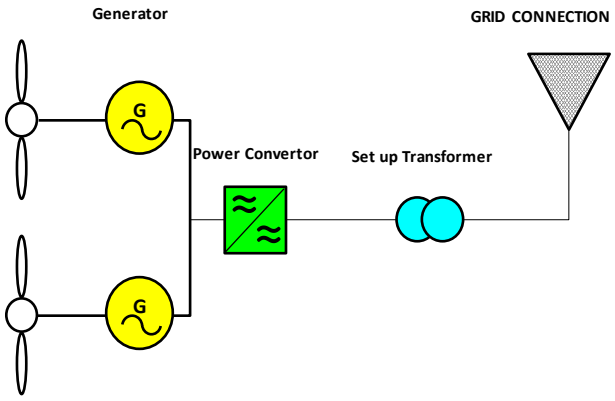

Figure 3.5 Multiple turbines, generators & single converter, step-up transformer & AC link

Source: DTI (2007)

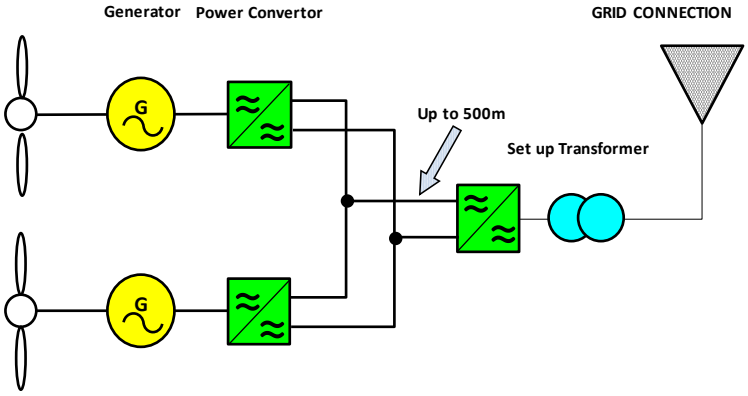

Figure 3.6 Multiple turbines, generators, generator-side inverters, active DC link cable, single onshore single grid side inverter, step-up transformer

Source: DTI (2007)

3.4 A Generic TSD

Based on the general taxonomy classification shown in Table 3.1, the author proposes a generic classification of a TSD device, by codes, to develop a system Reliability Block Diagram (RBD) and major critical sub-systems applicable to a

variety of TSD configurations, see Figure 3.7. Further, each sub-system's block diagram can be expanded to show individual sub-assemblies block diagrams, see Figure 3.8. These activities are well-known in reliability prediction analyses; however, the application of coding provides specifics, unique to each sub-assembly; this coding will be applied to five devices under study.

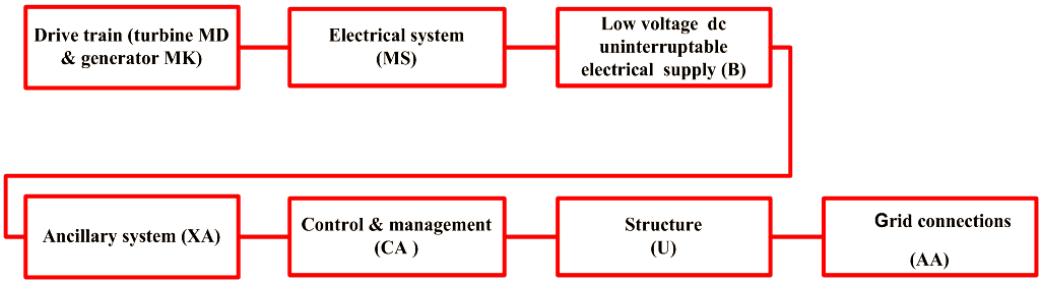

Figure 3.7 Generic device reliability block diagram (RBD)

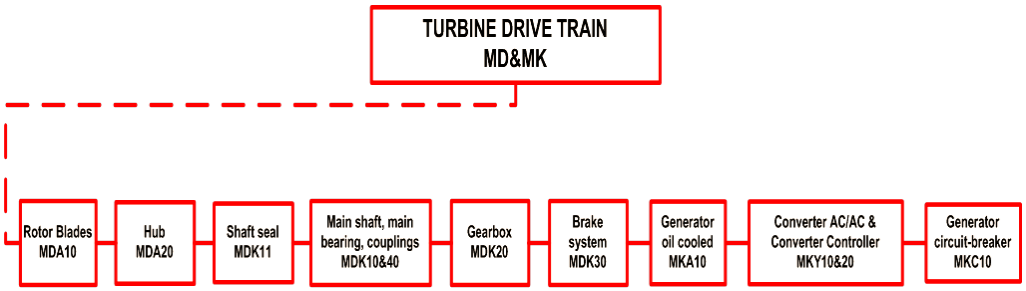

Figure 3.8 Generic turbine drive train RBD.

3.5 TSD Horizontal Axis Turbine Prototype Examples

The horizontal axis tidal turbine with different sea-bed fixing options has been considered by the marine renewable energy industry. Below are five devices, which are in the prototype stage, currently installed in UK, Canadian or French waters, suitable for consideration in this Thesis. The author was able to extract generic design principles and characteristics for these devices available from the public

domain and with some consultation with device inventors. The reader should take into account that the data presented in Tables 3.2-3.6 is conditional and was not made based upon detailed device design knowledge but upon the generic design principles and characteristics. In addition, these design principles and characteristics are developing, based upon new updates available to developers, enabling them to minimize cost and increase energy efficiency. The following five generic device prototypes will be studied in more detail in Chapter 5 as a part of the methodology for reliability model prediction and analysis.

3.5.1 *Semi-Submerged Tethered, Single Turbine*

An example of a semi-submerged, floating, tethered, downstream tidal and ocean current energy device with a single, slow–speed, horizontal axis turbine is shown in Figure 3.9. The concept is similar to a WT and based upon the Evopod product (Mackie 2008b). Table 3.2 summarizes the device features and design characteristics.

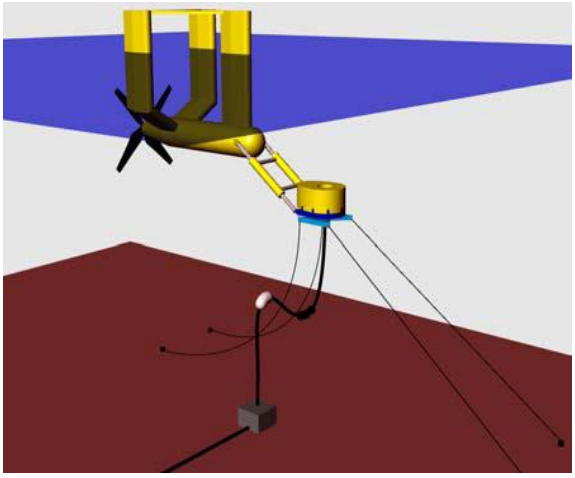

Figure 3.9 A moored semi-submerged device with a horizontal axis turbine

Source: Mackie (2008b)

Table 3.2 TSD1 Generic Design Features Based on Evopod Series

Features	Design Characteristics
The power train consists of a gearbox, induction generator, converter, switchgear and transformer, controls, instrumentation and data logging equipment, utilizing components similar to a WT.	Induction generator; nameplate rating 1.2 MW
	Rotor diameter - 14 m to 18m depending upon flow conditions
Marine features, shaft, seals, stern bearing, power export swivel, utilize components of marine standard.	Nacelle diameter about 3.50 m
	Nacelle length overall - 21.5 m
The longitudinal separation of the struts in the multi-strut version provides some damping against the device pitching in surface waves.	Rated flow speed - 3.0 m/s
	Depth of water mean sea level - 300m
The device requires a controllable pitch turbine for limiting the power absorption when the flow is faster than the rated speed.	The device is free to yaw with the changing current direction
	Pitch system designed for limited pitch control
The pitch adjustment required by the turbine is only about +/-10 degrees However, this is not a fully reversing pitch system needed for a bi-directional tidal regime.	Off-shore distance - 1 to 2 km
	First line maintenance possible on site
	Could be detached for maintenance off-site

3.5.2 *Submerged Fixed Tower, Twin Turbines*

Figure 3.10, based on the SeaGen device (Fraenkel 2007b), shows an example of a seabed-fixed, tidal ocean current energy device supported on a fixed tower, with twin, slow–speed, horizontal-axis flow turbines, similar to a WT, mounted on a cross-beam that can be raised above sea-level. The rotor blades have a pitch control system similar to a WT but that can operate over the full-span from $+90^{o}$ to -90^{o} to allow the rotor to extract energy from the ebb and flood tides, so the device can be operated in a bi-directional tidal regime. The structure is designed to minimise water disturbance in bi-directional water flow. Table 3.3 summarizes device features and design characteristics.

Figure 3.10 SeaGen twin horizontal axis turbines on fixed support tower

Source: Fraenkel,(2007b)

Table 3.3 TSD 2 Generic Design Features Based on Sea Gen Series

Features	Design Characteristics
The rotor drives mounted in separate nacelles on the cross-beam consist of a power train consisting of a gearbox and generator. The gearbox has an innovative design with two planetary stages and one spur stage. The gearbox and generator are designed to be cooled by the passing ocean current and do not need additional cooling systems. The tower structure is piled into the sea-bed. The pitch system is designed for a bi-directional tidal regime.	Squirrel cage induction generator Converter fully rated for 2 x 0.6MW = 1.2MW Rotor diameter - 16 m Rated flow- 2.4 m/s Distance between drive trains - 27 m. Cross-beam length - 29 m Weight of each drive train - 27 tonnes Weight of cross-beam with 2 drive trains - 151 tonnes Depth of water mean sea level - 26.2 m Tower total height above sea-bed - 40.7 m Tower diameter- 3.025 m Off-shore distance - 1 to 2 km Service of drive trains possible on and off-sites

3.5.3 *Sea-bed Fixed, Single Turbine, Direct Drive Generator*

An example of a submerged, tidal and ocean current energy device arranged on a gravity base, fixed support, special design structure, with bi-directional, slow-rotation, horizontal axis, open-centre rotor turbine, that could be lowered to the sea bottom is shown in Figure 3.11 based upon the OpenHydro product (OpenHydro Group Ltd. 2011). The rotor blades allow the rotor to extract energy from the ebb and flood tides, so the device can be operated in a bi-directional tidal regime. The system structure is designed to minimise water disturbance due to bi-directional flow. Table 3.4 summarizes the device features and design characteristics.

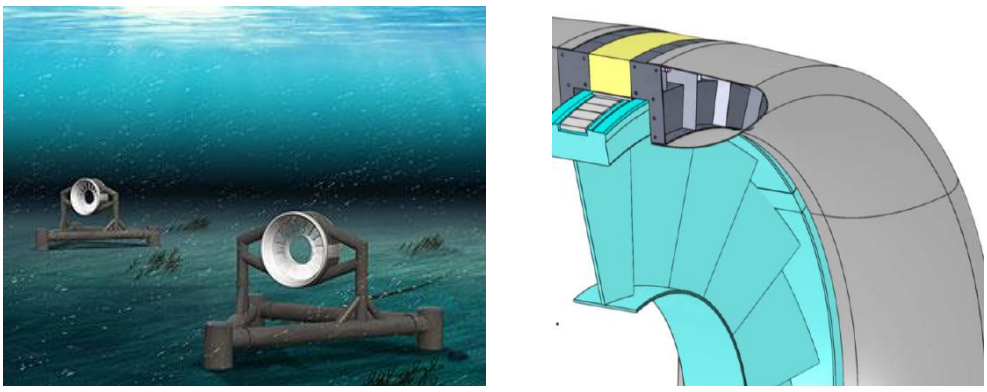

Figure 3.11 OpenHydro single horizontal axis turbine, sub-sea gravity base

Source: URL: OpenHydro Group Ltd. (2011)

Table 3.4 TSD 3 Generic Design Features Based on Open Hydro Series

Device Features	Device Characteristics
Rim-mounted turbine. Only one moving part of the whole system, the rotor rotating within the stator. Water lubricated generator bearings. Offshore station contains rotor with turbine blades and magnets, stator with coils and rectifier. Onshore station contains converter, switchgear, transformer, controls, instrumentation and data logging equipment, utilizing similar components to a WT. Retention of rotor blades within the outer housing. A large number of permanent magnets are embedded in the outer generator rotor rim. A large number of coils are embedded in the inner annular rim of the stator. Marine features, power export swivel utilizing components similar to marine standards. Gravity-based support structure. The device does not require a controllable pitch turbine for limiting the power absorption when tidal flow is faster than the rated speed. Design avoids the need for oils, greases or other lubricating fluids.	Direct drive permanent magnet synchronous generator Nameplate rating 1.0MW. Rotor diameter - 6, 10 or 16m depending upon flow conditions Rated tidal flow speed - 3.0 m/s, designed for extreme weather climate for tidal flow up to 8,5 knots. Designed with no seals or gearbox. Off-shore distance $\geq$ 0.5 km. Depth of water mean sea level – shallow/ and deep waters Service of drive train possible only off site

3.5.4 *Floating Tethered, Twin Turbines*

An example of a floating, tethered, downstream tidal and ocean current energy device with two, slow–speed, horizontal axis turbine is shown in Figure 3.12 based upon the SRTT product (Francis and Hamilton 2007) and similar to the Evopod but with twin turbines. Table 3.5 summarizes the device features and design characteristics.

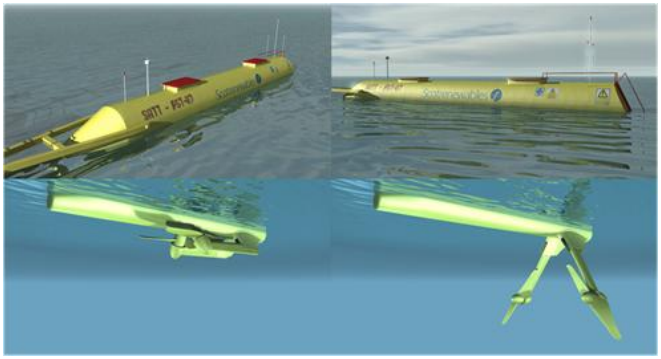

Figure 3.12 SRTT floating two axis fixed pitch turbine, moored

Source: Francis and Hamilton (2007)

Table 3.5 TSD 4 Generic Design Features Based on SRTT

Features	**Design Characteristics**
Main floating nacelle or hull has a single buoyancy cylindrical tube with two parallel horizontal axis rotors attached to the hull by moving legs. The rotor drive is mounted in a separate power take-off nacelle consisting of a power train with a gearbox and a generator. Converter, switchgear and transformer, controls, instrumentation and data logging equipment, utilizing components similar to a WT. Marine features, shaft, seals, bearings, power export swivel, utilize components of marine standard. Device is moored to sea bed Passive Yaw System for energy efficiency Fixed Pitch Rotor Blades	Permanent magnet synchronous generators Nameplate rating 2 x 0.6MW = 1.2MW Rotor diameter 2 x 12 m, can be modified based on tidal site. Rated flow 3.0 m/s Weight 400 Tonnes Depth of water mean sea level > 25 m Rotors total height below waterline 12 m Nacelle length 32 m Off-shore distance - 1 to 2 km Service of drive trains possible on and off-sites

3.5.5 *Sea-bed Fixed, Single Turbine, Permanent Magnet Generator*

Figure 3.13, based on the AR series devices (Atlantis Resources Corporation Pte Ltd. 2009), shows another example of a submerged, tidal device arranged on a gravity base, a fixed-support structure, a pylon with bi-directional, slow-moving, horizontal-axis turbine lowered to the bottom. The blades allow the rotor to run from ebb and flood tides. The following Table 3.6 summarizes the device features and design characteristics.

Figure 3.13 AR series horizontal axis turbine on fixed support tower

Source: URL: Atlantis Resources Corporation Pte Ltd (2009).

Table 3.6 TSD 5 Generic Design Features Based on AR Series

Device Features	**Device Characteristics**
Offshore station: rotor with turbine blades and magnets, stator with coils and rectifier	Permanent magnet synchronous generator
Onshore power station: inverter drive, switchgear and transformer, controls, instrumentation and data logging equipment, utilizing components similar to a WT	Nameplate rating 1.0MW
Retention of rotor blades within the outer housing	Rotor diameter – 18 meters
Gravity based support structure, mono-pylon	Rated flow velocity – 2.6m/s
Fixed pitch blades	Depth of water mean sea level – shallow/and deep water
The device does not require a controllable pitch turbine for limiting the power absorption when the flow is faster than the rated speed.	Off-shore distance > 0.5 km
	Service of drive trains possible off site

3.6 Summary

To create reliability prediction models, a TSD taxonomy is needed; however, no detailed taxonomy is publicly available. The author of this Thesis has developed a general taxonomy that can aid in developing a reliability prediction model.

A typical TSD consists of eight sub-systems, which can in turn be broken down into their own sub-assemblies and specified by a code:

- Drive train (DT);
- Electrical system (MS);
- Low voltage (LV) electrical systems (B);
- Grid connection (AA);
- Ancillary system (XA);
- Control & management (CA);
- Corrosion protection (BA);
- Structure (U).

The systems vary considerably between TSDs and may not be present in every device. There are overlapping systems in individual designs.

4. Developing a Methodology for TSD Reliability

> *The prediction of failures involves uncertainty, and problems associated with failures are inherently probabilistic. Their solution requires optimal tools to analyze strength of evidence and process and understand failure events and processes to gauge confidence in a design's reliability.*
>
> Modarres, Kaminskiy and Krivtsov (2010)

4.1 Introduction

It is crucial to the success of developing a TSD prototype system to have a reliability prediction model that can apply probabilistic assessment to the prediction of incident failures and of future performance, and to compare architectures in order to develop devices with low failure rates. The author's research aims to develop the methodology of system reliability assessment. This chapter addresses conceptual development of generic reliability prediction models for TSDs, which, for the purposes of this Thesis, have been applied to five horizontal-axis TSD designs as shown in Chapter 5. Sections 4.2 and 4.3 provide a brief introduction to the reliability concepts and equations that are used in the following sections.

4.2 Basic Reliability Modelling Concepts

In speaking of TSD reliability concepts, it is useful to present the definition of reliability and of reliability modelling based on probability. A list of definitions of terms for reliability and maintainability is published in MIL-STD-721C (1981) and a full description of the application of these terms can be found in MIL-HDB-338B (1998). In addition, RIAC&DACS (2005) have summarised and presented the

definitions of reliability and maintainability. For the purposes of this Thesis, the relevant terminology is defined in Appendix 1.

Based on MIL-STD-721C, reliability in general is the probability that a component or system will perform its intended function for a specific time interval under stated conditions. Reliability or probability is measured quantitatively and consists of several reliability characteristics. The results can be different for non-repairable and repairable components/assemblies/systems. The equations presented in this section are well-known in the field of reliability and also can be found, for example, in Modarres et al. (2010).

The most commonly-used reliability functions for the non-repairables are:

- Reliability survival function *R(t)*;
- Failure function *F(t)*;
- Instantaneous probability of failure *f(t)*;
- Hazard rate *h(t)* or failure intensity *λ(t);*
- Failure rate, assuming constant λ (Failures/year).

The reliability survival function *R(t)* and the constant failure rate λ are sufficient to analyse and compare the probability of failure for non-repairable sub-systems and systems in TSDs at the conceptual stage.

Mathematically, the reliability survivor function *R(t)* or probability that a system or component will survive after a specified time *t*, can be expressed as:

$$R(t) = 1 - F(t) = 1 - \int_0^t f(t)dt$$

Equation 4.1

The hazard rate *h(t)* indicates the instantaneous probability that a given system or component will fail, assuming that the system/component is still operational:

$$h(t) = \frac{f(t)}{R(t)} = \frac{F'(t)}{1 - F(t)R(t)}$$

Equation 4.2

The probability is usually high at the start of operational life, as a result of manufacturing defects or mishandling. Towards the end of the system's or component's life, the probability of failure increases due to general wear and tear and the system/component cannot be repaired or replaced. However, there is usually an intermediate period where the probability is more or less constant. As a function of time, this probability has the 'bath-tub' shape shown in Figure 4.1. For reliability analysis, the intermediate period during which the hazard rate is constant, is used for reliability prediction.

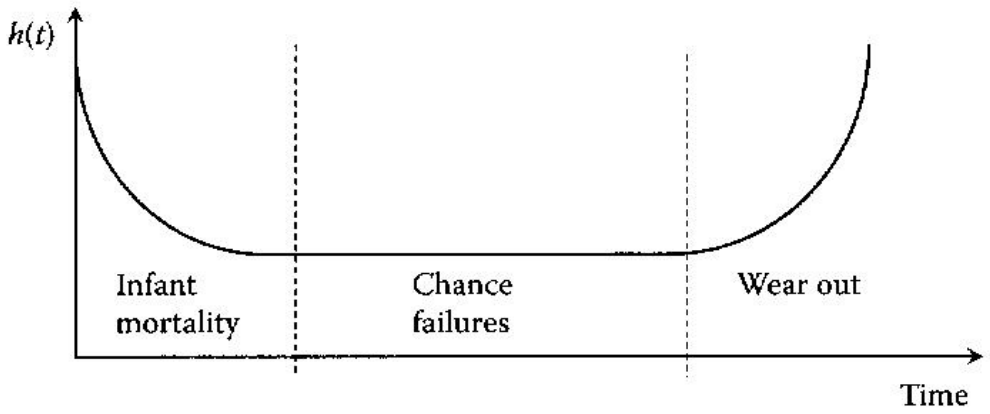

Figure 4.1 Hypothetical hazard rate, failure intensity curve, applicable to TSDs

Source: Modarres et al. (2010)

If the hazard rate *h(t)* becomes constant, λ, then

$$f(t) = \lambda e^{\lambda t}$$

Equation 4.3

and

$$R(t) = e^{\lambda t}$$

Equation 4.4

The reliability survivor function *R(t)*, time t = 1 year between services, shown in Equation 4.4, will be used in this Thesis as the reliability characteristic for TSD analysis.

For a device with all components in series, i.e. where the failure of any one component will cause system failure if there is no redundancy, the total predicted system reliability *R(t)* over time *t* is the product of the reliabilities of the component systems:

$$R(t) = \prod_i R\,i(t)$$

Equation 4.5

and the total predicted system failure rate λ_{tot} ,where component *i* has a constant failure rate λ_i , yields:

$$\lambda_{tot} = \sum \lambda_i$$

Equation 4.6

Different systems have different configurations of components and sub-assemblies and different interconnections. Table 4.1 shows the reliability characteristics of different system arrangements, assuming that the system is not repairable.

Table 4.1 Reliability Characteristics Calculation for Non-Repairable Systems

System	**Active redundancy**	***Reliability, R(t)***	***Failure Rate, λ***
1	1 of 1 must be working	$e^{-\lambda t}$	λ
2	1 of 2 must be working	$2e^{-\lambda t} - e^{-2\lambda t}$	$2\lambda/3$
3	1 of 3 must be working	$3e^{-\lambda t} - 3e^{-2\lambda t} + e^{-3\lambda t}$	$6\lambda/5$

Source: RIAC&DACS (2005)

A summary of effective redundancy equations for calculating reliability survivor functions and failure rate estimation for different system configurations is presented in RIAC&DACS (2005).

For non-repairable systems with independent sub-assemblies, when the hazard function $h(t)$ or failure intensity $\lambda(t)$ is constant λ, with mission time t, an exponential probability distribution describes time-to-failure. This distribution was chosen due to its simplicity and because field data of failure rates are not available, so surrogate constant failure rates were used instead, which represent random variables. Surrogate data of sub-assembly constant failure rates are related to the useful lifetime of the hazard failure rate curve, Figure 4.2, and this data is applied to TSDs and analysed in Section 4.6. and Chapter 5.

According to Modarres et al. (2010), in the case of *components where the random-failure region is long, in comparison to the two other regions, this distribution might be adequate […] In general, the exponential distribution is considered as a good model for representing systems and complex, non-redundant components consisting of many interacting parts.*

TSD sub-assemblies should have long random-failure regions by design. Their architecture will consist of complex, non-redundant electronic and mechanical components, so it is reasonable to use the exponential time-to-failure distribution.

4.3 Different Reliability Prediction & Assessment Methods

Reliability prediction and assessment methods are defined in this Thesis as the process of quantitatively assessing a system design, relative to its specified reliability. Prediction analysis applies appropriate models, failure rates and repair

rates in order to evaluate systems, sub-systems, sub-assemblies or component reliability parameters.

When considering reliability prediction and assessment methods, it is important to understand that there are currently two main schools of modelling, with contrasting approaches to probability meanings and applications to different scenarios. These modelling methods are:

- Classical Modelling, as used in this Thesis;
- Bayesian Subjective Modelling, as used by e. g., Val and Chernin (2011); Val and Iliev (2011); Thies et al. (2012).

These two methods can be applied to TSD reliability prediction and assessment analyses, but at different stages of the design and development. In Appendix 3, Table 12.1, the author provides an overview of all the most commonly-used methods for the evaluation of the reliability of systems under different stages of development. This overview highlights the decision-making process on the chosen TSD reliability prediction modelling methodology used in this Thesis.

This author intends to apply the classical Reliability Modelling and Prediction (RMP) to the TSD rather than other system reliability and uncertainty prediction approaches because this approach has been well developed in MIL-HBDK217 (1991), RIAC&DACS (2005; see also RIAC 2010), Modarres et al. (2010) and is well-proven in practice for new technologies.

4.3.1 *Reliability Modelling & Prediction (RMP)*

As defined by RIAC&DACS (2005), a reliability model is a visual representation of the functional interdependencies of a system, with a framework of prediction analysis for reliability estimates, which will guide design decisions. Derived models assist in device failure predictions, visual representations of series, parallel

configurations and redundancies; they also show the reliability characteristics and factors possible for systems failures.

Models are derived from functional requirements, functional block diagrams (FBD) providing a basis for reliability block diagrams (RBDs) for calculating the total system annual failure rate or total system reliability for the devices. The RBD is used primarily to quantify the reliability survivor function of a system, sub-system or total device, thus it can be called an assessment or prediction method. Models can be simple or complex, including varying environments, operations, controls and human interactions. Development of the models depends on the types and amounts of reliability data available and the criticality of the device being analysed. Each block in a model may represent the maximum number of components with assigned λ_i under specific environments. Examples of derived graphical models for TSDs are presented in Chapter 5 and Appendix 4.

4.3.2 *Bayesian Subjective Modelling*

The Bayesian approach to reliability prediction is based on subjective interpretation of analysed data, where *P(E)* is a measure of the degree of belief one holds in a specified event *E* (Modarres et al. 2010). However, this method has its limitations.

The Bayesian method is based on three steps:

- Establishing the prior distribution;
- Deriving the likelihood distribution;
- Assessing the posterior distribution.

The major problem is the selection of the prior distribution, which depends upon the amount of available data and their format.

Val and Iliev (2011) demonstrated the applicability of the Bayesian method in their paper on the reliability of TSD main bearings. Although the method can be

used for component improvements simulation analysis, it is complex for comparisons of device architecture at the early stage of design.

The Bayesian method is a useful tool for assessing further systems reliability uncertainties and future prediction of components failure when the designer does not have sufficient data but some information is provided. This is another approach of analysing TSD sub-assembly uncertainties, which could be used as more TSD reliability data become.

4.4 Proposed Reliability Modelling Methodology

4.4.1 *RMP & Portfolio of Surrogate Data*

This Thesis is based on Reliability Modelling and Prediction analysis (RMP) of RIAC&DACS (2005), adapting a combination of:

- **Graphical models** consisting of FBDs and RBDs, presented in Chapter 5 and Appendix 4;
- **Mathematical models** based on Parts Count Reliability Prediction Technique (PCRPT) , as described below in 4.6 and presented in Chapter 5 and Appendix 4;
- **A Portfolio of Surrogate Data (PSD),** as described below in 4.4.2 and Appendix 4.

The RMP, based on PSD sources, was chosen as the appropriate quantitative method for prediction and assessment of failures for comparison of TSD designs due to specific issues associated with tidal device applications for the following reasons:

- Devices are in the early stage of design and deployment, hence, operational data are limited;
- TSD is new technology, hence, analysis by similarity to existing systems would be limited;
- RMP is applicable to both the mechanical and electrical sub-assemblies incorporated in TSDs.

The PSD was mainly drawn from the following sources:

- Wind turbine data: Hahn et al. (2007), Spinato et al. (2009), Tavner et al. (2010: 2012);
- Marine data: OREDA (1984-2002);
- Generic reliability databases: MIL-HDBK-217F(1991), NRPD-95 (1995);

- Integrated reliability databases: IEEE Gold Book (1997).

Based on Y-ARD Ltd (1980) and RIAC & DACS (2005), the sequence used for modelling reliability predictions for this study was to:

- Perform a robust parts classification for each device using robust methods, eg VGB PowerTech (2007);
- Establish a schematic diagram for each device based on the defined structure;
- Derive an FBD from that schematic diagram, showing the logical and functional interdependencies between sub-systems, assemblies and sub-assemblies, constituting an RBD;
- In the absence of historical reliability data, collect reliability data from surrogate data sources, using them to allocate failure rates for each FBD sub-assembly;
- In the unknown environment without historical reliability data establish lower and upper bound failure rates, λ_{Gi_min} and λ_{Gi_max}, for each sub-assembly from surrogate data and use the upper bound as the more conservative value;
- Adjust surrogate failure rate data to the tidal environment using two failure rate estimate approaches;
- Calculate predicted tidal environment failure rates;
- Evaluate the total device reliability, using the PCRPT from MIL-HDBK-217F (1991), MIL-HDBK-338B (1998), assuming sub-assembly times-to-failure were exponential, that is hazard rates are the results of random failures and a constant failure rate applies.

The parts classification of the systems and sub-systems was performed according to VGB PowerTech (2007) because the taxonomy of tidal and wind turbines is similar. System reliability considerations require identification of all the sub-systems of any system. The criticality of each part may not be identical but the failure rates are statistically significant.

FBDs depict the functional interdependencies of the sub-systems, assemblies and sub-assemblies of each device. Assuming that each sub-assembly is independent of others and that sub-assemblies operate in a single environment, the overall tidal device reliability, based on the experience of wind-turbine operation, can be analysed as a series or series-parallel network, using an RBD. The constituted RBDs of five horizontal-axis TSDs with different architectures were used to quantify the reliability survivor function of each device and so could be considered an assessment or prediction method.

To evaluate total system reliability the PCRPT can be used on RBD models. This technique assumes that the average failure rate for each sub-system or component is constant during useful life, Figure 4.1, and that the time-to-failure of sub-systems is exponentially distributed.

4.4.2 *Reliability Data from Surrogate Sources*

The author created a PSD from the data sources of several industries. Surrogate data were used for a number of reasons:

- No reliability data is yet available for TSDs;
- The architectures and core technologies of TSDs and WTs are similar;
- WMEP database contains failure rates for about 1,500 fixed- and variable-speed WTs, with geared or direct drives in operation for up to 15 years.

4.4.3 *Wind Industry Databases-WMEP, LWK & Windstats*

Hahn, Durstewitz and Rohrig (2007) analysed the reliability of German WTs and components, providing figures of failure frequency and downtimes voluntarily reported to ISET over 15 years and evaluated under Germany's Scientific Measurement and Evaluation Programme (WMEP) '250 MW Wind'. This database was for repairable, on-shore WTs, documenting 60,000 maintenance and repair episodes in which average annual evaluations show WT availability in the 97-98% range.

LWK and Windstats databases from 6,000 WTs in Germany and Denmark over 11 years of operation were surveyed by Spinato et al. (2009), focusing on a sub-set of 650 onshore machines, from which the data about the reliability of generators, gear-boxes and electricity converter sub-assemblies were analysed: see Figure 4.2. The authors concluded that, although the reliability is 'considerably below' that of such sub-assemblies in other industries, reliability was improving with time.

The European onshore WT database data are summarized by Tavner et al. (2010; 2012) and are presented in Figure 4.3, showing the average failure rate and the average downtime per component: see also Delorm et al. (2011).

The summary of WT databases indicates that electrical sub-systems are most vulnerable to failure.

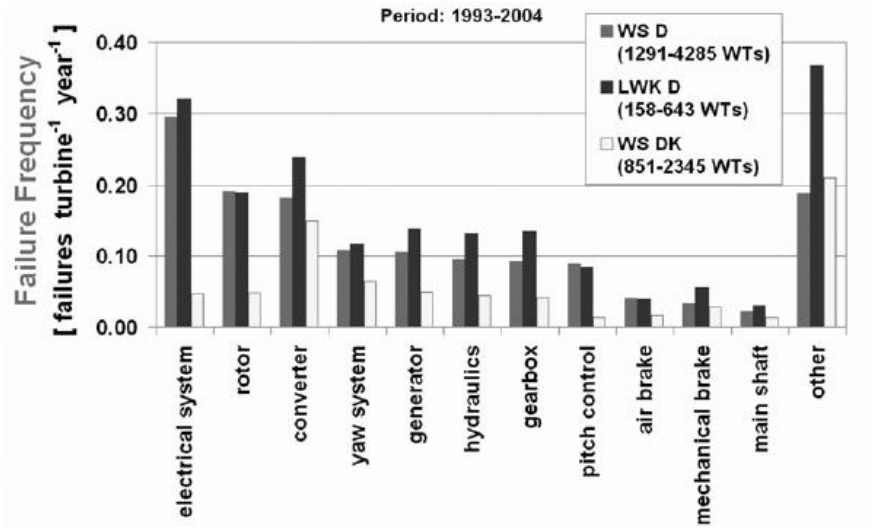

Figure 4.2 Reliability data on repairable onshore WTs

Source: Spinato et al. (2009)

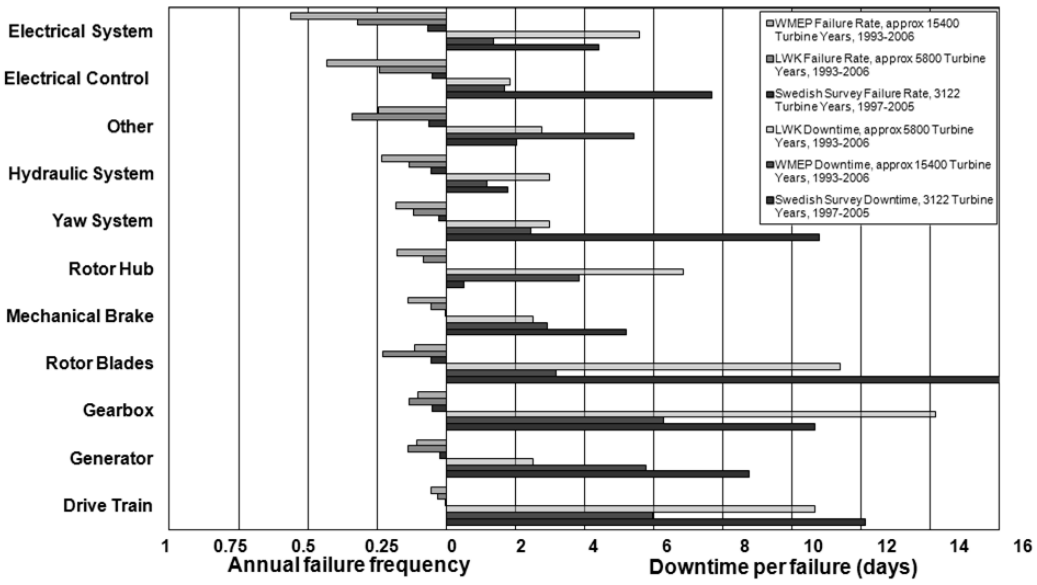

Figure 4.3 Onshore WT failure rates & downtimes, 3 surveys over 13 years

Source: Tavner et al. (2012)*;* based on Tavner et.al (2010)

4.4.4 *Petrochemical Industry Database-OREDA*

Since 1983 OREDA has collected reliability data from a wide range of equipment used in oil & gas exploration/production based on the experience of oil companies operating in the North and the Adriatic Seas (OREDA 1984-2009).

Most offshore and sub-sea equipment are covered by this database. Failure rate data is presented in a time window of 2-4 years operation of offshore equipment, for subsea equipment failures are collected on a total lifetime basis. The failure rates relate to generic sub-assemblies, which have physical boundary-defined parts with detailed statistical measures of the sample population. The information collected is from equipment performing under normal operating conditions. The source data is stored in a computer database, access to which is only available to participating OREDA oil companies.

4.4.5 *Generic Reliability Databases*

MIL-HDBK-217F

The handbook MIL-HDBK-217F (1991) was prepared under contract to the U.S. Department of Defense. It comprises failure rate estimates for components in electronic systems, failure rate data on both commercial and military electrical components, including resistors, capacitors, inductors, transformers & integrated circuits, suitable for use in reliability analyses.

Rausand and Hoyland (2004) observed that, compared to the OREDA (1984-2009) handbooks, the MIL-HDBK 217F failure rates are not field failure data; they are based on laboratory tests under controlled environmental stresses, e.g., temperature, humidity and voltage. The failure rates do not account for external stresses or common-cause failures.

Tables with adjustment factors for the data of MIL-HDBK-217F appeared in RIAC&DACS (2005) to accommodate uncertainties.

NPRD-95; NPRD 2011

The NPRD-95 (1995) provides reliability data, failure rate data, on non-electronics: mechanical, electromechanical and discrete electronic parts and assemblies of 25,000 parts of military and commercial applications.

The data has been updated as NPRD-2011 and gives a wider range of components (NPRD-2011). NPRD-2011 discloses summary and detailed data sorted by part type, quality level, environment and data source. The data is compiled from field experience of military, commercial and industrial applications and focuses on systems, sub-systems, assemblies, sub-assemblies and components not included in MIL-HDBK-217F (1991). The data is as follows: part descriptions, quality level, application environments, point estimates of failure rate, data sources, number of failures, total operating hours, miles, or cycles and detailed part characteristics. MIL-HDBK-217F, NPRD-95 and NPRD-2011 are complementary to each other.

4.4.6 *Integrated Reliability Database-IEEE Gold Book*

An extensive AIEE survey conducted a group led by Dickson in the 1960s was followed by several IEEE reliability surveys between 1973 and 1996 (IEEE 1998). The survey provides data on commercial power distribution systems and included generators, power transformers, rectifier transformers, circuit breakers, disconnect switches, cables, cable joints and terminators and electrical utility power supplies according IEEE (1998). The historical data provided can be used to compare alternative electrical technologies.

4.5 Predicted Sub-assembly Failure Rates in Tidal Environment

The main question mark over the surrogate data approach is the relevance of these data to the TSD environment, particularly related to the environments from which the surrogate data came, as summarized in Table 4.2.

Table 4.2 Environments of Surrogate Data Sources Used in the Model

Surrogate Data Source	Naval, Unsheltered Severe Environment NU	Naval, Sheltered Normal Environment NS	Ground, Fixed Severe Environment GF
LWK ,WMEP	-	-	X
OREDA	X	X	X
NPRD-95	X	X	X
MIL-HDBK217F	X	X	X

Some treatment is needed in applying these surrogate data to the marine environment, treatment in the form of environmental adjustment factors. Three different operational environments in which tidal devices were to be placed are presented in Table 4.2:

- GF-ground, fixed: severe environment;
- NS-naval, sheltered: normal environment;
- NU-naval, unsheltered: severe environment.

In general, WTs and electrical equipment are in the GF environment, whereas TSDs are in the NS or NU environment. Tidal environment sub-assembly failure rates could be predicted using surrogate data by applying a GF to NU or NS adjustment factor.

Environmental Adjustment Factors for electrical and electronic components from MIL-HDBK 217F (1991) are tabulated in RIAC&DAC (2005). The data had to be modified for this study, which considers component failure rates, λ_i, because MIL-HDBK-217F multipliers were intended for MTBFs. The modified data are presented in Table 4.3 and environmental definitions are described in references MIL-HDBK 217F (1991) and SD-18 (2006).

Table 4.3 Environmental Adjustment Factors, π_{Ei}

			To That Environment*				
	MIL-HDBK-217F (1991)		GB	GF	GM	NS	NU
		SD-18 (2006)	Protected	-	-	Normal	Severe
From This Environment	GB	Protected	-	2.0	5.0	3.3	10.0
	GF	-	0.5	-	2.5	1.7	3.3
	GM	-	0.2	0.4	-	0.7	1.4
	NS	Normal	0.3	0.6	1.4	-	2.0
	NU	Severe	0.1	0.3	0.6	0.5	-

*Environments defined in nomenclature

These factors cannot be used for mechanical sub-assemblies: the failure causes for their components differ (shock overload; deterioration of strength). For electrical assemblies, failures are due to overstress and production defects. The π_{Ei} for mechanical components in this method is equal to 1, multiplied by the highest surrogate failure rate, closely approximating the tidal environment: see Table 4.4. Future mechanical loading studies may yield a more precise adjustment factor.

Applying appropriate environmental adjustment factors will reduce errors in further predictions. The author did not find a previously defined rationale for this approach, so proposes two Failure Rate Estimates, FRE_{con} and FRE_{env}, see Table 4.4.

In the particular case of OREDA data, where the tidal environment differs from the oil & gas environment, the author has used OREDA failure rates at the upper limit of the 90% confidence interval to ensure the most conservative estimate.

Table 4.4 Failure Rate Estimates

Failure Rate Estimate	Method using surrogate data	Limitations
Conservative $\boldsymbol{FRE_{con}}$	No environmental adjustment applied. $\lambda_i^{(b)} = \lambda_{Gi\ max}$	Represents a conservative failure rate for a branch, *b*, but neglects environmental conditions.
Environmentally Adjusted Conservative $\boldsymbol{FRE_{env}}$	Multiplied by an environmental factor, π_{Ei}. $\lambda_i^{(b)} = \lambda_{Gi\_max}\ \pi_{Ei}$ For mechanical components: $\pi_{Ei} = 1$ For electrical/electronic components: π_{Ei} as defined in Table 4.3.	Represents a conservative failure rate for a branch, *b*, but takes account of environment.

4.6 Reliability Prediction Model Calculations

In the methodology of this Thesis, individual sub-assembly failure rates were combined into a total failure rate for two alternative operating constraints, as follows:

- Predicted total failure rates based on the assumption of a non-repairable series assembly of independent sub-assemblies operating up to full 100% of device power output for examples TSD1 to TSD5 for one calendar year: see Chapter 5.
- As above, but operating up to full 100% of device power output for TSD1 to TSD5, or 50% of device power output for TSD2 and TSD4, which incorporate twin-axis turbines, thus having implicit redundancy: see also Chapter 5.

To evaluate the total device reliability the PCRPT was used whereby the FBD was simplified to a series model, reducing any redundant sub-assemblies to an

equivalent single branch, *b*, then using sub-assembly failure rates to calculate the predicted failure rate for the i^{th} generic unit according to Tables 4.3-4.4:

either

$$\lambda_i^{(b)} = \lambda_{Gi\_max} \ (Failures/year)$$

Equation 4.7

or

$$\lambda_i^{(b)} = \lambda_{Gi\_max}\pi_{Ei} \ (Failures/year)$$

Equation 4.8

The predicted device failure rate models are as follows:

- Series network: For a TSD with all sub-assemblies in series, the device will fail if any one of the sub-assemblies fails. For a series reliability model of independent sub-assemblies with constant failure rates, the reliability model forms and total failure rate are expressed as:

$$\lambda_{tot\_Ns} = \sum_{b=1}^{N_s} \sum_{i=1}^{N_b} \lambda_i^{(b)}$$

Equation 4.9

- Series parallel network**:** For a device with N_s sub-assemblies in series and N_p assemblies with two identical branches in parallel with constant failure rates, for example TSDs 2 & 4 shown in Appendix 4, with twin-axis drive trains up to 50% power production (DT), an uninterrupted electrical assembly (B), a redundant ancillary assembly (XA), and twin-axis nacelle structures (U), and so on for other similarly redundant sub-assemblies with two identical branches in parallel (see Table 4.1), the reliability model forms and total failure rate are expressed as:

$$\lambda_{tot} = \lambda_{tot\_Ns} + \left(\frac{2}{3}\right)\lambda_{tot\_Np}$$

Equation 4.10

Where:

$$\lambda_{tot\_Np} = (\lambda_{DT} + \lambda_B + \lambda_{XA} + \lambda_{U\ +\ldots})$$

Equation 4.11

then:

$$\lambda_{tot} = \sum_{b=1}^{N_s} \sum_{i=1}^{N_b} \lambda_i^{(b)} + \frac{2}{3} (\lambda_{DT} + \lambda_B + \lambda_{XA} + \lambda_{U\ +\ldots})$$

Equation 4.12

Where:

$$\lambda_{DT} = \sum_{i=1}^{N_{DT}} \lambda_i^{(DT)}$$

Equation 4.13

is the total failure rate of a drive train (DT), equal to the sum of the failure rates of the single branch DT sub-assemblies

$$\lambda_B = \sum_{i=1}^{N_B} \lambda_i^{(B)}$$

Equation 4.14

is the total failure rate of an uninterrupted electrical assembly (B), single branch twin-axis assembly

$$\lambda_{XA} = \sum_{i=1}^{N_{XA}} \lambda_i^{(XA)}$$

Equation 4.15

is the total failure rate of an ancillary assembly (XA), single branch of twin-axis redundant assembly

$$\lambda_U = \sum_{i=1}^{N_U} \lambda_i^{(U)}$$

Equation 4.16

is the failure rate of a single branch twin-axis nacelle or support structure (U).

Therefore, the device reliability survivor function *R(t)* can be calculated as follows:

For series network:

$$R(t) = e^{-\lambda_{tot\_Ns}\, t}$$

Equation 4.17

For series/parallel network:

$$R(t) = e^{-\lambda_{tot}\, t}$$

Equation 4.18

The model uses a standard formula for assemblies with twin-axis redundant drive train branches to represent a single reliability parameter curve. The method can be extended to more complex assemblies using standard reliability equations published in RIAC & DACS (2005).

4.7 Summary

Judging from this limited data and early stage of device designs, the only valid reliability assessment method currently available is Reliability Modelling and Prediction, as described in this Thesis. Owing to intellectual property rights issues, the author is unable to obtain all the detailed TSD design information needed to execute the classical probabilistic FMEA or FTA reliability models. The same limitation applies to the data needed to carry out a Bayesian model. These methods are summarised in Appendix 3.

Due to the absence of historical information for tidal turbines at the present time, surrogate data sources with generic failure data adjusted to the tidal environment have been identified and a PSD has been established which will be used for reliability modelling and prediction comparison in Chapter 5 and Appendix 4.

5. Methodology Application & Reliability Comparison

5.1 Five Generic TSD Models

This chapter applies the methodology in Chapter 4 to five generic TSDs, the most predominant ones, shown in Figure 5.1; they are different types of offshore, horizontal-axis tidal turbines of generic manufacture rated from 1.0-1.2 MW. Historical reliability data from similarly-rated WTs and other relevant marine devices and sub-assemblies were used to compile the reliability for these generic TSDs; see Appendix 4, which will then be compared.

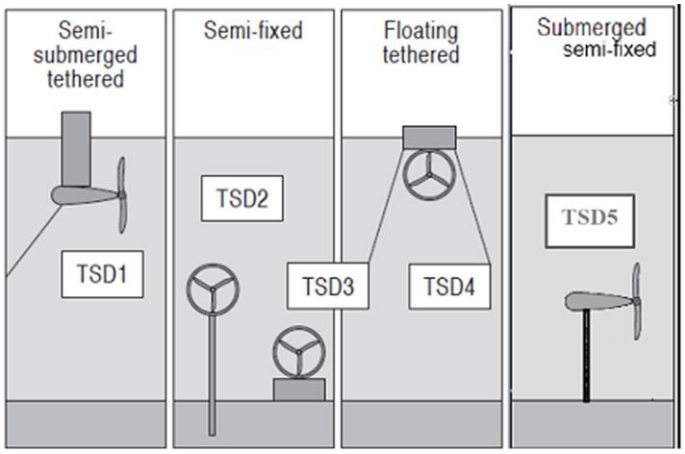

Figure 5.1 Horizontal-axis TSDs chosen for reliability comparison

Source: Adapted from Mackie (2008b)

The five TSDs 1-5, shown in Figure 5.1, were chosen as they have been recently considered for commercialization, as discussed in Chapter 2, with the prototype examples described in Chapter 3. These TSD types were chosen to emphasise the differences between sea-bed fixing options and the effects of these options on design, installation and maintenance:

- TSD1: moored, floating tethered, semi-submerged deep-water application, single-axis turbine, fixed pitch blades, induction generator, rated power 1.2MW;
- TSD2: sea-bed pile-mounted, shallow-water application, twin-axis turbines, variable pitch blades, induction generators, rated power 2 x 0.6MW = 1.2MW;
- TSD3: sea-bed bottom-mounted, gravity base, shallow or deep water application, single-axis ducted turbine, fixed pitch blades, permanent magnet generator, rated power 1.0MW;
- TSD4: moored, floating tethered, deep-water application, twin-axis turbines, fixed pitch blades, permanent magnet generators, rated power 2 x 0.6MW = 1.2MW;
- TSD5: submerged, semi-fixed pile-mounted, gravity base, shallow or deep water application, single-axis rotated turbine, fixed pitch blades, permanent magnet generator, rated power 1.0 MW.

The choice of the five models assumed:

- The devices are all new technology and in the prototype stage;
- The devices are immersed in the tidal environment during one year of service without maintenance;
- The sub-assembly times-to-failure are exponentially distributed, that is, failure rates are the result of random failures and the system operates in a single environment;
- The acceptable level of a device reliability is 0.80 or above, an arbitrary threshold suggested by RIAC (2010), in order to satisfy the TSD mission.

The boundaries of the study for each device are defined in Table 5.1, assuming the time used for the reliability survivor function $R(t)$, t = 1 calendar year.

Table 5.1 TSD1-5 Reliability Assessment Study Boundaries 1 year in Service

TSD1; TSD3; TSD5	TSD2; TSD 4
System requirements for 100% output power	Two of two drive trains are required for 50-100% power output One of two drive trains are required for 0-50% power output
Individual failure degrades performance from 100% to 0%; therefore any breakdowns of sub-system or components will cause the whole system to fail	Individual failures degrade performance from 100% to 0%; therefore any breakdowns of sub-system or components will cause the system to fail
For the purposes of this study the system is considered non-repairable for the operational period, although in practice the system could be repaired in-service but probably at specific shutdown periods when access to the tidal turbine is possible.	For the purposes of this study, the system is considered non-repairable for the operational period, although in practice the system could be repaired in-service but probably at specific shutdown periods when access to the tidal turbine is possible.

Based on the above assumptions, graphical models for TSDs1-5 were derived, then from these the appropriate mathematical models were developed.

The principles of TSD1-5 models are based on the design series available at the time of writing. Due to the novelty of the technology, developers are constantly updating their device designs; therefore, these reliability models are generic and only applicable to the system layout identified here and not to the absolute design. It should be noted that the scale of some of these devices such as TSD4 has been changed in the past few years and the design features may have been upgraded to

satisfy the demands of marine environments for energy efficiency and cost reduction. For example, Scotrenewables Tidal Power Ltd has tested the SR250 with different power drive train sub-assemblies compared to previous design SRTT with 1.2MW, as described by Francis and Hamilton (2007).

To formulate RBDs, a taxonomy of critical sub-assemblies which directly contribute to power production was derived.

The sub-assemblies of each device are arranged in Tables 13.2-13.6, Appendix 4, using a classification system, shown in Table 3.1, devised by VGB PowerTech (2007) for wind turbines.

Mathematical reliability models were then populated with surrogate failure rate data, adjusted for the tidal environment. The purpose of the mathematical model was to combine sub-assembly failure rates into a total predicted equipment failure rate, $\lambda_{tot,}$ as a first step to the prediction of device reliability. The author's prediction models proposed in Chapter 4 were then used to assess failures for devices, to identify generic reliability weaknesses and to indicate reliable architectures by comparison between the five generic TSDs.

Conditions for adjusting non-marine surrogate data to the tidal environment were applied, based on Tables 4.3-4.4. Two Failure Rate Estimates methods, shown in Table 4.4, were used for comparison between results adjusted and unadjusted to tidal environments.

The study used an upper bound failure rate λ_{Gi_max} for each sub-assembly, giving a conservative prediction for a novel technology. The failure rates were calculated using Equations 4.7 to 4.18. Device reliability was analysed as a series/parallel sub-assemblies network configuration, or decomposed to a series sub-assemblies

network, as shown in Chapter 4. The failure rate results are tabulated in Tables 13.2-13.6, Appendix 4, alongside the structure of the turbine.

The total failure rates, $\lambda_{tot,}$ and predicted survivor functions, *R(t),* were calculated based on the assumption of a non-repairable system, of N_s independent sub-assemblies, for 1 calendar year, with a power output up to 100% for all TSDs1 to 5 and up to 50%, for twin-axis TSDs 2 and 4.

For brevity, only the graphical models for TSD1 are presented in this chapter in Figures 5.2-5.3. The detailed device models for TSD1-5 will be presented in Appendix 4.

5.2 Development of TSD1 Reliability Model, Example

5.2.1 *TSD1 Reliability Model: Graphical*

For this example, a schematic diagram and an FBD have been developed for TSD1, following VGB PowerTech (2007), and presented in Figure 5.2-5.3.

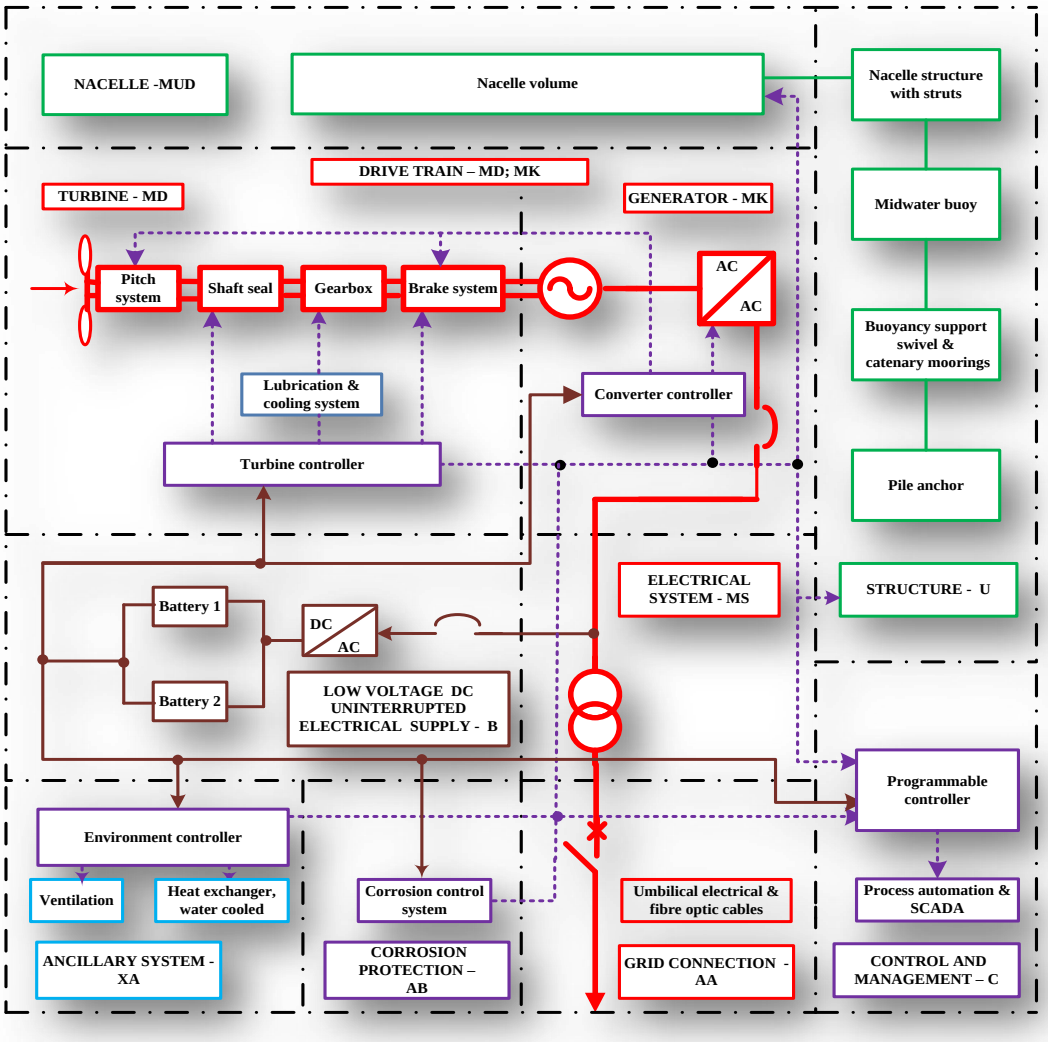

Figure 5.2 TSD1 schematic diagram

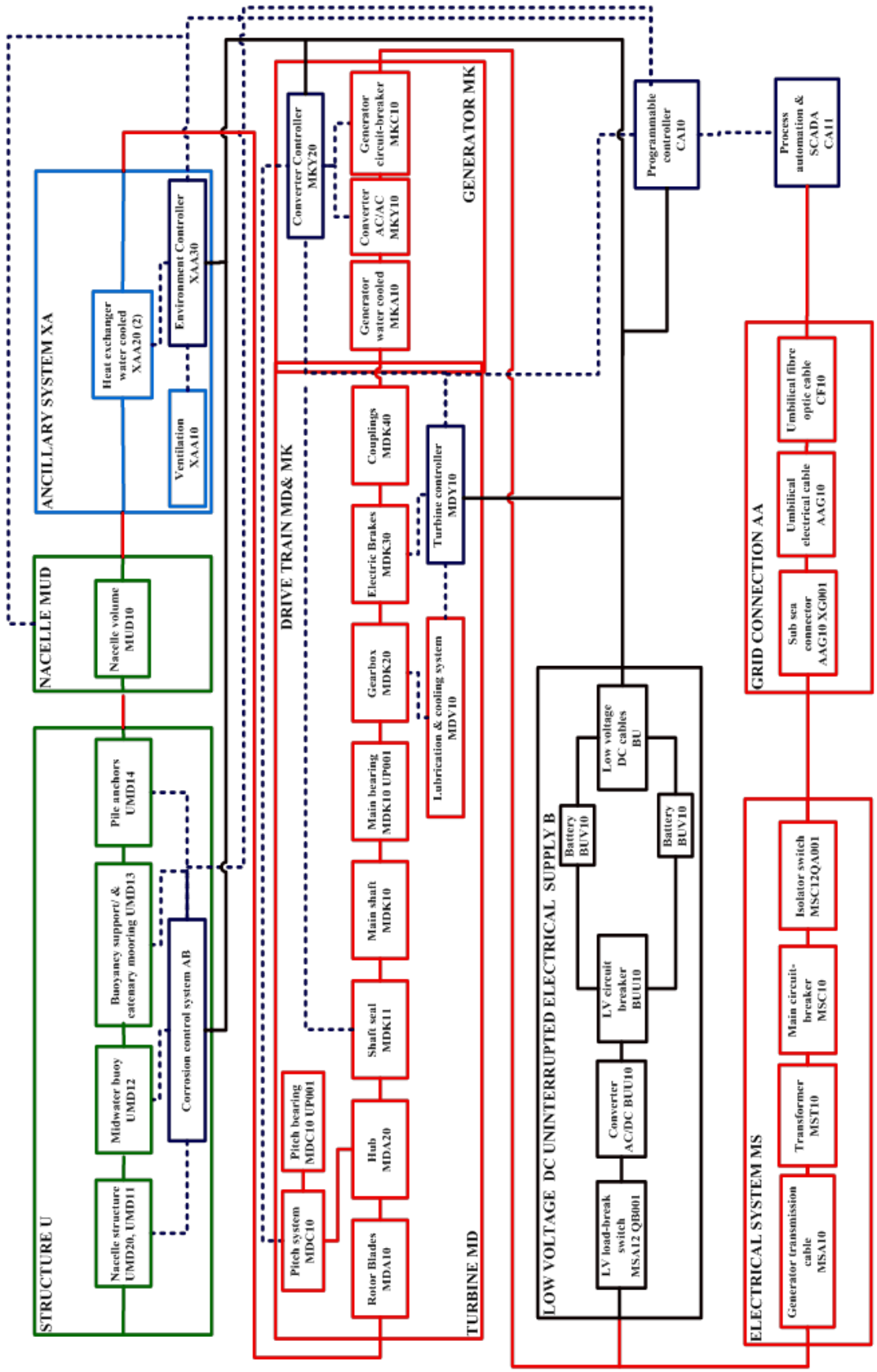

Figure 5.3 TSD1 FBD (Functional Block Diagram) or RBD1

For brevity, only a single Drive Train (DT) branch with sub-assemblies coded MD&MK, of the total TSD1 reliability model is detailed in this section, Figure 5.4. This branch was analysed as a series sub-assemblies network model; if one sub-assembly fails the entire branch will fail.

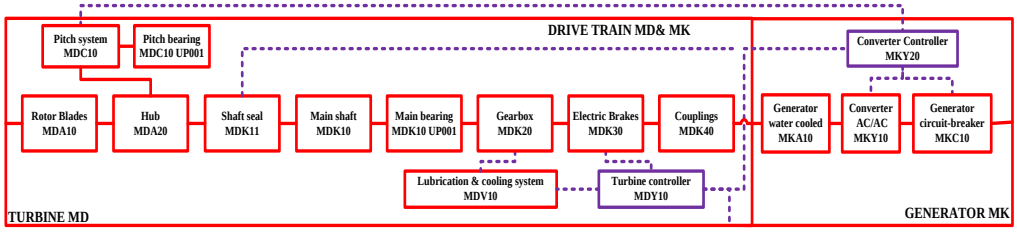

Figure 5.4 FBD for Drive Train of TSD1, extracted from Figure 5.3

5.2.2 *TSD1 Reliability Model: Mathematical*

The DT mathematical model based on FBD with critical sub-assemblies is developed and analysed in Table 5.2. The failure rates calculation of the critical sub-assemblies contributing directly to DT power production are tabulated here; in addition, the whole structure and reliability prediction calculations are shown for TSD1 in Appendix 4, Table 13.2.

Table 5.2 TSD1 DT Element Reliability Model, from Equations 4.4-4.6

Reliability characteristics for:				Surrogate failure rates (Failures/year)		Failure Rate Estimate (Failures/year)		
b	*i*	Code: MD& MK	Sub-assemblies	Data Source	λ_{Gi_min} - λ_{Gi_max}	FRE_{con} λ_{i_FREcon}	π_{Ei}	FRE_{env} λ_{i_FREenv}
Drive train (DT)	1	MDA10	Rotor blades, pitch electronics	WTs: Hahn et al. (2007) Spinato et al. (2009) Tavner et al. (2010; 2012)	0.115 - 0.230	0.230	3.3	0.759
	2-4	MDA20, MDC10, MDC10P 001	Hub, pitch system, pitch bearing	WTs: Hahn et al. (2007) Spinato et al. (2009) Tavner et al. (2010)	0.083 - 0.177	0.177	1.0	0.177
	5-7	MDK10, MDK10 UP001, MDK40	Main shaft, bearing, couplings	WTs: Hahn et al. (2007) Spinato et al. (2009) Tavner et al. (2010)	0.031 - 0.055	0.055	1.0	0.055
	8	MDK11	Shaft seal	NRPD-95 (1995)	0.061	0.061	1.0	0.061
	9	MDK20, MDV10	Gearbox, lubrication & cooling	WTs: Hahn et al. (2007) Spinato et al. (2009) Tavner et al. (2010)	0.101 - 0.134	0.134	1.0	0.134
	10	MDK30	Electric brakes	NRPD-95 (1995)	0.031	0.031	1.0	0.031
	11	MKA10	Generator water cooled	WTs: Hahn et al. (2007) Spinato et al. (2009) Tavner et al. (2010)	0.106 - 0.139	0.139	1.7	0.236
	12-13	MKY10, MKY11	Converter, AC/AC; converter controller	WTs: Hahn et al. (2007) Spinato et al. (2009) Tavner et al. (2010)	0.239 - 0.430	0.430	1.7	0.731
	14	MKC10	Generator circuit-breaker	MIL-HDBK-217F (1991)	0.020 - 0.175	0.175	1.0	0.175
Drive train estimated total failure rate, λ_{DT}(Failures/year)						*1.433*		*2.360*

5.2.3 *TSD1 Predicted Failure Rates: Calculation*

Drive train

For the single DT with N_{tot} = 14 independent sub-assemblies in the series network and up to 100% power output, the reliability mathematical model Equation 4.10 is applied. Therefore, the total DT sub-assemblies failure rate estimates are:

$$\lambda_{DT\_FREconv} = \sum_{i=1}^{14} \lambda_{i\_FREconv} = 1.433 \left(\frac{Failures}{year}\right) \quad \text{Equation 5.1}$$

$$\lambda_{DT\_FREenv} = \sum_{i=1}^{14} \lambda_{i\_FREenv} = 2.360 \left(\frac{Failures}{year}\right) \quad \text{Equation 5.2}$$

where, the total predicted failure rate, λ_{DT} of the single DT is equal to the sum of the individual sub-assembly failure rates of DT, adjusted or not to the tidal environment, as appropriate, according to Tables 4.4-4.5.

5.2.4 *TSD1 Total Device*

For the total TSD1 with N_{tot} = 45, Table 13.2, Appendix 4, independent sub-assemblies the reliability calculation is similar to the DT model. The differences are in the number of sub-assemblies and their connection network. Next, the PCRPT is applied to the total device structure to estimate the average failures per year of the total device sub-assemblies and, further, to predict the reliability survivor function after 1 year in service.

For the total TSD1, with up to 100% power output, assuming that all sub-assemblies are in a series network, with those sub-assemblies such as batteries and redundant auxiliaries decomposed into individual series network blocks, the total predicted failure rate ($\lambda_{tot100\%}$) for the device is:

- Conservative Failure Rate Estimate FRE_{con}, the sum of all individual sub-assembly failure rates, or
- Environmentally Adjusted Failure Rate Estimate FRE_{env}, the sum of failure rates of sub-assemblies within sub-systems

The choice of approach depends on the method of comparison: either total device reliability by number of sub-assemblies or total device reliability by sub-system comparison. For the total device reliability, the author will present FRE_{env} in this section. Reliability characteristics from the Appendix 4 Table 13.2 are:

The total device sub-assemblies failure rate is:

$$\lambda_{tot100\%\_Ns\_FREconv} = \sum_{i=1}^{42} \lambda_{i\_FREconv} = 4.345 \left(\frac{Failures}{year}\right)$$

Equation 5.3

$$\lambda_{tot100\%\_Ns\_FREenv} = \sum_{i=1}^{42} \lambda_{i\_FREenv} = 5.379 \left(\frac{Failures}{year}\right)$$

Equation 5.4

TSD1 reliability survivor function R*(t)* after 1 year service:

$$R(1year)_{100\%\_Ns\_FREconv} = e^{-\lambda_{i\_FREconv}\, t} = e^{-4.345\ x\ 1} = 1.30\ \%$$

Equation 5.5

$$R(1year)_{100\%\_FREenv} = e^{-\lambda_{i\_FREenv}\, t} = e^{-5.379\ x\ 1} = 0.46\ \%$$

Equation 5.6

5.3 Reliability Comparison: Predicted Survivor Functions

The previous section has described the way in which reliability prediction models were developed for five different types of horizontal-axis TSDs. Having all reliability characteristics available for the assessment of TSD1-5 by comparison, the

data can be summarised, analysed and device reliability comparisons made by several methods:

- Total annual predicted failure rates;
- Total annual predicted survivor functions;
- Reliability comparison of TSD by sub-assemblies and sub-systems;
- Reliability comparisons with other renewable energy extraction devices, for example wind and wave.

The results of the predicted reliability characteristics of TSD1 compared to the other four devices TSD2-5 are summarised in Table 5.3 and graphically presented in Figures 5.5-5.6 below. Since the publication of Delorm et al (2011a, b), the author has improved the FBD of TSD4, reducing the number of sub-assemblies, and therefore the results for this device have been updated in these tables.

Table 5.3 TSD1-5 Reliability Characteristics by Comparison

Total failure rates, λ_{tot} (Failures/unit/year)							
	TSD 3, 100%	*TSD 5, 100%*	*TSD 2, 50%*	*TSD 4, 50%*	*TSD 1, 100%*	*TSD 4, 100%*	*TSD 2, 100%*
FREcon, $\lambda_{\tau o \tau}$	*3.459*	*4.104*	*3.816*	*4.068*	*4.345*	*5.322*	*6.400*
FREenv, $\lambda_{\tau o \tau}$	*4.160*	*4.172*	*4.543*	*4.552*	*5.379*	*6.623*	*8.642*
Sub-assemblies, N_{tot}	*27*	*37*	*40*	*43*	*42*	*56*	*58*

Reliabilty survivor function, R(1yr)%							
	TSD 3, 100%	*TSD 5, 100%*	*TSD 2, 50%*	*TSD 4, 50%*	*TSD 1, 100%*	*TSD 4, 100%*	*TSD 2, 100%*
FREcon, R(1 yr)	*3.15%*	*1.65%*	*2.20%*	*1.71%*	*1.30%*	*0.49%*	*0.17%*
FREenv, R(1 yr)	*1.56%*	*1.54%*	*1.06%*	*1.05%*	*0.46%*	*0.13%*	*0.02%*
Sub-assemblies, N_{tot}	*27*	*37*	*40*	*43*	*42*	*56*	*58*

TSDs 1, 3 & 5 are single turbines with sub-assemblies in series and 100% power output; TSDs 2 & 4 (100%) are twin turbines with 100% output and all critical sub-

assemblies in series relationship; TSDs 2 & 4 (50%) are twin turbines, assuming one of two is operational, which reduces N_{tot} and power output to 50% (see Table 5.1).

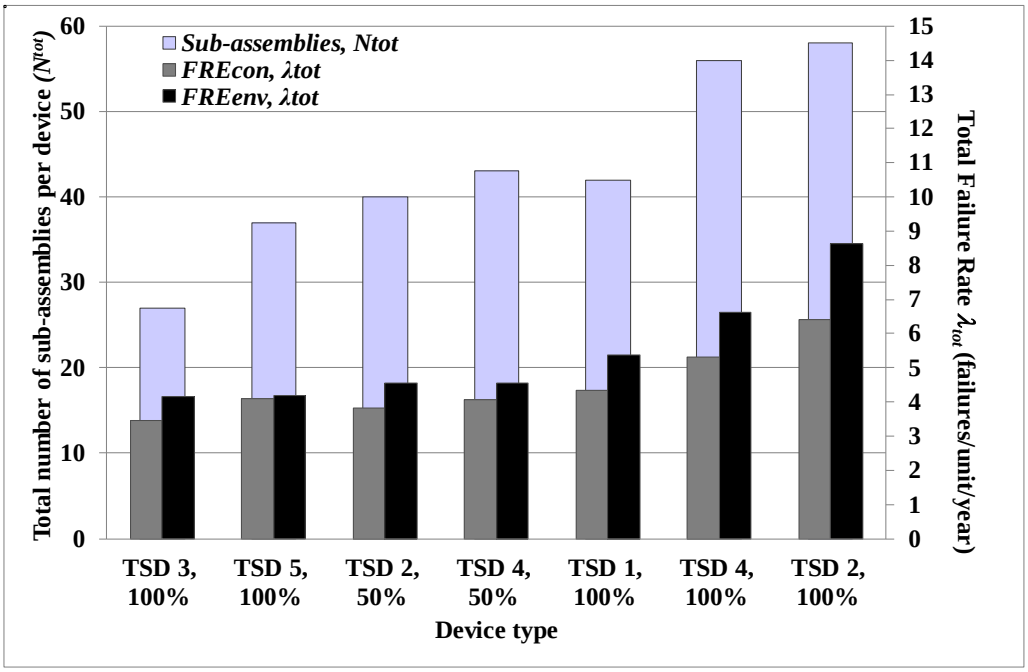

Figure 5.5 Predicted failure rates and number of sub-assemblies for TSD1-5

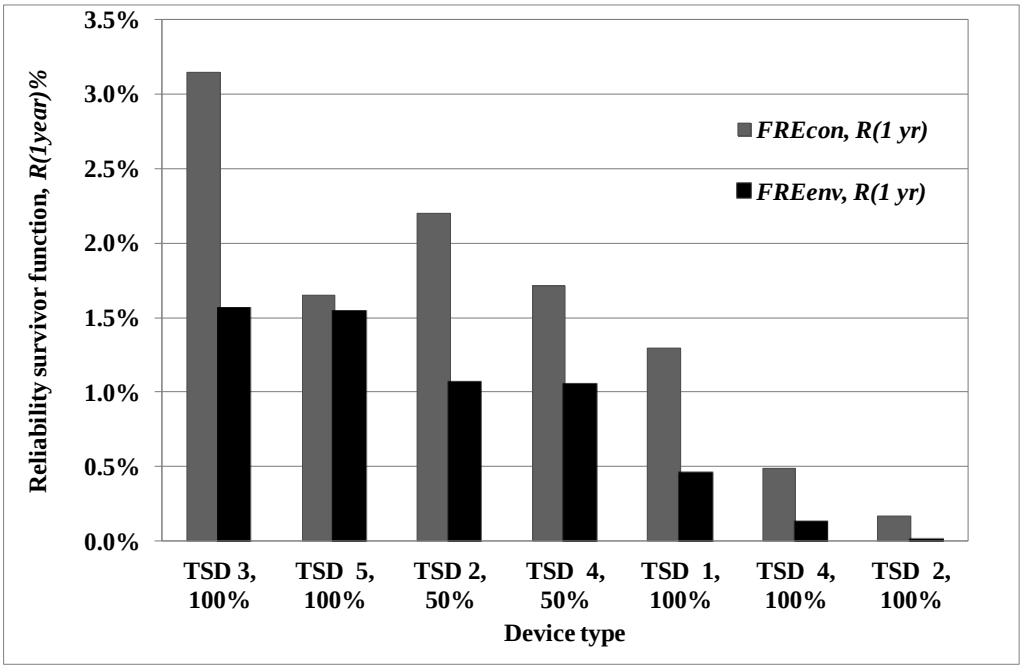

Figure 5.6 Predicted survivor functions for TSD1-5 after 1 year of operation.

The methodology obtained predicted total device failure rates λ_{tot} (failures/device/year) after one year in service, and reached the following conclusions:

- Predicted TSD failure rates increase with increasing device complexity, as expected;
- TSD3, with a sea-bed bottom-mounted, ducted single-axis turbine, offshore/onshore arrangements, has the lowest failure rate because of its simple technology and low N_{tot};
- N_{tot} increases for twin-axis TSDs 2 & 4 and therefore so do failure rates;
- TSDs 2 & 4 show improved failure rates when only 50% power is required because of the implicit redundancy of the twin-axis technology, and the reduced N_{tot} ;
- TSD2, when operating at 50% power, has a failure rate almost as low as TSD3, because it is utilising the sub-assemblies of only one drive train;
- TSD2, when operating at 100% power has a higher predicted failure rate than TSD4, operating at 100% power, because of the choice of the design layout and the sub-assemblies specifications, which affect the total failure rate and the number of sub-assemblies increase;
- The necessary significant failure rate improvements for tidal devices are possible.

The predictions are that a sea-bed bottom-mounted, ducted single-axis turbine such as TSD3 with the generator offshore and the remainder onshore (transformer, ancillary and onshore control sub-systems) would have the lowest failure rate because of its simple technology. Complexity increases for TSDs with twin-axis turbines with all sub-systems offshore, therefore so do failure rates.

5.4 Summary

The reliability results for the five devices summarised in Figures 5.5-5.6, show failure-and-survivor rate comparison between models in order to assess their architectures. In particular, Figure 5.5 shows that TSDs with more sub-assemblies have a higher failure rate. The twin-axis devices TSDs 2 & 4, which also have some intrinsic redundancy, the effect of which is visible in their higher failure rates when 100% power is expected, produce lower failure rates when only 50% power is required. However, at 50% of power, there is a risk that the loads imposed by single turbine operation might be damaging to the overall structure. In reality, therefore, these devices might not be suitable when only one of two turbines operates at up to 50% of total power.

The PCRPT was applied to calculate the average number of failures per year. It was assumed that assembly-redundant sub-assemblies are individual blocks. It is acknowledged that this approach can lead to error, which according to Faraci (2006), could be as much as 20% of the resultant failure rate; however, this will lead to a conservative but acceptable result.

Nevertheless, RMP and PSD using PCRPT have been shown to be an appropriate methodology for predicting TSD reliability and for making comparisons. However, the predictions are only as good as the model constructed and the data used: thus, this methodology is well suited to early stages of TSD design. As the design evolves, this method would be equally applicable for comparison of TSDs when more precise design and reliability data become available.

6. Model Validation & Discussion

6.1 Introduction

The following Chapter will set out validations of the models proposed and discuss their significance. Validation of these speculative reliability models for TSD under design or in the prototype stage is exceptionally difficult, in that although their structure is reasonably well-defined, the data concerning their sub-assembly and component failures is drawn from disparate sources and different environments. However, a degree of validation can be achieved by consideration of the models themselves and by comparison of the results with different forms of analysis. This will be done by considering the following:

- The TSD sub-assembly survivor and failure rates and the identification of least reliable sub-assemblies;
- Comparison of the predicted main bearing and blade sub-assembly failure rates with other, design-based, predictions;
- Interpretation of TSD predicted sub-assembly failure rates;
- Comparison with reliability of other renewable systems:
    - Tidal vs wind turbines;
    - Tidal vs wave devices;
- Statistical significance of the results.

6.2 Validation by Sub-assembly & Sub-system Analysis

6.2.1 *Analysis of Reliability Models*

One aim of this Thesis was to determine if any cost-effective modelled reliability methodologies can be applied and used for the reliability assessment of different TSD designs at the conceptual stage, comparing these designs in order to reduce reliability uncertainties, and also to facilitate the development of these devices as uninterruptible power suppliers.

The uniqueness of the methodology developed by the author consists in the use of the following models:

- Graphical models with robust parts classification of critical sub-assemblies of each generic version of TSDs based on VGB PowerTech (2007): see Chapter 4.4-4.5, Appendix 4;
- Mathematical models with a combination of PSD adjusted to the tidal environment: see Chapter 4.6, Appendix 4.

Concern over the use of these sources has been addressed by the use of environmental adjustment factors: see Table 4.4 and Chapter 4.5.

6.2.2 *Acceptable Survivor Rate*

The basic question "What is the highest acceptable failure rate for any single sub-assembly?" should be taken into consideration in order to make a device commercially acceptable. Below is a generic prediction of the acceptable reliability characteristics, excluding the effect of the tidal environment.

Based on the assumptions in Chapter 5.1, the acceptable level of a device reliability survivor rate is:

$$R(t)_{TSD} = \prod_{i=1}^{Ntot} R_i(t) \geq 0.80$$

Equation 6.1

Assuming all sub-assemblies have reliability characteristics: $R_i(t)$ = A (the minimum reliability), then the minimum device reliability will be:

$$R(t)_{TSD} \geq A^{Ntot}$$

Equation 6.2

where N_{tot} = total number of the sub-assemblies.

Therefore, an acceptable level of one generic sub-assembly reliability survivor rate can be calculated, and the result must be at least:

$$R(t)_{TSDi} = R_i(t)_{TSD}{}^{1/Ntot} = A \geq 0.8^{(1/Ntot)}$$

Equation 6.3

For example, a TSD with N_{tot} = 27, the reliability of any sub-assembly should be:

$$R(t)_{TSDi} \geq 0.80^{1/27} \geq 0.99$$

Equation 6.4

which brings the sub-assembly failure rate to a very low number to make the device commercially acceptable.

$$\lambda_{i\_FREenv} \leq 0.01 \ (Failures/year)$$

Equation 6.5

Therefore, ideally, the sub-assembly failure rates should be within this range in order to assure that the device will be reliable for a specified working time.

6.2.3 *Predicted Failure Rates*

This section presents analysis of TSD sub-assemblies reliability and predicted failure rates, based on the surrogate failure rate data, adjusted to the marine environment, that were presented in earlier sections under the model $FRE_{env,}$ Table 4.4.

Figures 6.1-6.5 present charts with generic sub-assemblies illustrating the differences in predicted failure rates. These charts are not intended to illustrate the effect of redundancy; they identify sub-assemblies with the highest number of failures per year. By such means, engineers could review their designs at a preliminary stage, predicting maintenance needs and considering further reliability analyses to reduce final cost.

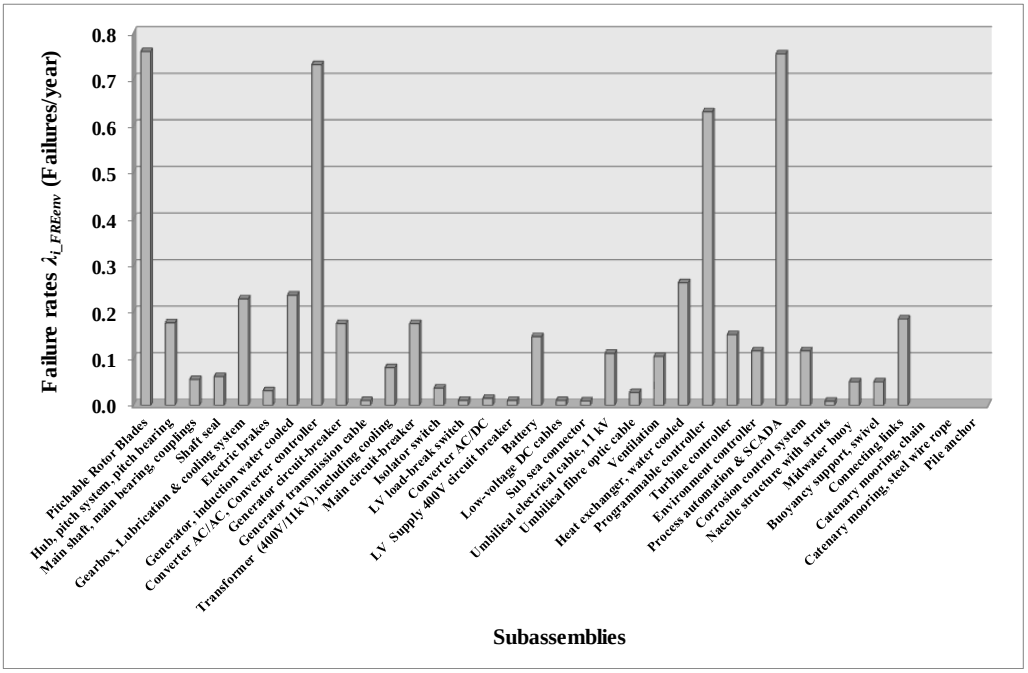

Figure 6.1 TSD1 adjusted single generic sub-assembly failure rates, λ_{i_FREenv}

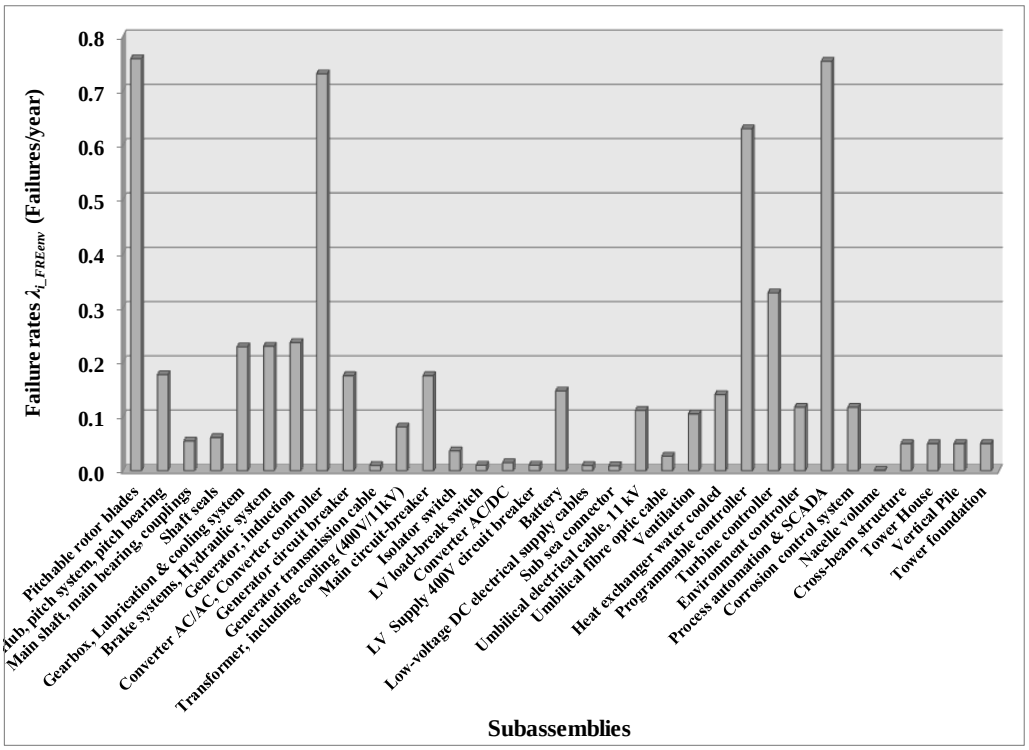

Figure 6.2 TSD2 adjusted single generic sub-assembly failure rates, λ_{i_FREenv}

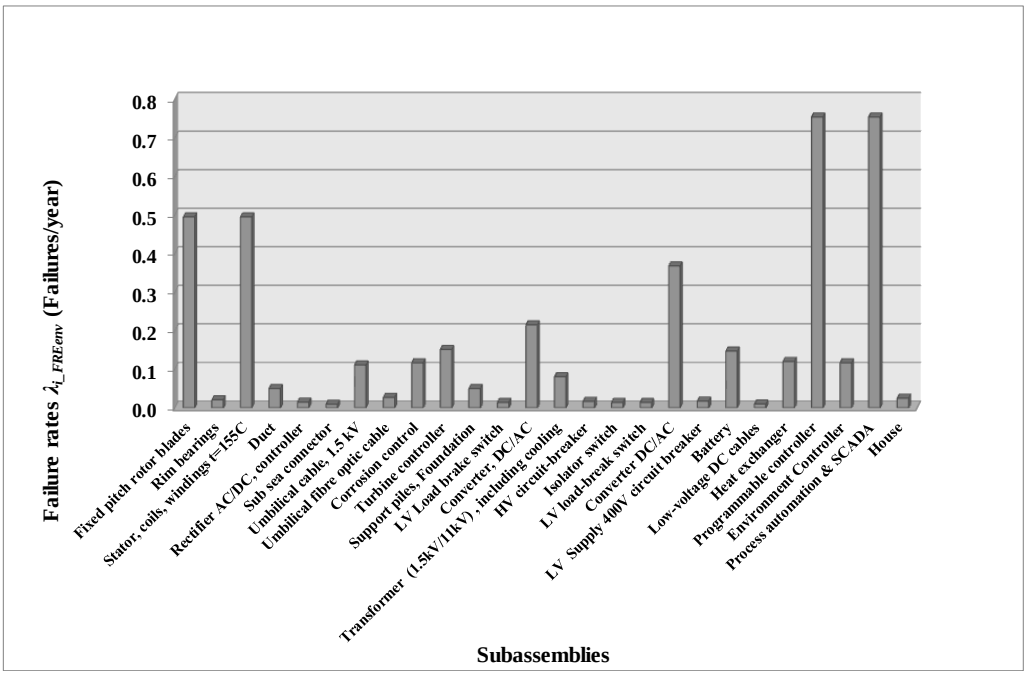

Figure 6.3 TSD3 adjusted single generic sub-assembly failure rates, λ_{i_FREenv}

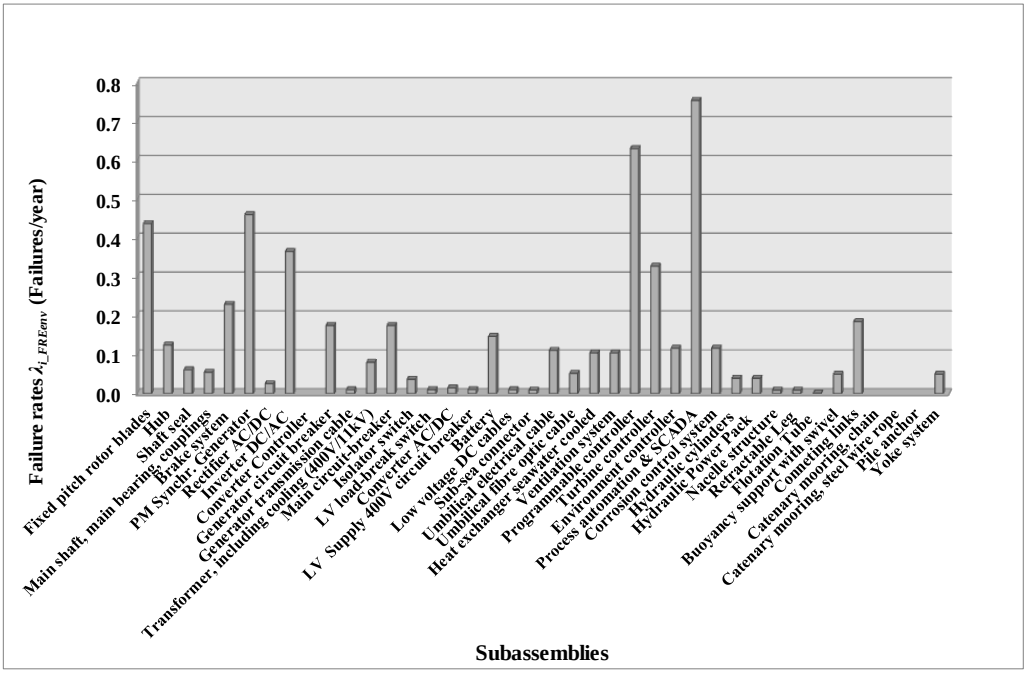

Figure 6.4 TSD4 adjusted single generic sub-assembly failure rates, λ_{i_FREenv}

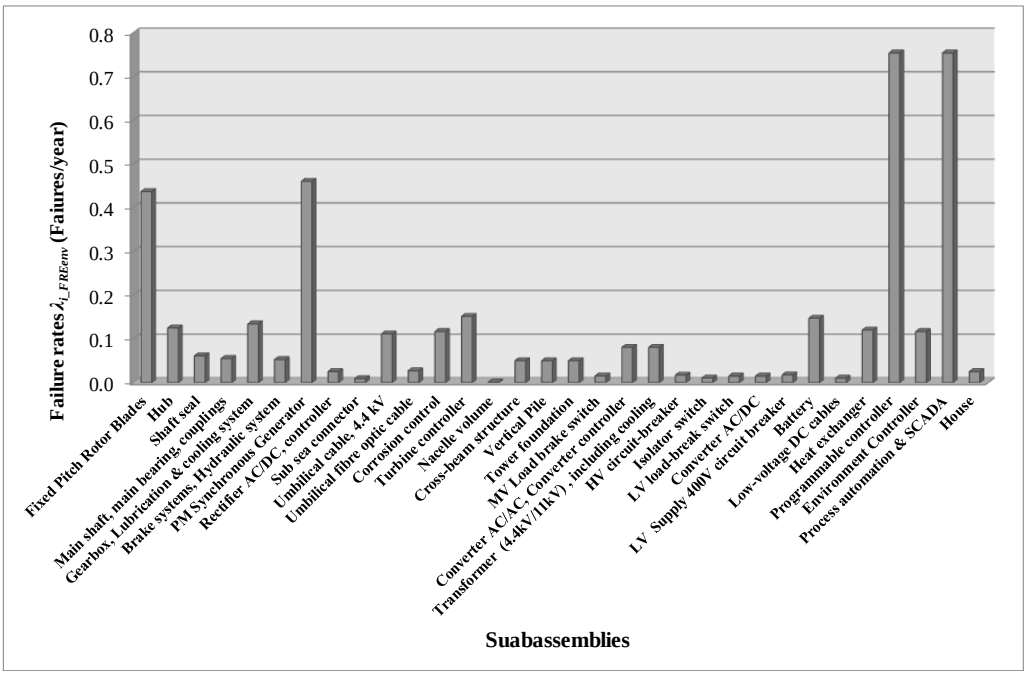

Figure 6.5 TSD5 adjusted single generic sub-assembly failure rates, λ_{i_FREenv}

The author identified the most unreliable sub-assemblies under tidal environmental conditions; these are summarised in Table 6.1. All unreliable hardware is shown in one table as a visual representation of predicted failure rate estimates. Not all sub-assemblies are in a given device.

Table 6.1 Summary of High Failure Rate Sub-Assemblies

	Sub-assembly	Environment*	Failure rate estimate, λ_{i_FREenv} (Failures/year)	Reliability survivor function *R(1 year)*
1	Rotor blades, pitch electronics	NU	0.759	0.468
2	Process automation & SCADA	GF	0.754	0.470
3	Converter AC/AC, Converter controller	NS	0.731	0.481
4	Programmable controller	NS/GF	0.630	0.533
5	Stator, winding coils	NU	0.495	0.610
6	PM Synchronous. Generator	NS	0.460	0.631
7	Induction Generator, water cooled	NU	0.236	0.790
8	Fixed pitch rotor blades	NU	0.437	0.646
9	Inverter DC/AC, Converter controller	NS	0.366	0.694
10	Turbine controller	NS	0.151	0.859
11	Gearbox, Lubrication & cooling system	NS	0.228	0.796
12	Brake systems, Hydraulic system	NS	0.230	0.795

*Environments defined in nomenclature

The predicted failure rate range of the above sub-assemblies was found to be higher than required by Equation 6.1, somewhere between:

$$\lambda_{i\_FREenv} = 0.230\text{-}0.759 \text{ Failures/year}$$

The highest failure rates are found in:

- Rotor blades with electronic pitch control systems;
- Process automation & SCADA;
- AC/AC converter and its controller;
- Programmable TSD controller.

The results, shown in Table 6.1, put the survivability factor for a year lower than 46% for the total system. Thus, for an independent sub-assembly such as the pitched rotor blades, the survivor function will be approximately

$R(1year)$ rotor blades-pitched = 0.468.

In terms of R_i(1 year) = 47% to 53%, total device reliability will be well below $R(t)_{TSD} < 0.80$.

Such results would be unacceptable for a year in service without maintenance: see Table 6.1. These electronic-based sub-assemblies are good candidates for improvement.

Analysis of TSD3 data of all critical sub-assemblies presented in earlier sections found that only the sub-sea connectors and LV DC cables are close to an acceptable level of reliability, near to 0.992, for the total device reliability to stay at 0.80.

In summary, the reliability of almost all sub-assemblies are candidates for improvement. This should be given high attention by all marine offshore industries.

6.2.4 *Identification of the Least Reliable Sub-Assemblies*

Based on graphical models developed in Appendix 4, the tidal device architectures are shown as a complex of mechanical, electrical, control, and structural sub-systems with dependency status, which makes the devices more vulnerable to failures. Knowing the ratio of device sub-systems reliability will improve the total device reliability at the development stage and lead to an improved maintenance strategy.

The sub-systems can be analysed with an assumption that they are composed of a number of sub-assemblies in a series relationship. Each sub-system was analysed as an individual independent block.

Figure 6.6 shows an example of the relationship of predicted sub-systems reliability characteristics for TSD1 (fully offshore technology) based on an exponential distribution. This shows clearly that TSD unreliability is concentrated in order of significance as follows:

- Drive train (MD+MK);
- Control systems (CA+ AB);
- Electrical systems (MS+AA);
- Structure (U);
- Ancillary Systems (XA).

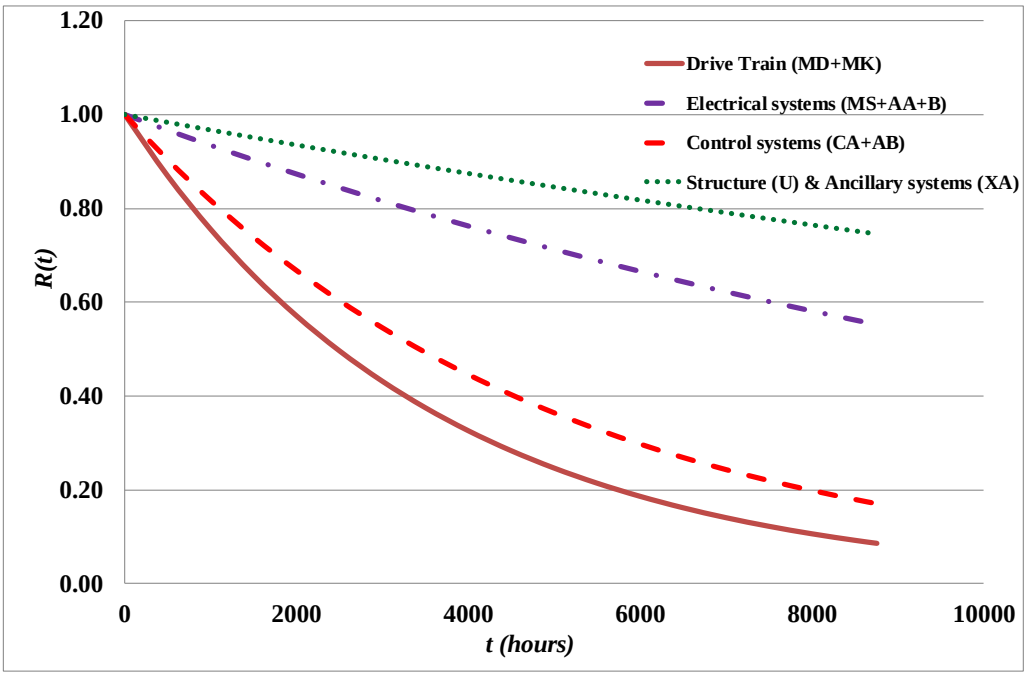

Figure 6.6 TSD1 sub-system reliability survivor functions

6.2.5 *Summary*

In this section, the author has shown that some sub-assemblies, and their arrangements, including sub-systems, are more critical than others in terms of system reliability. Estimating the relative importance factors of sub-assemblies for maintenance strategy requires in-depth knowledge of compiled TSD system and design variation, which was not available at this early stage of development.

6.3 Validation by Comparison of Prediction Methods

6.3.1 *Description of Two Prediction Methods*

This section presents a comparison of results between different methods of evaluating the reliability of TSD drive train sub-assemblies, based on the assumption of constant failure rates only**.** The sub-assemblies considered are the rotor blades and pitch system, and the main bearing. The methods to be compared are as follows:

- Classical probability prediction, as used in this Thesis, for the conceptual stage of design, using sub-assembly failure rates from surrogate data. This approach requires knowledge of device architecture and availability, relying heavily on past information, not the tidal environment. It is a “top-down” approach.
- Structural reliability theory, the method used by Val and Chernin (2011) and Val and Iliev (2011), applied to assessment during the development stage when more information on sub-assembly characteristics and stresses are available. It is useful for sub-assembly reliability assessment and estimation as a part of reliability design and testing programme. Monte Carlo simulation and Bayesian analysis were used in this method, requiring detailed knowledge of sub-assembly characteristics and stresses. The

approach is based on a multiplicative method, with a number of coefficients and various scenarios. The data used for this method were illustrative, representing only one type of blade and bearing. This is a "bottom-up" approach.

According to RIAC (2010), reliability modelling takes three main steps: prediction, assessment and estimation, as illustrated in Figure 6.7.

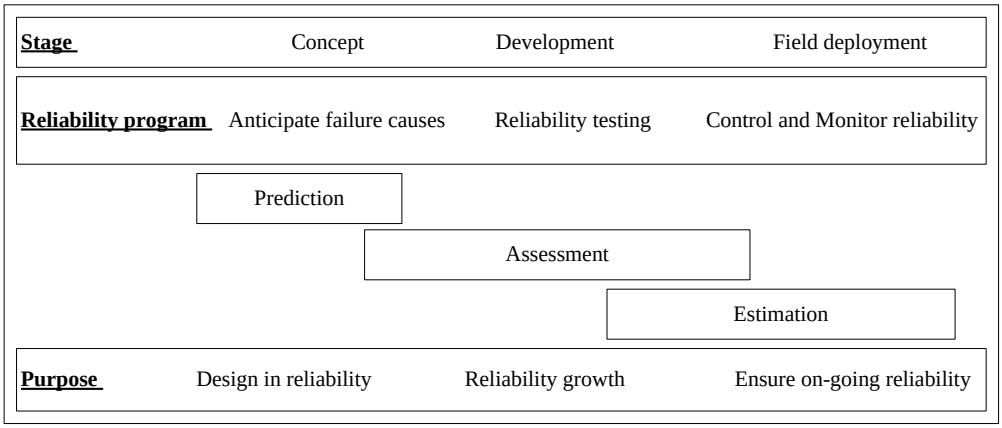

Figure 6.7 Reliability prediction, assessment and estimation

Source: Adapted from RIAC (2010)

The method presented in this Thesis represents prediction; the method of Val and Chernin (2011) and Val and Iliev (2011) represents assessment and estimation. Each method has its limitations:

- classical probability prediction: wind turbine main bearing failure rates were not specifically defined, being combined with those for the main shaft and couplings;

- structural reliability assessment:

- main bearing failure rates were limited to one bearing example only, *i.e.* SKF29240E;
- turbine blade design used in the example was non-optimal, not coming from a real tidal turbine but selected for illustrative purposes.

A comparison of results from the two methods is presented in Table 6.2.

Table 6.2 Comparing Results From Two Reliability Methods

Sub-assembly	**Prediction Method**		**Assessment Methods**							
	This Thesis		**Val and Chernin**		**Val and Iliev**					
	$\lambda_{i\_FREcon} = \lambda_{Gi\_max}$	$\lambda_{i\_FREenv} = \lambda_{Gi\_max}\ \pi_E$	λ_{ob} under u_r = 2.0 m/s	λ_{ob} under u_r = 2.5 m/s	$\lambda_{0.05}$ at COV_{Cm}=0.1	$\lambda_{0.95}$ at COV_{Cm}=0.1	$\lambda_{0.05}$ at COV_{Cm}=0.5	$\lambda_{0.95}$ at COV_{cm}=0.5	$\lambda_{0.05}$ at COV_{Cm}=1.0	$\lambda_{0.95}$ at COV_{cm}=1.0
Pitchable rotor blade	0.230	0.759	0.002	0.126	-	-	-	-	-	-
Main shaft, main bearing, coupling	0.055	0.055	-	-	0.039	0.147	0.024	0.187	0.011	0.245

u_r	Rated tidal stream velocity, m/s
λ_{ob}	Obtained Failure Rate (Failures/year)
$\lambda_{0.05}$	Prior Distribution Failure Rate (Failures/year), 5% confidence limit
$\lambda_{0.95}$	Prior Distribution Failure Rate (Failures/year), 95% confidence limit
C_m	Multiplier, representing uncertainties associated with the modification method
$COV_{Cm=0.1}$	Coefficient of variation for C_m =0.1 - strong belief
$COV_{Cm=0.5}$	Coefficient of variation for C_m =0.5 - medium belief
$COV_{Cm}^{=1.0}$	Coefficient of variation for C_m =1.0 - weak belief

6.3.2 *Summary*

The results for TSD turbine blades, pitch mechanism and main bearing, summarised in Table 6.2, are complementary. It can be seen that for the turbine blades the failure rate, obtained from the bottom-up approach, ranges from 0.002-0.126 failures/sub-assembly/year, much lower than predicted by the top-down approach of this Thesis, 0.230-0.759 failures/sub-assembly/year. This result tells us that predicted failure rates during the conceptual phase can be drastically improved by detailed design during the assessment stage.

The failure rates for bearings were more complex, being based on many factors. However, they can be summarised from the bottom-up approach with $COV_{Cm} = 0.1$, degree of weak belief, producing the lowest failure rate of 0.011 failures/sub-assembly/year with a 5% confidence limit and the highest failure rate of 0.245 failures/sub-assembly/year with a 95% confidence level. From the top-down approach the main bearing with main shaft and coupling failure rate was 0.055 failures/sub-assembly/year, lying between the results of Val and Chernin (2011) and Val and Iliev (2011).

6.4 Validation by Comparison to Other Renewable Systems

6.4.1 *Tidal vs Wind Turbines*

A validation of the methodology presented in this Thesis would be to compare the predicted reliability values obtained from the five TSDs from this Thesis with measured reliabilities of onshore WTs of similar size, as presented by Spinato et al. (2009). The similarities of sub-assemblies used in the power trains of these two technologies make this comparison interesting and the results are shown in Figure 6.8. The horizontal band represents the range of measured failure rates of onshore WTs of similar rating, Spinato et al. (2009).

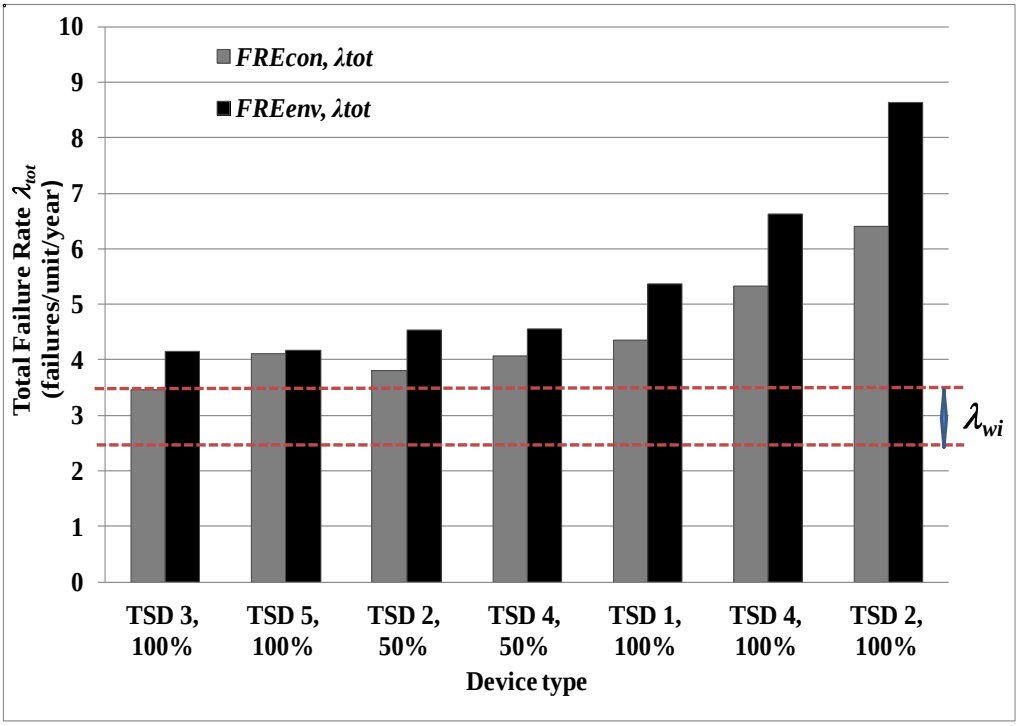

Figure 6.8 Comparison of predicted TSD & WT failure rates

Source: Delorm et al (2011)

From Figure 6.8, the predicted failure rates for the five TSDs (λ_{tot_FREenv} = 4.160 to 8.642 failures/year) show that they are less reliable than onshore WTs of similar

power output (λ_{wi} = 2.5-3.5 failures/year) and the predicted TSD failure rates range from 150-200% of wind turbine failure rates. This is to be expected, bearing in mind that the TSD technology is in its infancy and operating in a harsher environment. However, it suggests that these predicted TSD failure rates are representative and that the industry either needs to reduce them in some radical way or provide more accessible methods of repair. Significant failure rate improvements for devices could be possible in time, bearing in mind Figure 6.8, where failure rates can be improved if sub-assembly counts are reduced.

Moreover, the data in Figure 6.8 were obtained from WTs undergoing regular service at least twice a year. Onshore WTs can be maintained at any time, and failure rates would naturally be lower compared to an offshore device for which the shortest practical maintenance interval is likely to be one year (Wolfram 2006). Considerable experience is being gained of offshore WTs, and Feng et al. (2010) gives a good summary of UK Round 1 offshore wind farm operations. However, WT failure rates in these circumstances are not being released due to confidentiality.

In order to bring the WT and TSD data to the same analogous confidence level, the structure and numbers of type of devices considered should be similar. Therefore, the generic model structures of TSDs 1-5 in this Thesis must be similar to the generic structures of the WTs described in Chapter 3.2 and shown in Figure 6.9, following VGB PowerTech (2007). Based on the above two assumptions of TSD and WT similarity in structure, see Figure 6.9, and in the number of data analysed, one can conclude of a similar confidence level of the failure rates applied to TSDs. Therefore the comparison of two types of technology with horizontal drive trains can be compared and analysed. However, failure rate results will be very dependent on differences of operational environment.

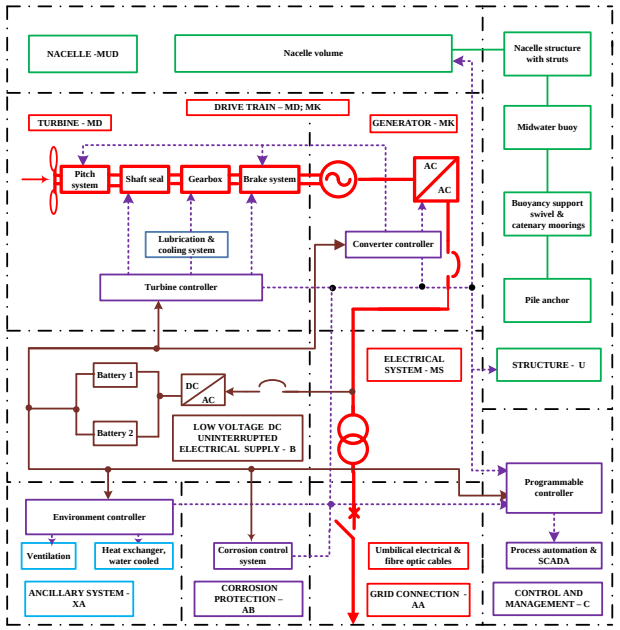

(a)

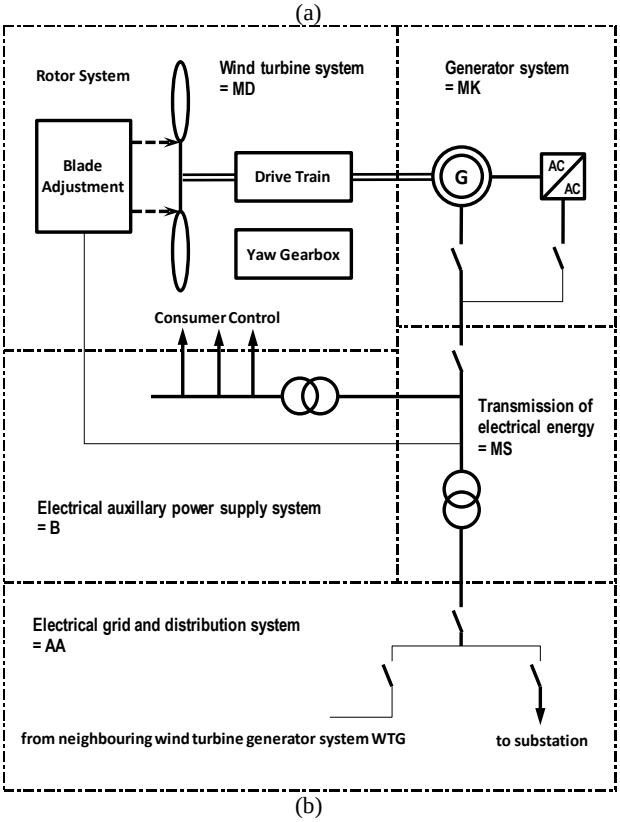

(b)

Figure 6.9 Structural comparison of TSD and WT

(a) TSD1 by T. Delorm

(b) WT (adapted from VGB PowerTech 2007; redrawn by Ko Okazaki)

6.4.2 *Tidal vs Wave Devices*

A further way to validate the methodology presented in this Thesis would be to compare its results with a recent WEC reliability assessment on a Wave Energy Converter (WEC), presented by Thies et al. (2009), and that of devices considered in this Thesis using a similar approach. To analyse a generic linear WEC 1 with hydraulic couplings and six hydraulic Power Take-Off (PTO) modules, different parallel arrangements were compared, based upon the structure shown in Fig 6.10.

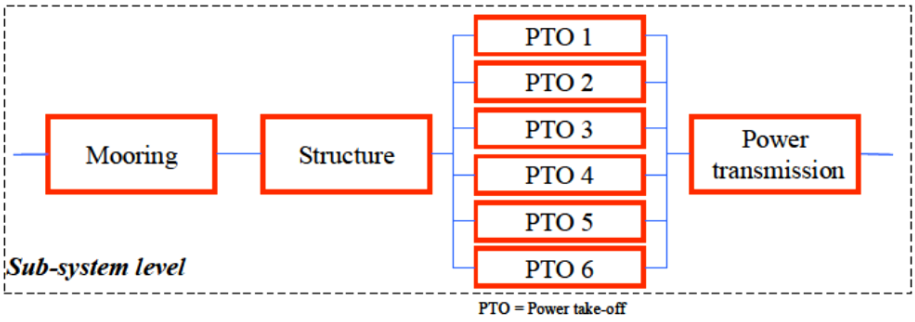

Figure 6.10 Wave energy converter analysed by Thies et al. (2009)

Each power module could contribute up to 1/6 of the total power production, assumed to be 750kW. The device was assessed as six independent WEC systems with six levels of power take-off starting from PTO1 to PTO6. The systems were analysed as series and series/parallel connected blocks with different redundancy configurations of PTO sub-assemblies. The study concentrated on investigating early stage reliability problems for the six such WECs in an array and identifying critical components in the wave environment.

Both studies used surrogate constant failure rate data from publicly available sources and applied exponential data distribution, assuming devices are not

repairable during one year in service, but Thies et al. did not use the same surrogate data as this Thesis, see Table 6.3.

Table 6.3 Comparing TSD and WEC Surrogate Failure Rate Databases

Surrogate data sources used in this Thesis on TSDs		**Surrogate data sources used by Thies et al. (2009) on WEC**	
Description	**References**	**Description**	**References**
Wind power LWK & WMEP	Hahn et al. (2007) Spinato et al. (2009) Tavner et al. (2010; 2012)	-	-
OREDA	OREDA (1984-2009)	OREDA	OREDA (1997)
NPRD-95	NPRD-95 (1995) NPRD-2011 (2011)	AME	AME (1992)
MIL-HNDBK 217F	MIL-HDBK-217F, Notes 2 (1991)	FARADIP	FARADIP.THREE (2006)
IEEE Gold Book	IEEE Gold Book (1997)	GREEN	Green and Bourne (1978)

This comparison of results from WEC 1 by Thies et al. (2009) with those from TSDs 1-5, as illustrated in Figure 5.1, shows that, for the TSDs, both analyses give broadly similar predicted failure rates for this particular WEC, with its six PTOs considered successively in parallel reliabilities to that of the analyzed wave device technology as illustrated in Figures 6.11-6.12.

Predicted models validate that sub-systems redundancy, such as drive trains, can increase and decrees systems reliability and require careful critical evaluation. The redundancy effect is illustrated in Figures 6.11-6.12.

- A configuration WEC1 with two PTOs, required to be working during one year of operation for specified power production, demonstrate higher reliability characteristics compared to other five options: λ_{tot} =2.287 Failures/year and R(1 year) = 10.16.

- A configuration such as six PTOs in series shows that after proposed 2800 hours of operation the system is no longer reliable at all. Failure rate of PTO1-6 in series not acceptable: λ_{tot} =21.133 Failures/year*;* R(*1 year)* = 0.

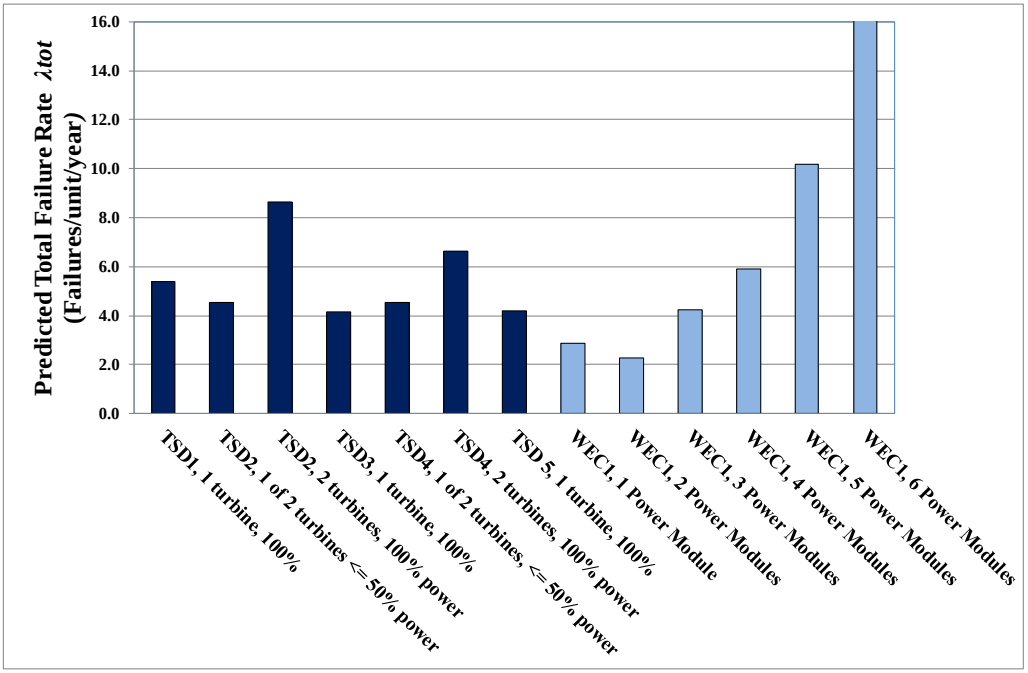

Figure 6.11 Predicted failure rates intensity for TSDs1-5 and WEC1 in 6

The predicted survivability of 100 such TSD or WEC systems in the water for 1 year is shown in Fig 6.12 and again the number of surviving devices is small but similar between TSDs and WEC. The WEC with six power modules in series failed after only 2800 hours of operation, therefore reliability after one year is not applicable.

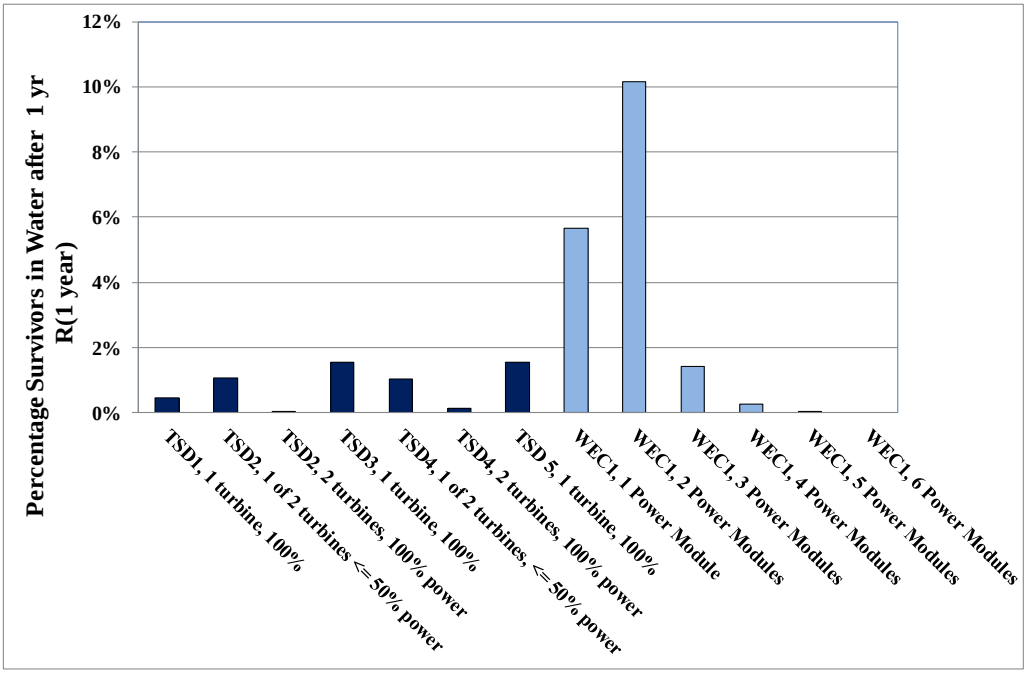

Figure 6.12 Probability of survivors 1-year operation, 100 TSDs or WECs

It is obvious from Table 6.3, and Figures 6.11 and 6.12 that TSD and WEC reliability model results have similarities based upon their functional specifications. Both systems are emerging technologies and both harvesting energy from the marine environment. The systems can be divided into similar sub-systems, such as moorings, support structure, main body structure, drive train, electrical or transmission lines, control systems and additional auxiliary systems.

Reliability models for analysing these technologies have been chosen based on traditional approaches, and multiplicative failure rate adjustment factors applied to surrogate data. Both studies assumed devices are non-repairable units during one year in marine environment. The differences between TSD and WEC assessment models are in the application of surrogate data, adjustment factors to tidal or wave environments, and the mathematical prediction models for survival factors. The author's mathematical reliability models for calculating total failure rates for the

series-parallel networks and further survivor functions were described in Chapter 4.6 and based on theory of Table 6.2.1-3 of RIAC&DACS (2005). Thies et al. applied a different approach for calculating network reliability characteristics *R(t)* similar to Table 6.2.1-2 of RIAC & DACS (2005). The author's method in this Thesis is simpler, but gives an error greater than 20%, as stated in Chapter 5.4.

This comparison shows that both ocean energy converters are facing similar problems in relation to total systems reliability. The TSD drive train and WEC PTO can be considered the most vulnerable sub-systems in the marine environment, see Table 6.4. After 2000 hours of operation the drive train *R(t)* is reduced to less than 0.8: see TSD Figure 6.6 and also Thies et al. (2009) Figure 5. In order to increase the number of hours of system operation without falling below the 0.8 line level, the devices can be designed with lower failure rates and/or a higher level of redundancy. However, this will affect the cost of applications of the device.

Table 6.4 Failure Rate Intensities: TSD1 Sub-Systems Compared to WEC

Device/sub-assemblies	Time (t) year	TSD1/Drive train (MD-MK)	TSD1/Electrical systems (MS+AA+B)	TSD1/Structure (U)	TSD1/Control systems (CA+AB)	TSD1/Ancillary systems (XA)	WEC/PTO	WEC/Power transmission
λtot (Failures/year)	1	2.454	0.594	0.280	1.769	0.280	2.420	0.470

6.4.3 *Comparison with a real TSD Failure Distribution*

The previous subchapters presented TSD reliability prediction models' validation based on an analytical approach using discrete analysis of constant failure rates. However, for a new technology, the most valuable way to validate the models would

be to compare the predicted model distribution of failures with the operational distribution of failures.

In a recent publication, presented at SuperGen Marine 2011 by MCT SeaGen Fraenkel (2011), the first commercial prototype tidal energy device, full analyses of measured shut-down faults over a period of one year's operation in Strangford Lough is shown in Figure 6.13. The distribution of failures observed during operation can be compared with the reliability prediction of TSD2.

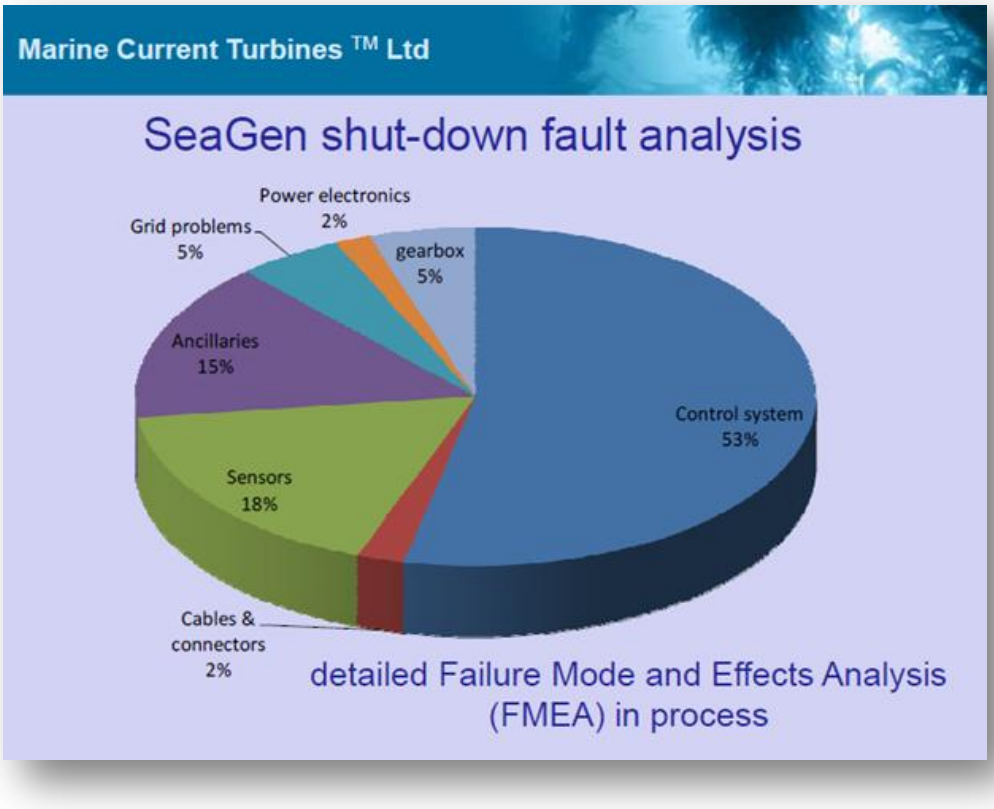

Figure 6.13 Measured SeaGen shut-down fault analysis

Source: Fraenkel, Supergen Marine General Assembly, 2011

The TSD2 structure in Figures 13.3-13.4, Appendix 4, is similar to the MCT SeaGen in functional structure, number of general sub-assemblies, and total power production. The TSD2 models were checked against first-year operational shut-down

data of SeaGen. Figure 6.14 shows operational results at the front and predicted distribution behind. The key points are:

- Finding how the resulting models, based on PSD adjusted to tidal environment, fit the operational results model at an early stage of development;
- Comparing boundaries between predicted failure intensity results and operational observed data, to validate PSD adjusted to tidal environment where no historical data are available.

Comparison of similar sub-assemblies of tidal energy technologies with power production up to 1200 MW shows these results:

- The failure distribution between major sub-systems is similar to that observed in the field. The highest shut-down rates came from control systems – 71% (SeaGen) and 65% (TSD2), as expected.
- The failure intensity of both devices during one year of operation without repair at an early stage of development and commercialization are similar. The highest failure rate is found in control systems/sensors:
    - SeaGen: λ_{ics_seagen} = 1.992 Failures/Turbine/year
    - TSD2: $\lambda_{FREenvics\_TSD2}$ = 1.836 Failures/Turbine/year

The comparison shows that control systems are most vulnerable. According to Fraenkel (2011), control system problems can be overcome at the early stage of operation; when it is "tuned," problems become relatively rare and virtually disappear. This applies to any control system specification. It needs to be set to be over-protective at the starting point of operation in order to avoid early failure of the total device.

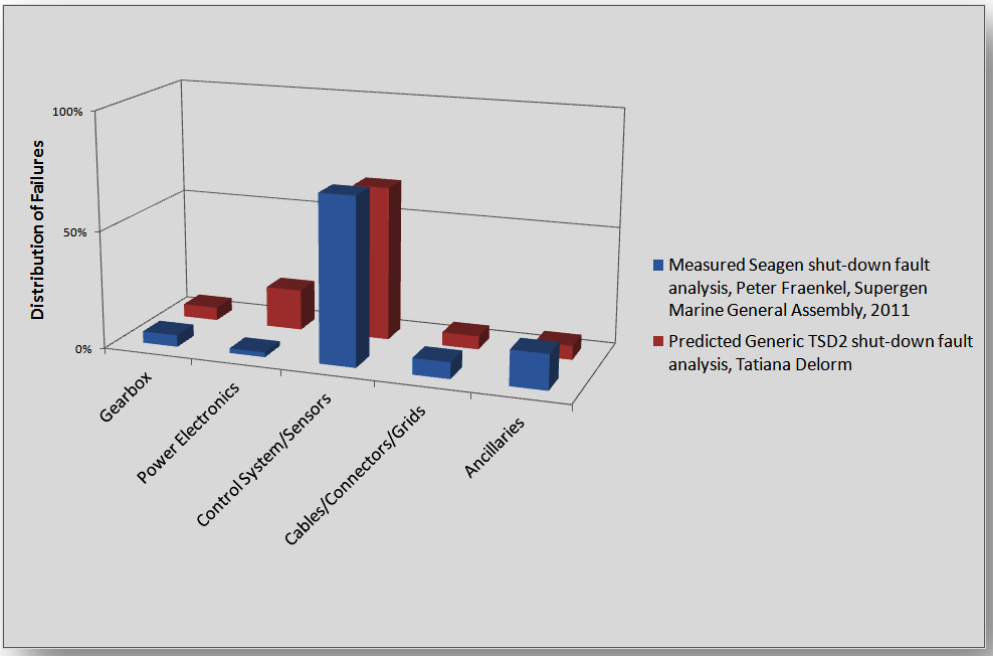

Figure 6.14 Distribution of Failures/year: TSD2 and Operational SeaGen

6.4.4 *Summary*

The summary of all these renewable device comparisons are:

- A portfolio of surrogate data collected for TSD and WEC technologies adjusted to the marine environment in a consistent way can provide TSD & WEC developers with predicted primary levels of failure rates during the first year of operation;
- The results in Figure 6.14 show clearly that TSD2 was able to predict the distribution of failures experienced by SeaGen in Strangford Lough during its first year of operation, validating the model approach;
- Increasing the number of sub-assemblies decreases the system reliability;
- Increasing generation capacity in a WEC with parallel PTO systems decreases the system reliability but increases redundancy. The same is demonstrated in TSDs with duplicate drive trains;
- Redundancy increases the total system reliability, however it needs careful design review for system configuration design in order to achieve the most reliable architecture because it also increases the number of vulnerable components;
- Predicted total failure rates for the WECs considered were from 2.287 - 21.133 Failures/year based on sub-system arrangements;
- Predicted total failure rate ranges for TSDs were from 4.160 - 8.349 Failures/year based on sub-systems arrangement;
- WECs with a configuration of several drive trains in series are confirmed to be unreliable;

- Predicted failure rates for WECs and TSDs are higher than for onshore WT due to the novelty of these technologies and the harsh environment in which they are placed.

These comparisons have limitations. The details of the identified RBD systems, sub-systems, assemblies, sub-assemblies and components of the TSD and WEC comparison were studied in the generic form only. As more data become available, further comparisons would be valuable. The cost of device development and maintenance was not taken into account in the author's modeling. This research will become easier when more marine devices are studied in the natural environment.

.

6.5 Statistical Significance of Results

When predicting reliability characteristics, based on the methodology proposed in Chapter 4 and applied in Chapter 5, one may question the confidence limits and the validity of the model results evaluated in this Thesis.

6.5.1 *Confidence Factors & Acceptance Range*

The confidence factors in a model can be expressed by the establishment of confidence intervals. *Confidence limits* cannot be applied to the results of these mathematical models because:

- Due to the fact that TSD are in the very early stage of development, there are no data from testing or sampling in the environment. By definition, without an experimentally derived data set, one cannot derive confidence intervals; therefore, confidence factors should not be created or used to indicate the reliability of the calculated estimates because these will increase data uncertainties.
- Confidence limits can only be constructed when you know the count of all of the failures that make up the 'population' of the part types for which you want to construct them. If this information is unknown, there is a great deal of risk in trying to apply the confidence limits from one application (with known data) and apply them to a different application (from a more severe environment). It is even more risky to apply confidence levels from one part type in one application to a different part type in a second application because of the lack of information about the number of failures that may have occurred and the specific characteristics of the environment (Nicholls, *pers. comm.* 2010).

Databases such as MIL-HDBK-217 and NPRD-95 do not have confidence factors linked with them because of the variation in population size, device type and environment. In contrast, the data from OREDA were from components measured in their natural operational environment; therefore, confidence intervals are associated with them. To ensure the most conservative estimate for the tidal environment, unlike the OREDA oil & gas environment, the author used OREDA failure rates at the upper limit of the 90% confidence interval

Despite the fact that the derived reliability characteristics data do not have assigned confidence factors, the data are believed to be applicable and acceptable for design comparison, because they fall within a range that has shown correlation with real-life operation of onshore wind turbines of similar rating, as presented in Figure 6.8. The lowest values of this range, calculated as FRE_{con} where no environmental adjustment was applied to the failure rate data from the databases, and the highest values, calculated as FRE_{env} where the data were multiplied by an environmental factor, form a range which is acceptable at this stage of research.

Confidence in the usefulness and accuracy of this data is also based on the fact that the failure rate data from wind turbine surrogate data was taken from a large population of European databases with measurements made over years of operation.

In summary, the author believes that at this stage of research, in order not to increase quantitative uncertainties, confidence factors should not be extrapolated or hypothesized because the range of TSD failure rate values came from data of different distribution and variation.

6.5.2 *Validity of Multiplicative Factor for Total Failure Rate*

The author has used the traditional method of reliability prediction. To calculate device total number of failures per year, the PCRPT was applied, assuming system redundant units are individual blocks. As described in Chapter 4.6, the technique is based on assigning surrogate data to each sub-assembly, multiplied by environmental adjustment factors, which also may include number of other multiplicative factors. The quality factor π_{Qi} was not taken into consideration, assumed to be equal to 1. Factors such as human reliability and software reliability factors were also considered equal to 1. This PCRPT was used because no specific product design and reliability information exist for these TSDs; however, as stated in Chapter 5, this approach can lead to error, the magnitude of which, as suggested by Faracci (2006), could be as much as 20%.

The environmental adjustment factors according to Table 4.3 do not include a correction factor for the correlation of wind turbulence and tidal turbulence. The reason for this is the absence of data for tidal turbulence because, as Wood et al. (2010) explained, the variation of flow patterns is too complex and requires more research. Even if this data were available, there is no information on how turbulence itself can either increase or decrease device failure rates. This is a subject for further investigation.

The author's approach to calculating the sub-assembly predicted failure rate in the tidal environment using surrogate WT data would be: equate the rate in the tidal environment to the surrogate wind database failure rate in a GF environment multiplied by an adjustment factor from GF to NU or NS. The conversion factors of RIAC&DACS (2005) were established using a generic prediction of reliability of electronic assemblies, using MIL-HDBK-217F. The environmental factors were

changed for each component in order to derive the multiplying factors for the assembly. These factors should not be used for predicting the reliability of mechanical components because MIL-HDBK-217F does not predict these and because the relationship of environmental differences for the mechanical components will probably be different and possibly more significant than those for electronic components. This approach was suggested by Nicholls (2010) *pers.comm*.

6.5.3 *Summary*

In the absence of historical reliability data and a known environment, the author used the highest generic failure data from surrogate data for each sub-assembly, making conservative predictions due to the novelty of the technology. The issue of the statistical significance of this approach and the confidence levels associated with its results should be dealt with in future research.

6.6 Discussion

6.6.1 *General*

The Reliability Modelling and Predictions Method, based on PCRPT, can be used before part-level testing. It provides quantitative direct results, accompanied by PSD adjusted to the tidal environment, constantly applied to predicted reliability models. The total predicted failure rates describe system failure probability, which depends on several factors not available at the time of writing. Therefore, the two reliability Failure Rate Estimations presented in Table 4.4 can demonstrate a wider operational range of total failure rates calculations for prediction and comparison.

The author's proposed approach is therefore appropriate for TSDs only in the early design phase. Using surrogate data, it produces informative comparative reliability results. In the future, other investigators could develop and apply this

method more widely. For example, if the method outlined in this Thesis were applied to a different type of power converter such as an offshore wind turbine at the early stage of design, the method would remain the same, but the surrogate data would have to be replaced or updated.

6.6.2 *Failure Rate & Complexity*

Figures 5.5 and 6.8 show that the TSDs with more sub-assemblies have a higher failure rate. This becomes more complicated in the twin-axis devices such as TSDs 2 & 4, which also have some intrinsic redundancy, the effect of which is visible in their higher failure rates when 100% power is expected and lower failure rates when only 50% power is required.

6.6.3 *Impact of Maintenance on Reliability Estimation*

Assuming non-repairable operation for all devices for 1 year, the survivors after 1 year in the water have been predicted to be less than 2 in 100 as shown in Figure 5.6. This is very low and would be commercially unacceptable, suggesting that predicted failure rates must be reduced or the annual maintenance concept will be untenable. This also suggests that fixed devices, without maintenance access, will suffer poor survivor rates, unless failure rates are dramatically reduced. On the other hand, devices with maintenance access, either by unmooring or the use of a sea-bed pile and turbine raising, may achieve much better survivor rates.

6.6.4 *Limitations*

Dynamic and peak-stress effects, such as wave-slam or exceptional tidal ranges, have not been considered in this Thesis. Issues of fouling have not been dealt with, either. Both could be included in further research if appropriate adjustment factors become available.

7. Conclusions

7.1 Background

This Thesis has established a new methodology for analysing TSDs in the early design phase, using surrogate data theoretically adjusted to the tidal environment. This methodology has produced informative comparative reliability results and identified the most reliable architecture amongst the TSDs studied. Despite the lack of historical reliability data for TSDs, analogous data has been found and has been presented as a portfolio of surrogate failure rate data, in order to derive the primary level of total device reliability characteristics during first year of operation. As demonstrated above, surrogate data were compiled from published wind turbine databases, OREDA, NPRD-95, MIL-HDBK 217F and IEEE Gold Book databases, which have then been used for TSD reliability characteristic prediction.

Reliability analyses were based on an exponential distribution of failure probability, assuming constant failure rate during useful sub-assembly life spans. Environmentally-adjusted conservative estimates for five horizontal-axis TSDs1-5 with power production from 0.6MW – 1,2MW were analysed and compared for different architectures and the annual reliability characteristics were compared.

7.2 Surrogate Failure Rate Data

In the course of this research the most critical questions raised by developers and scientists relating to the relevance of surrogate failure rate data have been answered, uncertainties with environmental factors to the tidal stream technology have been illuminated and, by applying MIL-HDBK217F environmental factors to surrogate data, environmentally-adjusted conservative failure rate estimates have been

obtained. The annual estimated reliability characteristics for each device can now be compared.

The two approaches to Failure Rate Estimation used in this research demonstrate a calculated operational range of total failure rates for comparison. The estimates provide an overview of data from the lowest possible estimated results, justified for tidal environments, to the highest results, which are still under research.

Reliability predictions using surrogate data are clearly useful for comparing design approaches, not for making absolute predictions. The total predicted failure rates describe system failure probability, which depend on several factors not available at the time of research.

7.3 TSD, Wind & WEC System Result Comparison

The derived methodology compared and validated the predicted TSDs' total failure rates λ_{tot} (Failures/Year), with WTs and WEC1 reliability prediction results during one year in service, and reached the following conclusions:

- Drive train and control sub-system technology can be considered the most vulnerable in the marine environment;
- Control sub-systems can be tuned to increase reliability during early operation;
- Increasing generation capacity in a parallel PTO systems decreases overall system reliability by increasing components but increases redundancy;
- Redundancy must therefore be carefully analysed in order to design reliable devices;

The methodology concluded that overall differences between predicted reliability characteristics of the five TSDs, WTs and WECs are not large. However, this result should not be treated as absolute.

7.4 Sub-assembly & Sub-system Result Assessment

The comparative analysis of reliability characteristics for the five TSD sub-assemblies has found that the electronic-based hardware is most vulnerable. The highest predicted failure intensity has been identified in the electronics of pitched rotor blades, process automation & SCADA, converter AC/AC with converter controllers and program controllers.

The research shows that sub-systems reliability highly depends on the control system. These results are also confirmed by a comparison of TSDs with a WEC predicted estimate and by the first published failure intensity data from SeaGen, presented in this Thesis.

Reliability estimates have been described in Chapter 5 for models at the conceptual stage but significant failure rate improvements for tidal device sub-assemblies should be considered at the later stage, design and development. For example, design improvements in turbine blades can reduce failure rate to 0.002 - 0.126 failures/device/year and bring reliability of this sub-assembly to the lowest acceptable level of $\lambda_i \leq 0.01$.

7.5 The Conceptually Most Effective TSD Architecture

The methodology obtained predicted device survival rates *R(t)* for the five devices after one year in service results, showing that assuming non-repairable operation for a year, the device predicted failure rates show the percentage surviving in the water after 1 year will be small.

- Consequently, either:
  - Device failure rates must be dramatically reduced, or;
  - Fixed devices without maintenance access will suffer poor survivor rates;
  - Devices with maintenance access, either by unmooring or the use of a sea-bed pile and turbine raising, must achieve better survival rates.

7.6 Limitations of Models in this Thesis

The models in this Thesis exhibit the following limitations:

- Surrogate data were derived from repairable sources, representing different population sizes and failure mechanisms in environments different from those that may arise for tidal devices;
- An appropriate rationale for the use of surrogate data and their adjustment for the tidal environment is not yet agreed, so the author has proposed using two failure rate estimates, with effective upper and lower bound limits;
- This reliability prediction analysis, suitable for the early design stage, considered main sub-assemblies only, as shown in the FBD, and did not 'drill-down' into all components;
- 'Naval, Sheltered' or 'Naval, Unsheltered' environments were considered closest to the tidal environment where the TSD devices will operate;
- As explained in Chapter 6, environmental adjustment factors such as the dynamic and peak-stress effects of wave-slam or exceptional tidal ranges could not be considered because of the lack of applicable data. The effects

of fouling were also not considered in this Thesis. Future research should be undertaken to investigate these environmental factors.

- Load-sharing systems analysis has not been taken into account for sub-assemblies in parallel due to the lack of available data.

Due to these limitations, the failure and survivor rate results derived in this Thesis are an approximation to reality and cannot be treated as definitive.

The proposed models need to be applied to a wider range of tidal devices in order to develop the methodology and raise confidence in it. The author recommends that the failure rate estimation approach should be used for further early stage design TSD analysis, using surrogate data adjusted to the tidal environment.

8. Further Work

8.1 Examination of Other Devices

The proposed models need to be applied to a wider range of tidal devices in order to raise confidence in the application of reliability models and life cycle prediction. Analysing other variables of systems design could show that other options may be more reliable than those predicted in this Thesis, and should be further investigated. It is recommended that the failure rate estimation approach should be used for further early-stage design TSD analyses using surrogate data adjusted to the tidal environment. It would be useful to propose projects in conjunction with commercial developers for using such surrogate data with the restricted model approach that has been demonstrated in this Thesis.

8.2 Optimisation of Models

8.2.1 *General*

The approach for predictions of failure rate intensity reported in this Thesis was based on a traditional multiplicative technique, which could include application of numerical adjustment factors, multiplied to an appropriate surrogate sub-assembly failure rate. In preparing this Thesis, environmental factors, unknown at the time of research, were not taken into consideration and were assumed to be equal to 1. The following factors have an effect on reliability and should be taken into consideration.

8.2.2 *Ocean Turbulence Effect*

Further work is needed to investigate the ocean turbulence dynamic effect on reliability prediction of a total device and its individual systems, sub-systems, assemblies, sub-assemblies and components, including the establishment of

adjustment factors, π_{Tbi}, to represent turbulence effects. Investigating the turbulence effect on structural reliability, materials and control systems is also under-researched. Such study would reduce uncertainties in reliability data and allow the upgrade of the prediction models proposed in this Thesis, which are based on the multiplicative approach where turbulence was not considered.

8.2.3 *Increasing Wave Heights*

Further work is needed to investigate wave height, another dynamic effect, on the reliability of the TSD structure, drive train, control systems. The damage force ratio and failure rate intensity should be investigated in order to predict a further wave dynamic adjustment factor, π_{Wi}, so that the reliability models proposed in this Thesis can be upgraded.

8.2.4 *Corrosion & Human Factors*

In addition, the effect of corrosion and human factors on device reliability should be considered, and prediction adjustment factors (π_{Cri} and $\pi_{Hi,}$) derived so that the reliability models proposed in this Thesis can be upgraded with new data.

The interaction of turbulence, wave height increase, corrosion and human factors forcing damage to the total device and failure is common for all modern technical systems. This confrontation of natural and human design effects can lead to different failure mechanisms. Surrogate data could be examined to create a portfolio of adjustment factors and build a database for computer simulation algorithms for reliability prediction and analysis of TSDs, which could lead to model optimization and reducing uncertainties at the subsequent prediction stages. The above work will be beneficial for reduction of prediction models uncertainty.

8.3 Application of an Alternative Reliability Theory

Bearing in mind that this marine technology is emergent, future work is needed to investigate state-of-the art reliability prediction such as Bayesian analyses of failure modes, which can be provide better failure rate predictions and uncertainties reduction, as described in Chapters 2 & 4. This work should be pursued particularly for those sub-assemblies and sub-systems most at risk, for example, the drive train. All levels of simulation analyses including the algorithms presented in Table 4.1 should be considered for further applications.

8.4 Other Suggested Areas for Further Work

Other areas for future work not presented in this Thesis, but which would be beneficial to total device reliability, survivability and life cycle prediction are as follows:

- In the first stage of prediction, the following need to be further examined:
    - New forms of system design;
    - Application of fundamental science to study the behaviour of the device and device arrays in a tidal environment, which could lead to new fundamental knowledge leading to clarification of tidal phenomena and to comprehensive standards for the development of tidal devices based on laws of nature;
    - Reliability analysis of arrays of shared electrical systems, as for example, on wind farms where there may be electrical and mechanical linkages between turbines.

- Use of new materials, which is clearly a major issue for the technical innovation of TSDs but is beyond the scope of this Thesis.
- Application of this methodology to vertical or other TSD designs.

- From the point of view of methodology, the following areas are crucial:
  - Methodology for testing sub-assemblies and sub-systems in the tidal environment;
  - Methodology in systems reliability evaluation: control, diagnostics, prognostication and collection of information received from testing;
  - Methodology of systems survivability and exploration of models in which this concept can be utilized.
- Standardisation procedures for TSDs, as little standardization has yet been done.

In summary, as devices are developed, device life cycle and survivability must be investigated further.

9. References

[AME] Advanced Mechanics and Engineering Ltd. 1992. Reliability and Availability Assessments of Wave Energy Devices. Report ETSU 1690 Energy Technology Support Unit, AEA Technology, Harwell, UK.

Ainsworth, D. and Thake, J. 2006. Final Report on Preliminary Works Associated with 1MW Tidal Turbine. Project Reference: T/06/00233/00/00, Marine Current Turbines Ltd., UK.

Atlantis Resources Corporation Pte Ltd 2009. Marine Power. Available from: http://www.atlantisresourcescorporation.com/. Accessed 2011 September 10.

[BERR] Department for Business Enterprise and Regulatory Reforms. 2008. Atlas of UK Marine Renewable Energy Resources. Atlas Pages. ABPmer The Met Office Proudman Oceanographic Laboratory.

[BV] Black & Veatch Consulting Ltd. 2004. Tidal Stream Energy Resource and Technology Summary Report. Carbon Trust, UK.

[BV] Black & Veatch Consulting Ltd. 2005. Phase II UK Tidal Stream Energy Resource Assessment. Carbon Trust, UK.

Boyle, G. editor. 2004. Renewable Energy: Power for a Sustainable Future, Oxford University Press, Oxford.

Cabinet Office. 2001. Performance and Innovation Unit: Renewable Energy in the UK. Building for the Future of the Environment, London.

CAPP Manual - 30605. 2012. Capital Asset Accounting Useful Life. Office of the Comptroller, Commonwealth of Virginia, USA.

Cederstrom, M., Thorsall, P.-E., Hildenwall, B. and Westberg, S.-B. 2005. Incident with Loss of Seven Post-Tensioned 72 Ton Anchors in a Dam. Dam Safety 2005. Proceedings of the Annual Conference, Association of State Dam Safety Officials, Lexington, Ky.

Corcoran, P. 2009. OpenHydro Corporate Presentation, 3rd International Tidal Energy Summit. London.

Criscimagna, N. H. 2010. Criscimagna Consulting LLC. *Personal communication*

Douglas, J. F., Gasiorek, J. M., Swaffield J. A. 1995. Fluid Mechanics 3rd Edition, Longman Publishers. London.

De Laleu, V. 2009. La Rance Tidal Power Plant. 40-year Operation Feedback – Lessons Learnt. BHA Annual Conference, Liverpool, 14 - 15 October 2009. Available from: http://www.british-hydro.org/downloads/La%20Rance-BHA-Oct%202009.pdf . Accessed 2011 November 25.

Delorm, T. M., Zappala, D. And Tavner, P. J. 2011. Tidal stream device reliability comparison models. Proceedings of the Institution of Mechanical Engineers, Part O: Jurnal of Risk and Reliability. DOI:10.1177/1748006X11422620.

Delorm, T.M and Tavner, P. J. 2011a. Reliability methodology for evaluating tidal stream devices. 11th International Conference on Applications of Statistics and Probability in Civil Engineering – ICASP 11, Zurich, 1-4 August, 2011. Faber, Kohler & Nishijima (eds), Taylor & Francis Group. London.

Delorm, T. M. and Tavner, P. J. 2011b. Poster: Reliability Prediction Models for Tidal Stream Devices. SuperGen UK Centre for Marine Energy Research Annual Assembly 2011. Available from: http://www.supergen-marine.org.uk/drupal/files/events/assembly_2011_posters/Delorm2011SuperGen.pdf. Accessed 2013 October 4.

Delorm, T. M. and Tavner, P. J. 2010. Poster: Tidal Stream and Ocean Current Energy Converter Reliability. SuperGen UK Centre for Marine Energy Research Annual Assembly 2010. Available from: http://www.supergen-marine.org.uk/drupal/files/events/assembly_2010_posters/delorm_2010_reliability.pdf. Accessed 2013 October 3.

Delorm, T. M. and Tavner, P. J. 2009. Poster: Tidal Stream and Ocean Current Energy Converter Reliability. SuperGen UK Centre for Marine Energy Research Annual Assembly 2009. Available from: http://www.supergen-marine.org.uk/drupal/files/events/assembly_2009_posters/tatiana_delorm.pdf. Accessed 2013 October 3.

[DOE] Department of Energy, USA. 2011. Marine and Hydrokinetic Technology Database. Available from: http://www1.eere.energy.gov/. Accessed 2011 November 12.

[DTI] Department of Trade and Industry. 2003. Energy White Paper: our energy future - creating a low carbon economy. The Stationery Office (TSO). Available from: http://webarchive.nationalarchives.gov.uk/+/http://www.berr.gov.uk/files/file10719.pdf . Accessed 2011 Nov 9.

[DTI] Department of Trade and Industry. 2007. Economic Viability of a Simple Tidal Stream Energy Capture Device. Available from: http://www.berr.gov.uk/files/file37093.pdf. Accessed 2011 November 24.

[DTI] Department of Trade and Industry. 2010. The World Offshore Renewable Energy Report 2004-2008.

[EET] Elemental Energy Technologies Ltd 2012. SeaUrchin video. Home page on the Internet. Available from: http://www.seao2.com/oceanenergy/images/sea-urchin.jpg. Accessed 2013 July 13.

[EPRI] Electrical Power Research Institute. Hagerman, G., Polagye, B., Bedard. R. and Previsic, M. September 2006. Methodology for Estimating Tidal Current Energy Resources and Power Production by Tidal In-Stream Energy Conversion (TISEC) Devices. TP-001-NA, Rev. 3.

[EPRI] Electrical Power Research Institute. Bedard. R., November 9, 2005. Survey and Characterization - Tidal in Stream Energy Converters (TISEC) Devices. TP-004-NA.

[EPRI] Electrical Power Research Institute. Polagye, B and Previsic, M., Bedard. R. June 10, 2006. System Level Design, Performance and Cost of Knik Arm Alaska Tidal Power Plant. TP-006-AK Technical Report.

Ersdal, G. 2005. Assessment of existing offshore structures for life extension. Doctoral Thesis, University of Stavanger.

[ESRU] Energy Systems Research Unit. 2013. Baseload Supply Strategy. Available from: http://www.esru.strath.ac.uk/EandE/Web_sites/03-04/marine/strat_siteselect.htm Accessed 2013 April 29.

[EMEC] European Marine Energy Centre Ltd. Available from: http://www.emec.org.uk/. Accessed 2011 Nov 12.

Faraci, V. 2006. Calculating Failure Rates of Series/Parallel Networks, Journal of the System Reliability Center.

FARADIP.THREE. 2006. Failure rate data in perspective, Database, Issue 4.1, Technis.

Feng Y, Tavner PJ and Long H, 2010. Early Experiences with UK Round 1 Offshore Wind Farms, accepted Proceedings of the Institution of Civil Engineers, Energy, 2010.

Flinn, J., Bittencourt-Ferreira, C., 2008. Reliability Estimation Method for Wave and Tidal Energy Converters, Proceedings of the 2nd International Conference on Ocean Energy (ICOE), Brest, France.

Flinn, J., Bittencourt-Ferreira, C. 2011. Uncertain and Unavoidable-Reliability Estimation in Wave and Tidal Energy Systems, 11th International Conference on Applications of Statistics and Probability in Civil Engineering - ICASP'11, Zurich, Switzerland.

Fraenkel, P. L. and Musgrove, P. 1979. Tidal and River Current Energy Systems, IEE Conference on Future Energy Concepts, IEE Publication No 171, 114-117.

Fraenkel, P. L. 2007a. Supporting Structures for Water Current Turbines. Patent US 7307356B2.

Fraenkel, P. L. 2007b. Marine Current Turbines: Moving from Experimental Test Rigs to a Commercial Technology. ASME-OMAE07. 26th International Conference on Offshore Mechanics & Arctic Engineering San Diego, USA. OMAE2007-29642. June 10-15, 2007.

Fraenkel, P. L. 2011. SuperGen Marine Energy Research Consortium Assembly, Edinburg, UK.

Francis, M and Hamilton, M. 2007. SRTT Floating Tidal Turbine Production Design Study With Independent Verification. Report 07/1463. Department for Business, Enterprise and Regulatory Reform. London.

Gorlov, A. M. 2001. Tidal Energy, Northeastern University, Boston, MA, Academic Press.

Green, A. E. and Bourne, A. J. 1978. Reliability Technology. New York: Wiley

Hardisty, J. 2009. The Analysis of Tidal Stream Power. John Wiley & Sons, Ltd.

Hahn, B., Durstewitz, M., Rohrig, K. (2007). Reliability of Wind Turbines. Proceedings of the Euromech Colloquium 464b 2005 Oldenburg, Springer-Verlag Berlin Heidelberg New York, pp. 329-332.

Han, J.S., Kim, Y.H., Son, Y. J. and Choi, H.S. 2010. A comparison study on the fatique life of mooring systems with different composition. 9th International Conference on Hydrodynamics, Shanghai, China.

Harris, L.M. 1972. Deepwater Floating Drilling Operations. Petroleum Publishing Company, Oklahoma, USA.

IEEE Gold Book. 1997. Recommended Practice for the Design of Reliability Industrial and Commercial Power Systems, IEEE Std. 493.

[IPCC] Intergovernmental Panel on Climate Change. 2011. Renewable Energy Sources and Climate Change Mitigation Special Report of the Intergovernmental Panel on Climate Change. Technical Support Unit Working Group III. Potsdam Institute for Climate Impact Research (PIK). Cambridge University Press. Available from: http://www.ipcc.ch/pdf/special-reports/srren/SRREN_Full_Report.pdf. Accessed 2012 July 10.

Lynch, J. Permanent Magnet Generators, Northern Power Systems, 2009.

Mackie, G. 2008a. Floating Apparatus for Deploying in Marine Current for Gaining Energy, US Patent 7541688B2; GB Patent 2422978.

Mackie, G. 2008b. Development for Evopod Tidal Stream Turbine. Proceedings of the International Conference on Marine Renewable Energy, The Royal Institute of Naval Architects, London.

Mackie, G. 2009. Renewable Energy Module: Marine and Offshore Devices. REFLEX Module 10 – SPG 8010. Newcastle University. UK.

Mermiris, N. and Hifi. A. 2008. Risk-Based Decision - Making Framework for Marine Renewable Energy Installations. Proceedings of the International Conference on Marine Renewable Energy, The Royal Institute of Naval Architects. London.

Modarres, Kaminskiy and Krivtsov. 2010. Reliability Engineering and Risk Analysis: A Practical Guide, Second Edition. Boca Raton, FL: CRC Press.

Mosleh, A. 2011. Advanced Reliability Method Module. University of Maryland College Park, US.

Metoc 2010. The World Offshore Renewable Energy Report 2004-2008. Department of Trade and Industry's Renewables. 2010 Target Team, UK.

MIL-STD-721C. 1981. Military Standard. Definition of Terms for Reliability and Maintainability - Revision C. US Department of Defence.

MIL-HDBK-338B. 1998. Electronic Design Reliability Handbook, US Department of Defence.

MIL-HDBK-217F. 1991. Military Handbook. Reliability Prediction of Electronic Equipment - Revision F. US Department of Defence.

MIL-HDBK-217F, Notes 2. 1995. Military Handbook. Reliability Prediction of Electronic Equipment – Notece 2. US Department of Defence.

Nicolls, D. 2006 First quarter. So, Who are You and What Did You Do With The RIAC?. The Journal of the Reliability Information Analysis Centre. Available from: https://acc.dau.mil/adl/en-US/31009/file/5573/Journal-updated-3-10%202.pdf. Accessed 2013 February 12.

Nicolls, D. 2010. Reliability Information Analysis Center (RIAC). *Personal communication.*

[NOAA/NOS] National Oceanic and Atmospheric Administration /National Ocean Service. 2000. Tide and Current Glossary. Available from: http://co-ops.nos.noaa.gov/publications/glossary2.pdf. Accessed 2013 February 12.

[NOAA/NOS] National Oceanic and Atmospheric Administration /National Ocean Service. 2013. Tidal Range Predictions. US Department of Commerce. Available from: http://tidesandcurrents.noaa.gov/, version 2013 May 20. Accessed 2013 February 7.

Nobeltec Tides & Currents. 2011. PC Navigation Software. Nobeltec, Inc. Available from: http://cms.nobeltec.com/cms/Products/NavigationData/TidesCurrents.aspx. Accessed 2013 February 7.

Noble Denton Europe Ltd. 2006. Floating production system JIP FPS mooring integrity. Research Report 444 for the Health and Safety Executive (HSE).

NPRD-95. 1995. Non Electronic Parts Reliability Data, Reliability Information and Analysis Center (RAC), Utica, New York, USA.

NPRD-2011. 2011. Non Electronic Parts Reliability Data, Reliability Information and Analysis Center (RAC), Utica, New York, USA.

Okorie, O. P., Owen, A., Pollard, P. and Hossain,, M. 2011. Study of Coherent Structures Suitable for Numerical Testing of Tidal Current Energy Devices.

Okorie, O. P. 2011. Scale effects in testing of a monopole support structure submerged in tidal currents. Available from: http://openair.rgu.ac.uk. Accessed 2012 November 1.

OpenHydro Group Ltd. 2011. Open-Centre Turbine. Homepage on the Internet. Available from http://www.openhydro.com/. Accessed 2011 October 1.

[OREDA] Offshore Reliability Data1984-2009:

1984. Offshore Reliability Data Handbook. VERITEC – Marine Technology Consultants, PennWellBooks, 1st edition.

1997. Offshore Reliability Data Handbook. SINTEF Industrial Management. Det Norske Veritas, Norway, 3rd edition.

2002. Offshore Reliability Data Handbook. SINTEF Industrial Management. Det Norske Veritas, Norway, 4th edition.

2009. Offshore Reliability Data Handbook. SINTEF Industrial Management. Det Norske Veritas, Norway, 5th edition.

Papanikolaou, A. 2006. Analysis of AFRAMAX Tankers Accidents. International workshop on marine oil pollution control, Athens, Greece.

Rausand, M. and Hoyland, A. 2004. System Reliability Theory: Models, Statistical Methods, and Applications, 2nd edition, John Wiley & Sons, Inc.

[RIAC&DACS] Reliability Information Analysis Center and Data Analysis Center for Software. 2005. System Reliability Toolkit, A Practical Guide for Understanding and Implementing a Program for System Reliability. US Department of Defence.

[RIAC] Reliability Information Analysis Center. 2010. Reliability Modeling - The RIAC Guide to Reliability Prediction, Assessment and Estimation. US Department of Defence.

Richard, J., Bard, J., Rudolph, C. and M. Milovich. 2012. Assessing the Capabilities of Acoustic Doppler Sensors for Quantifying Dynamic Phenomena in Tidal Streams. 4th International Conference on Ocean Energy - ICOE 2012, Dublin 17-19th October 2012, Republic of Ireland.

Salter S.H. 2012. Are Nearly all Tidal Stream Turbine Designs Wrong? 4th International Conference on Ocean Energy - ICOE 2012, Dublin 17-19th October 2012, Republic of Ireland.

SD-18. 2006. Program Guide for Parts Requirements and Application. Defense Standardization Program. Naval Surface Weapons Center, Crain, IN.

Smith D. J. 2001. Reliability, Maintainability and Risk, Butterworth-Heinemann, Oxford.

Spinato, F., Tavner, P. J., van Bussel, G. J. and Koutoulakos, E. 2009. Reliability of Wind Turbine Sub-assemblies. IET Renewable Power Generation 3(4): 387-401.

Spooner, E. 2008. A Hydroelectric Turbine. Patent EP 1879 280 A1.

Schureman, P. 1971. US Department of Commerce, Coast and Geodetic Survey. Manual of harmonic analysis and prediction of tides. Special publication No.98 revised 1940 edition. United States Government Printing Office, Wachington DC, 1958.

Tavner, P. J., Xiang, J. P. and Spinato, F. Improving the Reliability of Wind Turbine and its Impact on Overall Distribution Network Reliability. Proceedings of CIRED Conference, Turin, 2005.

Tavner, P. J., Xiang, J. and Spinato, F. 2007. Reliability Analysis for Wind Turbines: Wind Energy pp. 1-18. Vol 10.

Tavner, P. J., Faulstich, S. and van Bussel G. J. W. 2010. Reliability & Availability of Wind Turbine Electrical & Electronic Components. EPE: European Power Electronics and Drives Association J., 20(4): 44-50.

Tavner, P. J. 2012. Wind Turbine Reliabiltiy – Can we see the Effects of Turbulence. Presentation. Durham University School of Engineering and Computer Sciences.

Thies, P. R. 2009. Reliability of Wave Energy Converters. Dissertation for University of Exeter in Cornwall. University of Flensburg. Unpublished.

Thies, P. R., Flinn, J., Smith, G. H. 2009. Is it a Showstopper? Reliability Assessment and Criticality Analysis for Wave Energy Converters. 8th European Wave and Tidal Energy Conference, Uppsala, Sweden, 7-10 September.

Thies, P.R. and Johanning, L. 2010. Development of A Marine Component Testing Facility For Marine Energy Converters. Proceedings of the 3rd International Conference on Ocean Energy – ICOE 2010, 6th–8th October 2010, Bilbao, Spain.

Thies, P. R., Johanning, L., and Smith G. H .2011. Towards Component Reliability Testing for Marine Energy Converters. Ocean Engineering, Vol. 38, issue 2-3, pp. 360–370.

Thies, P. R., Smith, G. H. and Johanning, L 2012. Addressing Failure Rate Uncertainties of Marine Energy Converters. Renewable Energy, Vol. 44, pp. 359-367. Available from: www.elsevier.com/locate/renene. Accessed 2013 December 10.

University of Southampton, 2008. Tidal-current Energy Device Development and Evaluation Protocol, URN 09/1317. Department of Energy and Climate Change, UK. Available from: http://webarchive.nationalarchives.gov.uk/+/http://www.berr.gov.uk/files/file48401.pdf. Accessed 2012 January 10th.

Usachev, N., Shpolyanskii, Y. B., Istorik, B. L., Pastukhov, V. P., Kondrashov, Y. V., Borodin, V. V., Savchenkov, S. N. and Kushnerik, V. I. 2007. Construction of a Standard Floating Power Generating Unit for a Tidal Power Plant, Power Technology and Engineering 41(6).

Val, D.V. 2009. Aspects of Reliability Assessment of Tidal Stream Turbines. Proceedings of the 10th International Conference on Structural Safety and Reliability - ICOSSAR 2009, Osaka, Japan, 13-17 September 2009.

Val, D.V. and Chernin, L. 2011. Reliability of Tidal Stream Turbine Blades. Applications of Statistics and Probability in Civil Engineering. Faber, Kohler & Nishijima (eds), Taylor & Francis Group. London.

Val, D.V. and Iliev, C. 2011. Reliability of Power Train Components in Tidal Stream Turbines. 11th International Conference on Applications of Statistics and Probability in Civil Engineering – ICASP 11, Zurich, 1-4 August, 2011. Faber, Kohler & Nishijima (eds), Taylor & Francis Group. London.

VGB PowerTech. 2007. Guideline: Reference Designation System for Power Plants (RDS-PP). Application Explanation for Wind Power Plants, VGB-B 116 D2, Germany.

Watson, R.T., Zinyowera, M.C., and Moss R.H. eds. 1996. Technologies, Policies and Measures for Meetigating Climate Change. Technical paper for Intergovernmental Panel on Climate Change (IPCC) Group II. Available from: http://www.ipcc.ch/pdf/technical-papers/paper-I-en.pdf. Accessed 2011 November 10.

Wicks, M., Member of Parliament. 2008. PRASEG Sustainable Energy Awards Ceremony, The Commonwealth Club. London.

Windows WXTide32 Tide and Current Prediction Program. Available from: http://www.wxtide32.com/download.html. Accessed 2013 January 20.

Wood, J.K., Bahaj, A.S., Turnock, S. R., Wang L. and Evans, M. 2010. Tribological Design Constraints of Marine Renewable Energy Systems. Philosophical Transactions of The Royal Society A (2010) 368, 4807-4827.

Wolfram, J. 2006. On Assessing The Reliability and Availability of Marine Energy Converters: The Problems of a New Technology, Proceedings of the Institution of Mechanical Engineers, IMechE, 220(O), pp. 55-68.

Y-ARD Ltd 1980. Reliability Study of Wave Power Devices. Memorandum No 3551/80 Report ETSU 1581. Energy Technology Support Unit. AEA Technology. Harwell, UK.

10. **Appendix 1: Terminology**

This section defines the terminology for power plant industries and reliability terms used in this Thesis. The terminologies were adapted from DOE (2011), RIAC&DACS (2005) and VGB PowerTech (2007) but some were created to satisfy the Thesis content.

Table 10.1 Basic Definitions of Terms

Term	Definition
Alternating Current, AC	Electric charge flow is in directions periodically reversible
Ancillary systems	Systems which are not directly required for the power plant process. This includes heating, ventilation, air-conditioning systems etc.
Availability factor	A measure of the degree to which an item is in an operable state at any time
Axial Flow Turbine	Turbine with two or three rotor blades mounted on a horizontal shaft to form a rotor; the kinetic motion of the water current creates lift on the blades causing the rotor to turn driving a mechanical generator. These turbines must be oriented in the direction of flow. There are shrouded and open rotor models.
Code letter	Alphabetic character providing classifying information
Component	An individual part of equipment
Cross Flow Turbine	Turbine with two or three blades mounted along a vertical shaft to form a rotor; the kinetic motion of the water current creates lift on the blades causing the rotor to turn driving a mechanical generator. These turbines can operate with flow from multiple directions without reorientation. There are shrouded and open rotor models.
Direct current, DC	Electric charge flow is only in one direction
Device/Equipment/System	A complete piece of machinery able of performing a required function on its own
Exponential distribution	A probability density function, describes systems which have a constant failure rates
Failure of the item as a function of time $F(t)$	The probability that the item will fail before time t
Failure Rate $\lambda(t)$	The total number of failures within the item population, divided by the total time expanded by the population, during a particular measurement interval under stated conditions
Hub	Fixture for attaching the blades or blade assembly to the rotor shaft

Hazard rate *h(t)*	Instantaneous failure rate, defined as a limit to failure intensity rate when time difference approaches to zero
Mission reliability	The total amount of mission time, divided by the total number of critical failures during a stated series of missions. (MIL-STD-721B)
Nacelle	Housing which contains the drive train and other elements
Oscillating Hydrofoil (Example of a Reciprocating Device)	Turbine is similar to an airplane wing but in water; yaw control systems adjusts their angle relative to the water stream, creating lift and drag forces that cause device oscillation; mechanical energy from this oscillation feeds into a power conversion system.
Random failures	Failures occurring during 'useful life period' of equipment, they occur unpredictably.
Reliability	(1) The duration or probability of failure-free performance under stated conditions. (2) The probability that intended function item can perform its intended function for a specified interval under stated conditions. For non-redundant items, this is equivalent to definition (1). For redundant items, this is equivalent to definition of mission reliability. (MIL-STD-721B).
Redundancy	The existence one or more means (not necessarily identical) for accomplishing one or more function. Active redundancy has all items operating simultaneously. Standby redundancy has alternate means activated upon failure
Reliability Model	A system model for identification of framework which integrates sub-systems interrelations for reliability analysis and assessment
Reliability Survivor Function *R(t)*	The probability that an item will perform its intended function for a specified interval under stated conditions
Reliability Prediction	A measure for estimation product reliability performance figures of merit
Reciprocating Device:	Uses the flow of water to produce the lift or drag of an oscillating part transverse to the flow direction. This behavior can be induced by a vortex, the Magnus effect, or by flow flutter.
System	A set of interrelated objects
Sub-system	An element within a system
Support structure	Part of a tidal turbine comprising the tower and foundation
Object	Entity treated in the process of design, engineering, operation, maintenance and demolition

11. **Appendix 2: Types of TSD Technology**

The following list taken from the European Marine Energy Centre (EMEC) Ltd website, http://www.emec.org.uk/marine-energy/tidal-developers/. Accessed 2012 May 1.

Table 11.1 Current TSDs under consideration

COMPANY	TECHNOLOGY	BASE COUNTRY
Alstom Hydro	Clean Current Tidal Turbine	France
Aquamarine Power	Neptune	UK
Aquantis Inc	C-Plane	USA
Atlantis Resources Corp	AK-1000	UK
Atlantisstrom	Atlantisstrom	Germany
Aquascientific	Aquascientific Turbine	UK
Balkee Tide and Wave Electricity Generator	TWPEG	Mauritius
BioPower Systems Pty Ltd	bioStream	Australia
Blue Energy	Blue Energy Ocean Turbine (Davis Hydro Turbine)	Canada
Bluewater	BlueTec	Netherlands
BluStream	MegaWatForce	France
Bourne Energy	CurrentStar / TidalStar / OceanStar	USA
Cetus Energy	Cetus Turbine	Australia
Clean Current Power Systems	Clean Current Tidal Turbine	Canada
Crest Energy		New Zealand
Current2Current	Tidal Turbine	UK
Current Power AB	Current Power	Sweden
Ecofys	Wave Rotor	Netherlands
Edinburgh Designs	Vertical-axis, variable pitch tidal turbine	UK
Edinburgh University	Polo	UK
Fieldstone Tidal Energy	Fieldstone Tidal Energy	USA
Firth Tidal Energy	Sea Caisson & Turbine System (SEACATS)	UK
Flumill	Flumill Power Tower	Norway
Free Flow 69	Osprey	USA
Free Flow Power Corporation	SmarTurbine	USA
GCK Technology	Gorlov Turbine	USA
Greener Works Limited	Relentless™ Turbine	UK
Greenheat Systems Ltd	Gentec Venturi	UK
Hales Energy Ltd	Hales Tidal Turbine	UK
Hammerfest Strom	Tidal Stream Turbine	Norway
Hydra Tidal Energy Technology AS	Morild ©	Norway
Hydro Green Energy	Hydrokinetic Turbine	USA
Hydro-Gen	Hydro-gen	France
HydroCoil Power, Inc	HydroCoil	USA
Hydrohelix Energies	Hydro-Helix	France
Hydrokinetic Laboratory	HyPEG	USA
Hydromine	The Hydro Mine	UK
Hydroventuri	Rochester Venturi	UK
Hydrovolts Inc	Hydrovolts	USA

Ing Arvid Nesheim	Waterturbine	Norway
Kepler Energy	Transverse Horizontal Axis Water Turbine (THAWT)	UK
Keys Hydro Power		USA
Kinetic Energy Systems	Hydrokinetic Generator, KESC Bowsprit Generator, KESC Tidal Generator	USA
Lucid Energy Technologies	Gorlov Helical Turbine (GHT)	USA
Lunar Energy	Rotech Tidal Turbine	UK
Magallanes Renovables	Magallanes Project	Spain
Marine Current Turbines	SeaGen, Seaflow	UK
Minesto	Deep Green Technology	Sweden
Natural Currents	Red Hawk	USA
Nautricity Ltd	CoRMaT	UK
Neo-Aerodynamic Ltd Company	Neo-Aerodynamic	USA
Neptune Systems	Tide Current Converter	Netherlands
Neptune Renewable Energy Ltd	Proteus	UK
New Energy Crop.	EnCurrent Vertical Axis Hydro Turbine	Canada
Norwegian Ocean Power	The Pulsus Turbine	Norway
Ocean Flow Energy	Evopod	UK
Ocean Renewable Power Company	OCGen	USA
Oceana Energy Company	TIDES	USA
Offshore Islands Ltd	Current Catcher	USA
OpenHydro	Open Centre Turbine	Ireland
Ponte di Archimede	Kobold Turbine / Enermar	Italy
Pulse Tidal	Pulse-Stream	UK
Robert Gordon University	Sea Snail	UK
Rotech	Rotech Tidal Turbine (RTT)	UK
Rugged Renewables	Savonius turbine	UK
Scotrenewables	SR250	UK
SMD Hydrovision	TiDEL	UK
Sustainable Marine Technologies (SMT)	PLAT-O	UK
Starfish Electronics Ltd	StarTider	UK
Statkraft	Tidevanndkraft	Norway
Swanturbines Ltd.	Swan Turbine	UK
Teamwork Tech.	Torcado	Netherlands
The Engineering Buisiness	Stingray	UK
Tidal Electric	Tidal Lagoons	UK/USA
Tidal Energy Ltd	Delta Stream	UK
Tidal Energy Pty Ltd	DHV Turbine	Australia
Tidal Generation Limited	Deep-gen	UK
Tidal Sails	Tidal Sails AS	Norway
TidalStream	TidalStream Triton Platform	UK
Tideng	Tideng	Denmark
Tocardo BV	Tocardo Turbines	Netherlands
UEK Corporation	Under-water Electric Kite	USA
University of Southampton	Southampton Integrated Tidal Generator	UK
Verdant Power	Various	USA
Voith Hydro	Hytide	Germany
Vortex Hydro Energy	VIVACE (Vortex Induced Vibrations Aquatic Clean Energy)	USA
Water Wall Turbine	WWTurbine	USA
Woodshed Technologies - CleanTechCom Ltd	Tidal Delay	Australia / UK

12. **Appendix 3: Reliability Assessment Methods**

Table 12.1[1] Most Commonly Used System Reliability Methods

RELIABILITY ASSESSMENT METHODS				
Methods	**Purpose**	**Application**	**Limitations**	**Use**
Reliability Modelling and Predictions: (RMP) Modelling – FBD & RBD Parts Count Reliability Prediction Technique (PCRPT)	To quantitatively evaluate the reliability of competing design. To direct reliability related design decisions. Identifies framework and integrates systems interrelationships for analyses and assessment. Uses system models, failure rates and repair rates to estimate device reliability. Enables trade-off with respect to different design approaches	Perform early in the design phase. More beneficial for new designed hardware. Applicable to all types of hardware. Surrogate data can be used before part-level testing provides first-hand data. However, predictions using surrogate data should be used for comparing design approaches, not for making absolute predictions	Deterministic & conservative assessment	Proposed for TSD system reliability assessment.
Failure Modes, and Effects and Analysis (FMEA)	Bottom up approach to identify single failure points and their effects. To assist in the efficient design of built-in test and fault isolations test. To identified interface problems.	Perform early in the design phase to help improve design. Use when investigation of all possible failures modes is critical. More appropriate for equipment performing critical functions (e.g., control systems)	Method is labor-intensive for use with highly complex or interconnected paths. It does not identify potential failure due to "human error", Need more data than RBD.	Will not be used for system evaluation as we do not have the information needed for FMEA
Fault Tree Analysis (FTA)	Top down functional analysis to identify effects of faults on system performance. Systematic deductive methodology for defining a single specific undesirable event. FTA can be considered an assessment but only if failure rates or probability of occurrence can be assigned to all sub-systems; otherwise, only the single point failures and multiple failure sets can be identified but no estimate of reliability can be made.	Use during initial device design when primary concern is safety, human error or some other explicit "top event". More limited in scope and easier to understand than FMECA. Results may be useful for troubleshooting after the device built.	Difficulty in distinguishing between dependent and independent events in the construction of the fault tree.	Will not be used for system evaluation as we do not have the information needed for FTA
System Simulations Analysis: Monte Carlo Algorithms Variety of Algorithms: Software Tools - RAPTOR, BlockSim, and AvSim+	To quantitatively evaluate the reliability of competing design. To direct reliability related design decisions. Uses system models, failure rates and repair rates to estimate device reliability. Enables trade-off with respect to different design approaches. Used for complex topologies when reduction to series and parallel connections not possible (i.e., RBD is insufficient). Used to evaluate additional aspects of system performance. Probabilistic reliability assessment. Provides dependency information, capacity information, changes between operating phases.	Perform early in the design phase as detailed data becomes available. More beneficial for new designed hardware. Applicable to all types of hardware.	Requires a lot of data	Proposed for future studies
Bayesian model	Further assessing systems reliability, uncertainties	Future prediction of sub-assemblies	Selection of prior distribution, the amount of available data	Proposed for future studies.

[1] The topology for this table was adapted from RIAC&DUCS (2005), Criscimagna, N. H. (2010), *pers. comm.* and modified to support the aim of author's proposed research.

13. **Appendix 4: Models & Results**

13.1 PSD: Portfolio of Surrogate Data

Table 13.1 Surrogate Failure Rate Data Sources

Data Source	Reference
[1]	Hahn et al. (2007)
[2]	Spinato et al. (2008)
[3]	Tavner et al. (2010; 2012)
[4]	NPRD-95 (1995)
[5]	OREDA (1984-2009)
[6]	MIL-HDBK-217F (1991)
[7]	IEEE Gold Book (1997)
[8]	Lynch (2009)
[9]	Noble Denton Europe Ltd (2006)
[10]	Papanikolaou (2006)
[11]	CAPP 30605 (2012)
[12]	Harris (1972)
[13]	Han et al. (2010)
[14]	Cederstrom et al. (2005)
[15]	Ersdal (2005)

13.2 TSD1

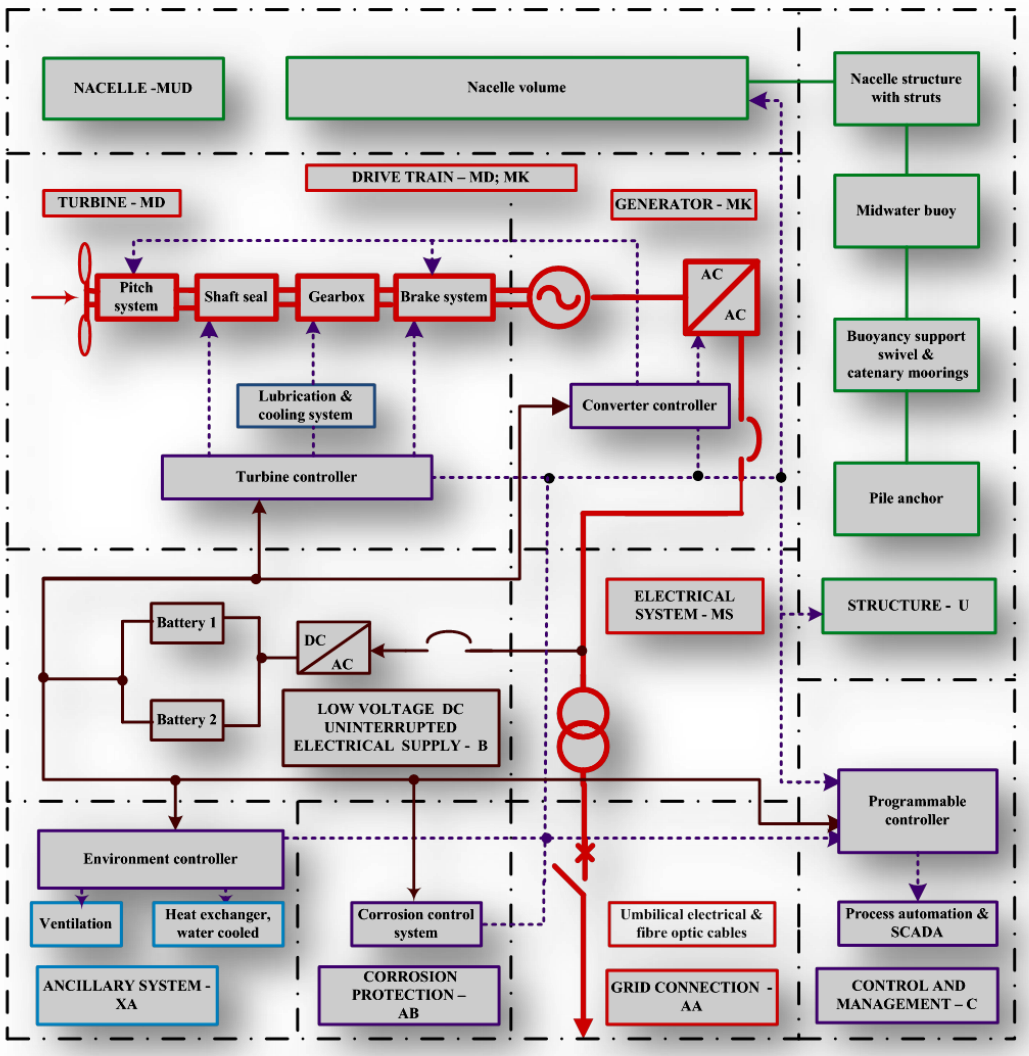

Figure 13.1 TSD1 schematic diagram

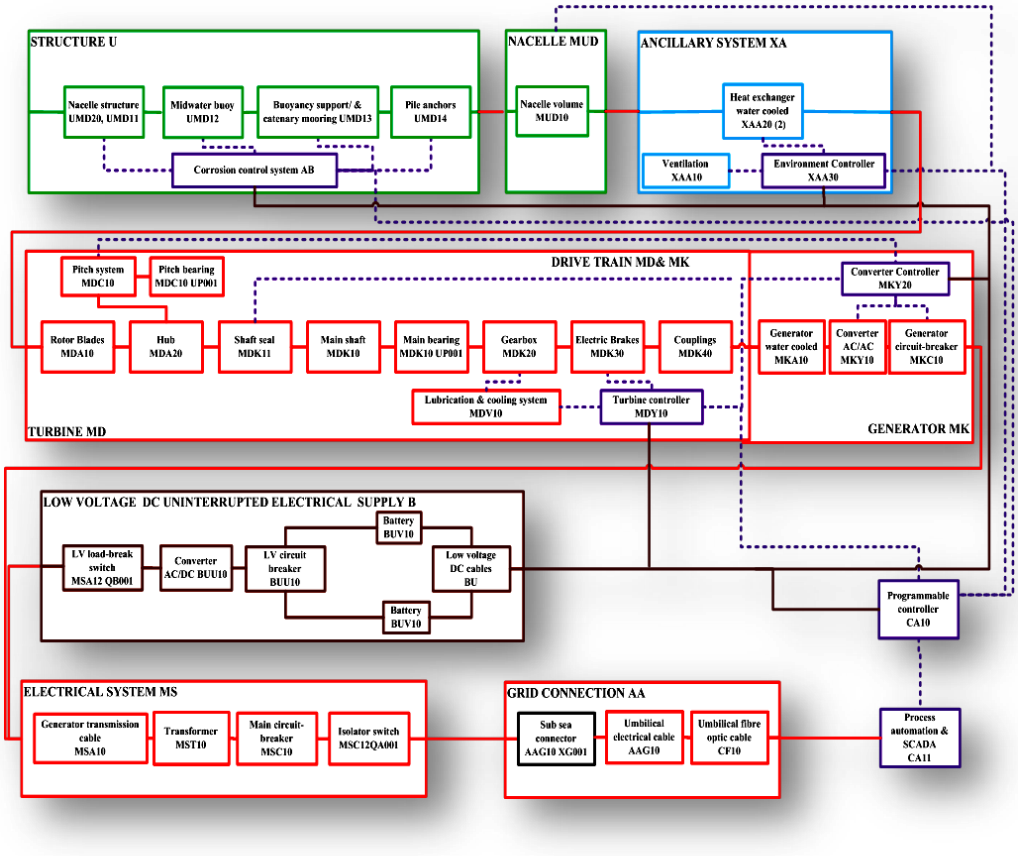

Figure 13.2 TSD1 FBD or RBD1

Table 13.2 TSD1 Parts Structure &Annual Failure Rate Range

RELIABILITY CHARACTERISTICS FOR:					Surrogate data failure rates (Failures/year)			Failure Rate Estimate λi_FREcon (Failures/year)	Failure Rate Estimate λi_FREenv (Failures/year)		
System/Branch	Number of subassembly i = 1 to Nb	VGB Code	Subassemblies	Qt	Data Source Table 13.1		λG_{i_min}	λG_{i_max}	Predicted total failure rate (Failures/year)	Environment adjustment	Adjusted single subassembly failure rates	Predicted total failure rate (Failures/year)
									$\lambda i\_FREcon = \lambda Gi\_max$	π_{Ei}	$\lambda Gi\_max * \pi Ei$	$\lambda i\_FREenv = \lambda Gi\_max * \pi Ei$
DRIVE TRAIN (MDK&MK)	1	MDA10	Pitchable Rotor Blades	3	[1]	[2]	0.115	0.230	0.230	3.3	0.759	0.759
	4	MDA20, MDC10, MDC10UP001	Hub, pitch system, pitch bearing	1	[1]	[2]	0.083	0.177	0.177	1.0	0.177	0.177
	7	MDK10, MDK10 UP001, MDK40	Main shaft, main bearing, couplings	1	[1]	[2]	0.031	0.055	0.055	1.0	0.055	0.055
	8	MDK11	Shaft seal	1	[4]		0.061	0.061	0.061	1.0	0.061	0.061
	10	MDK20, MDV10	Gearbox, Lubrication & cooling system	1	[1]	[2]	0.101	0.134	0.134	1.7	0.228	0.228
	11	MDK30	Electric brakes	1	[4]		0.031	0.031	0.031	1.0	0.031	0.031
	12	MKA10	Generator, induction water cooled	1	[1]	[2]	0.106	0.139	0.139	1.7	0.236	0.236
	14	MKY10, MKY20	Converter AC/AC, Converter controller	1	[1]	[2]	0.239	0.430	0.430	1.7	0.731	0.731
	15	MKC10	Generator circuit-breaker	1	[5]		0.020	0.175	0.175	1.0	0.175	0.175
ELECTRICAL SYSTEM (MS)	16	MSA10	Generator transmission cable	1	[4]		0.010	0.010	0.010	1.0	0.010	0.010
	17	MST10	Transformer (400V/11kV), including cooling	1	[5]		0.008	0.081	0.081	1.0	0.081	0.081
	18	MSC10	Main circuit-breaker	1	[5]		0.020	0.175	0.175	1.0	0.175	0.175
	19	MSC12 QA001	Isolator switch	1	[5]		0.000	0.037	0.037	1.0	0.037	0.037
LOW VOLTAGE DC UNINTERRUPTABLE ELECTRICAL SUPPLY (B)	20	MSA12 QB001	LV load-break switch	1	[5]		0.005	0.010	0.010	1.0	0.010	0.010
	21	BUU10	Converter AC/DC	1	[5]		0.000	0.015	0.015	1.0	0.015	0.015
	22	BUU11	LV Supply 400V circuit breaker	1	[5]		0.005	0.010	0.010	1.0	0.010	0.010
	23	BUV10	Battery	2	[5]		0.032	0.147	0.098	1.0	0.147	0.098
	24	BU	Low-voltage DC cables	1	[6]		0.010	0.010	0.010	1.0	0.010	0.010
GRID CONNECTION (AA)	25	AAG10 XG001	Sub sea connector	1	[5]		0.000	0.009	0.009	1.0	0.009	0.009
	26	AAG10	Umbilical electrical cable, 11kV	1	[5]		0.042	0.111	0.111	1.0	0.111	0.111
	27	CFA10	Umbilical fibre optic cable	1	[6]		0.010	0.016	0.016	1.7	0.027	0.027
ANCILLARY SYSTEM (XA)	28	XAA10	Ventilation	1	[4]		0.105	0.105	0.105	1.0	0.105	0.105
	29	XAA20	Heat exchanger, water cooled	2	[5]		0.002	0.263	0.175	1.0	0.263	0.175
CONTROL & MANAGEMENT (CA)	30	CA10	Programmable controller	1	[5]		0.241	0.630	0.630	1.0	0.630	0.630
	31	MDY10	Turbine controller	1	[5]		0.057	0.151	0.151	1.0	0.151	0.151
	32	XAA30	Environment controller	1	[5]		0.045	0.117	0.117	1.0	0.117	0.117
	33	CA11	Process automation & SCADA	1	[5]		0.286	0.754	0.754	1.0	0.754	0.754
CORROSION PROTECTION (AB)	34	AB	Corrosion control system	1	[5]		0.045	0.117	0.117	1.0	0.117	0.117
Nacelle MUD)	36	MUD10	Nacelle volume	1	10		0.001	0.001	0.001	3.0	0.003	0.003
STRUCTURE (U)	37	UMD20 EA001 UMD11UA001 UL002 UP001	Nacelle structure with struts	1	[10]		0.009	0.009	0.009	1.0	0.009	0.009
	38	UMD12 UA001 UL001	Midwater buoy	1	[10]	[15]	0.009	0.050	0.050	1.0	0.050	0.050
	39	UMD13UA001 UL001 UP001	Buoyancy support, swivel	1	[15]		0.050	0.050	0.050	1.0	0.050	0.050
	41		Connecting links	4	[12]	[9]	0.100	0.185	0.171	1.0	0.185	0.171
	43		Catenary mooring, chain with steel wire rope	4	[13]	[9]	0.024					
	45	UMD14	Pile anchor	4	[14]	[9]	0.008					
DEVICE TOTAL FAILURE RATE, $\lambda tot10056$ (Failures/unit/year)									4.345			5.379
RELIABILITY SURVIVOR FUNCTION, $R(1year)$, 36									1.3036			0.4636

13.3 TSD2

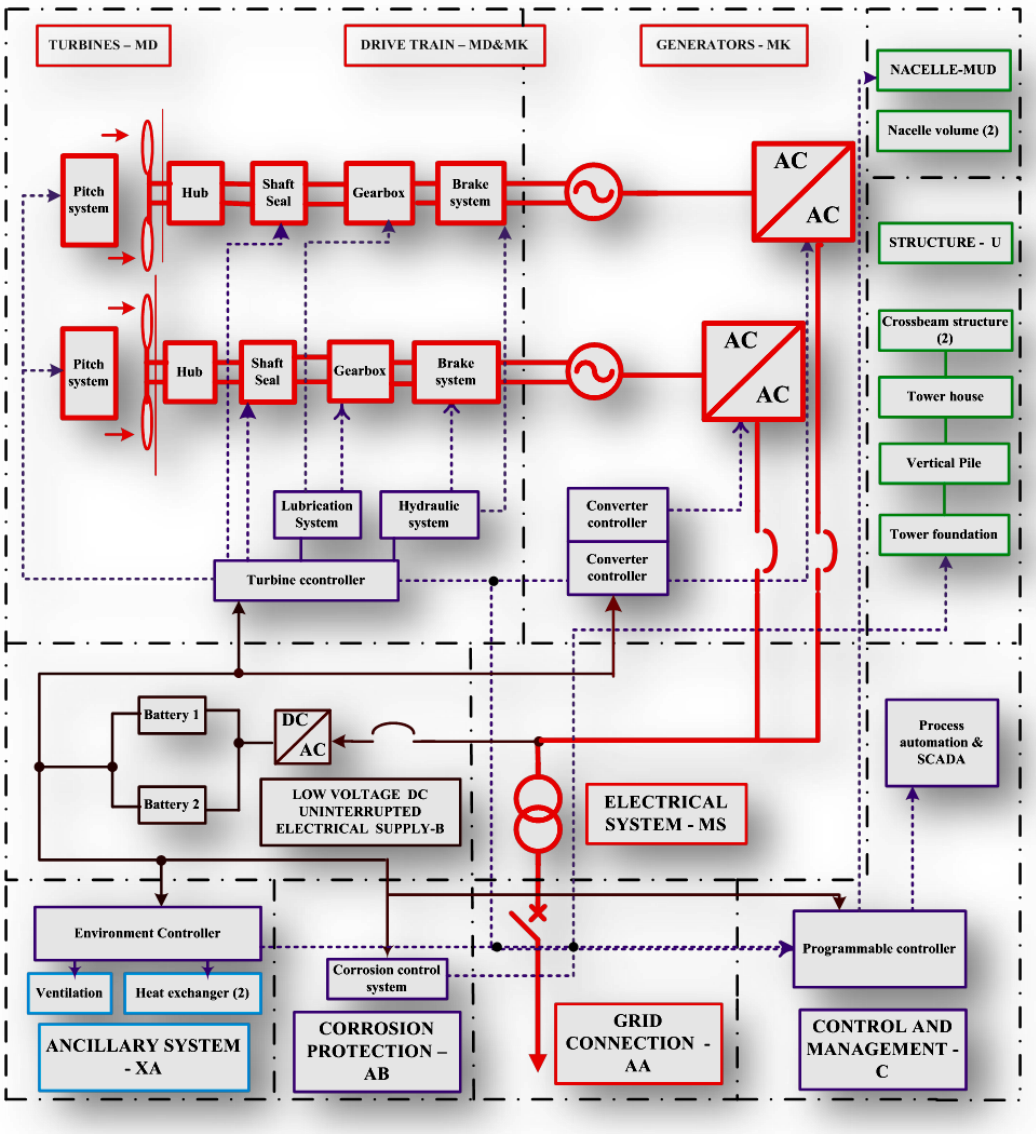

Figure 13.3 TSD2 schematic diagram

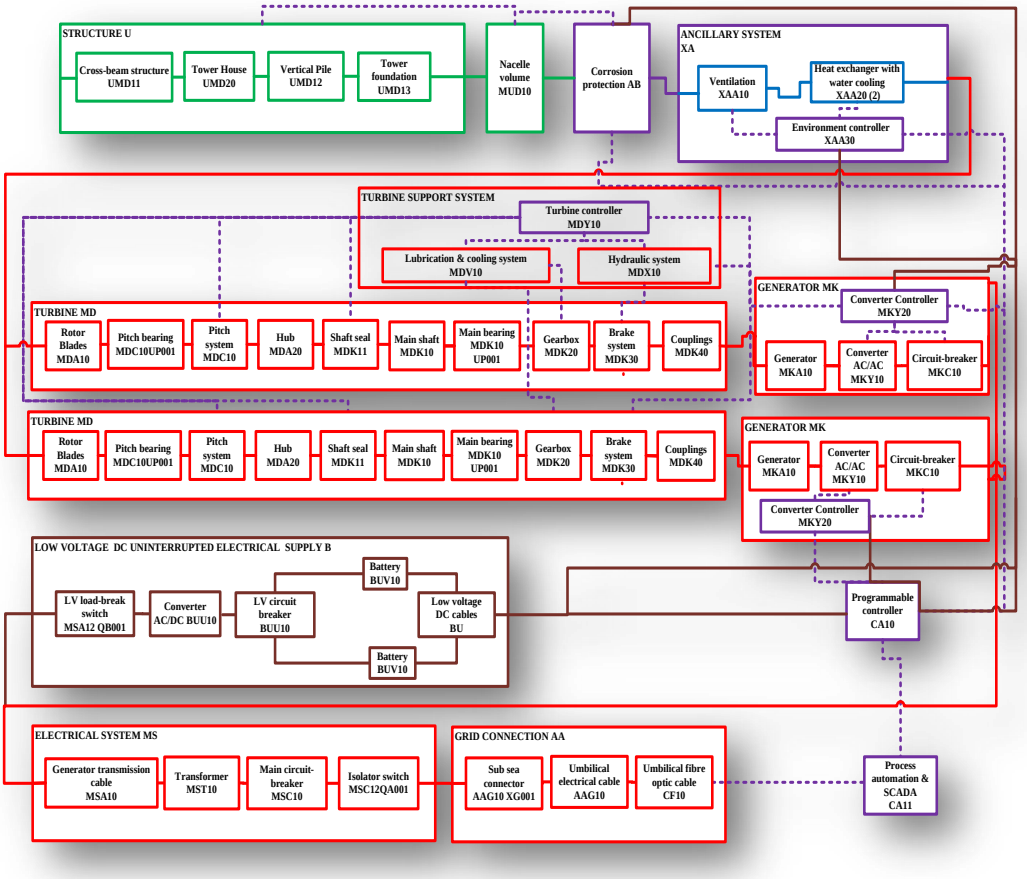

Figure.13.4 TSD2 functional block diagram (FBD) or RBD2

Table 13.3 TSD2 Parts Structure & Annual Failure Rate Range

RELIABILITY CHARACTERISTICS FOR:					Surrogate data failure rates (Failures/year)			Failure Rate Estimate λi_FREcon (Failures/year)		Failure Rate Estimate λi_FREenv (Failures/year)			
System/Branch	Number of subassembly i = 1 to N6	VGB Code	Subassemblies	Qt	Data Source Table 13.1	λG_{i_min}	λG_{i_max}	Predicted Total Failure Rate (Failures/year)		Environment adjustment factor	Adjusted single subassembly failure rates	Predicted total failure rate (Failures/year)	
								$\lambda i\_FREcon100\% = \lambda Gi\_max$	$\lambda i\_FREcon50\% = \lambda Gi\_max$	π_{Ei}	$\lambda Gi\_max * \pi Ei$	$\lambda i\_FREenv100\% = \lambda Gi\_max * \pi Ei$	$\lambda i\_FREenv50\% = \lambda Gi\_max * \pi E$
Drive Train (MDS& MK)	1	MDA10	Pitchable rotor blades	4	[1][2] [3]	0.115	0.230	0.460	1.031	3.3	0.759	1.518	1.775
	4	MDA20, MDC10, MDC10UP001	Hub, pitch system, pitch bearing	2	[1][2] [3]	0.083	0.177	0.354		1.0	0.177	0.354	
	7	MDK10, MDK10 UP001, MDK40	Main shaft, main bearing, couplings	2	[1][2] [3]	0.031	0.055	0.110		1.0	0.055	0.110	
	8	MDK11	Shaft seals	2	[4]	0.061	0.061	0.123		1.0	0.061	0.123	
	10	MDK20, MDV10	Gearbox, Lubrication & cooling system	2	[1][2] [3]	0.101	0.134	0.268		1.7	0.228	0.456	
	12	MDK30, MDX10	Brake systems, Hydraulic system	2	[1][2] [2]	0.055	0.135	0.270		1.7	0.230	0.459	
	13	MKA10	Generator, induction	2	[1][2] [3]	0.106	0.139	0.278		1.7	0.236	0.472	
	15	MKY10, MKY20	Converter AC/AC, Converter controller	2	[1][2] [3]	0.239	0.430	0.860		1.7	0.731	1.462	
	16	MKC10	Generator circuit breaker	2	[5]	0.020	0.175	0.350		1.0	0.175	0.350	
Electrical System (MS)	17	MSA10	Generator transmission cable	2	[4]	0.010	0.010	0.020		1.0	0.010	0.020	
	18	MST10	Transformer, including cooling (400V/11kV)	1	[5]	0.008	0.081	0.081	0.081	1.0	0.081	0.081	0.081
	19	MSC10	Main circuit-breaker	1	[5]	0.020	0.175	0.175	0.175	1.0	0.175	0.175	0.175
	20	MSC10 QA	Isolator switch	1	[5]	0.000	0.037	0.037	0.037	1.0	0.037	0.037	0.037
Low Voltage DC Uninterrupted Electrical Supply (B)	21	MSA12 QB001	LV load-break switch	1	[5]	0.005	0.011	0.011	0.011	1.0	0.011	0.011	0.011
	22	BUU10	Converter AC/DC	1	[5]	0.000	0.015	0.015	0.015	1.0	0.015	0.015	0.015
	23	BUU11	LV Supply 400V circuit breaker	1	[5]	0.005	0.011	0.011	0.011	1.0	0.011	0.011	0.011
	24	BUV10	Battery	2	[5]	0.032	0.147	0.098	0.098	1.0	0.147	0.098	0.098
	25	BU	Low-voltage DC electrical supply cables	2	[6]	0.010	0.010	0.020	0.007	1.0	0.010	0.020	0.007
Grid Connection (AA)	26	AAG10 XG001	Subsea connector	1	[5]	0.000	0.009	0.009	0.006	1.0	0.009	0.009	0.009
	27	AAG10	Umbilical electrical cable, 11 kV	1	[5]	0.042	0.111	0.111	0.111	1.0	0.111	0.111	0.111
	28	CFA10	Umbilical fibre optic cable	1	[6]	0.010	0.016	0.016	0.016	1.7	0.027	0.027	0.027
Ancyllary System (XA)	30	XAA10	Ventilation	1	[4]	0.105	0.105	0.105	0.105	1.0	0.105	0.105	0.105
	31	XAA20	Heat exchanger water cooled	2	[5]	0.006	0.140	0.094	0.094	1.0	0.140	0.094	0.062
Control & Management (CA)	33	CA10	Programmable controller	1	[5]	0.239	0.630	0.630	0.630	1.0	0.630	0.630	0.630
	34	MDY10	Turbine controller	1	[5]	0.124	0.328	0.655	0.218	1.0	0.328	0.655	0.218
	35	XAA30	Environment controller	1	[5]	0.044	0.117	0.117	0.117	1.0	0.117	0.117	0.117
	36	CA11	Process automation & SCADA	1	[5]	0.286	0.754	0.754	0.754	1.0	0.754	0.754	0.754
Corrosion Protection (AB)	37	AB	Corrosion control system	1	[5]	0.044	0.117	0.117	0.117	1.0	0.117	0.117	0.117
Nacelle MUD)	38	MUD10	Nacelle volume	2	[10]	0.001	0.001	0.002	0.034	1.0	0.001	0.002	0.034
Structure (U)	39	UMD11 UA001 UB001 UL0001	Cross-beam structure	2	[10] [15]	0.001	0.050	0.100		1.0	0.050	0.100	
	40	UMD20	Tower House	1	[10] [15]	0.001	0.050	0.050	0.050	1.0	0.050	0.050	0.050
	41	UMD12 UA001 UB001 UL001	Vertical Pile	1	[10] [15]	0.001	0.050	0.050	0.050	1.0	0.050	0.050	0.050
	42	UMD13	Tower foundation	1	[10] [15]	0.001	0.050	0.050	0.050	1.0	0.050	0.050	0.050
DEVICE TOTAL FAILURE RATE, $\lambda tot100\%$ (Failures/unit/year)								*6.400*	*3.816*			*8.642*	*4.543*
RELIABILITY SURVIVOR FUNCTION, R(1 year), 36								*0.16636*	*2.20236*			*0.01836*	*1.06436*

13.4 TSD3

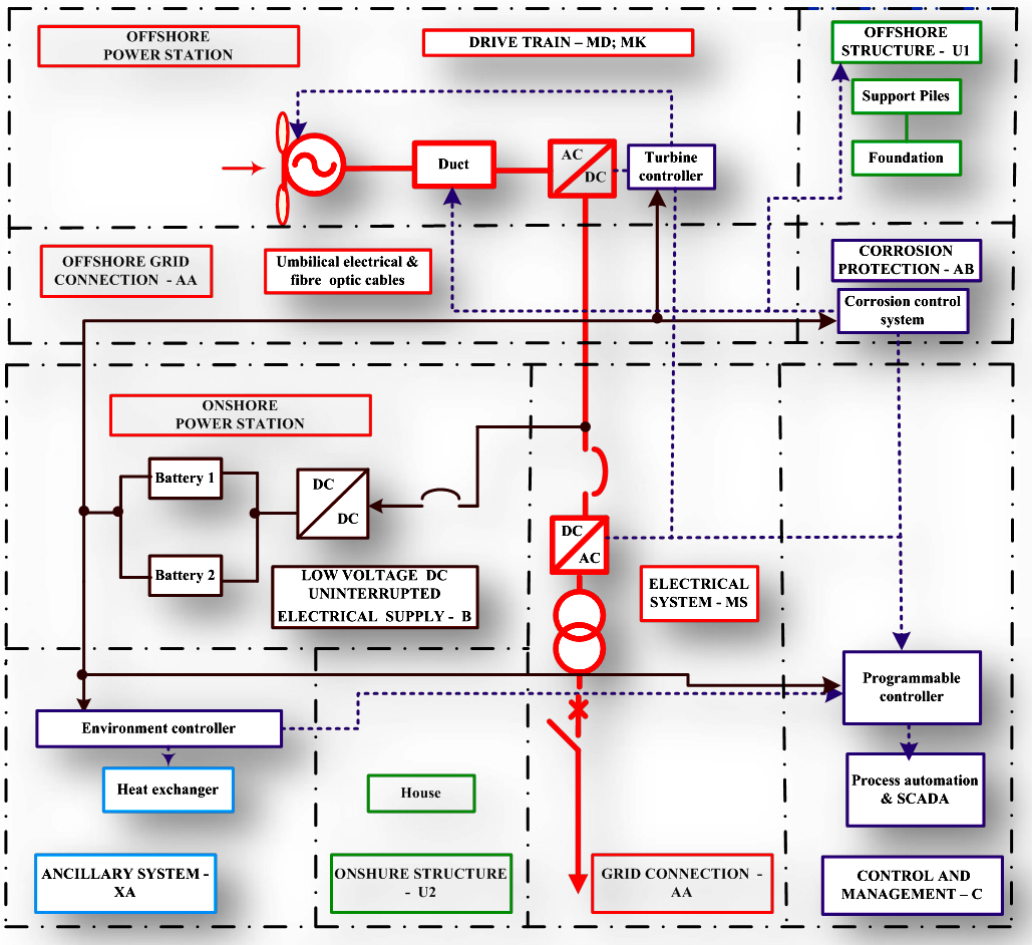

Figure 13.5 TSD3 schematic diagram

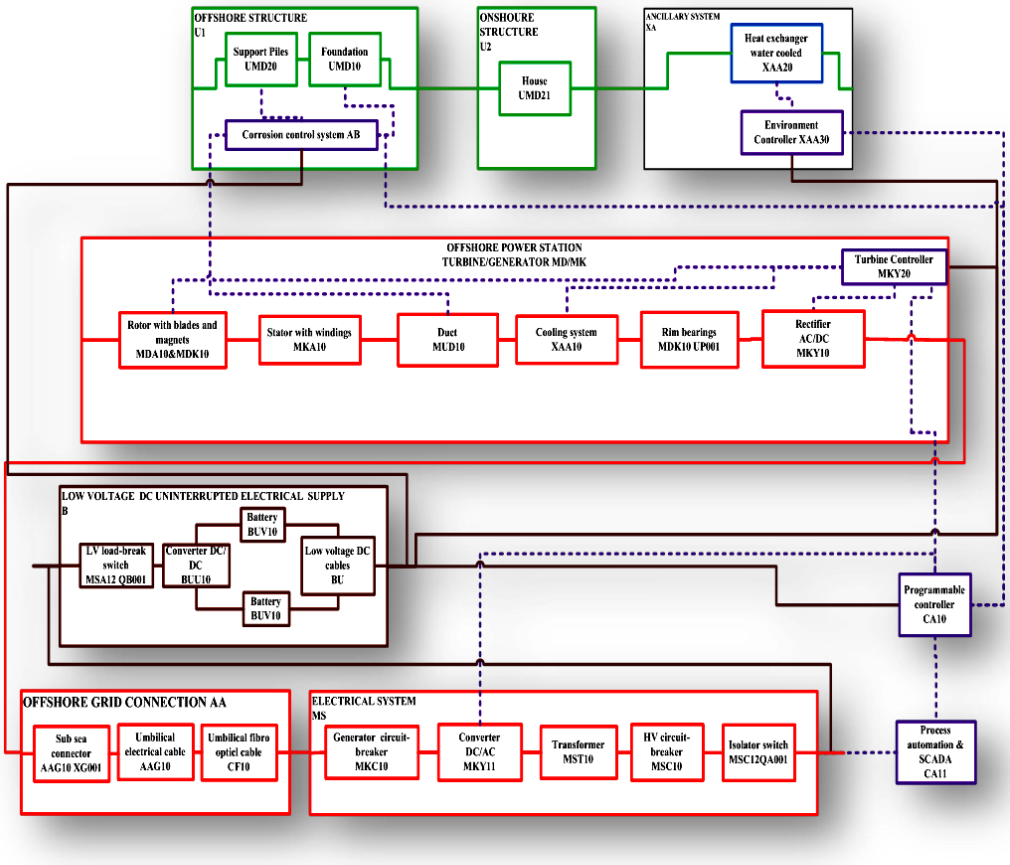

Figure 13.6 TSD3 functional block diagram (FBD) or RBD3

Table 13.4 TSD3 Parts Structure & Annual Failure Rate Range

RELIABILITY CHARACTERISTICS FOR:					Surrogate data failure rates (Failures/year)			Failure Rate Estimate λi_FREcon (Failures/year)	Failure Rate Estimate λi_FREenv		
System/Branch	Number of subassembly i =1 to Nb	VGB Code	Subassemblies	Qt	Data Source Table 12.1	λGi_min	λGi_max	Predicted total failure rate (Failures/year)	Environment adjustment factor	Adjusted single subassembly failure rates	Predicted total failure rate (Failures/year)
								$\lambda i\_FREcon = \lambda Gi\_max$	πEi	$\lambda Gi\_max * \pi Ei$	$\lambda i\_FREenv = \lambda Gi\_max * \pi Ei$
DRIVE TRAIN (MD&MK)	1	MDA10	Fixed pitch rotor blades	N	[8]	0.050	0.150	0.150	3.3	0.495	0.495
	2	MDK10 UP001	Rim bearings	1	[8]	0.021	0.021	0.021	1.0	0.021	0.021
	3	MKA10	Stator, coils, windings t=155C	1	[8]	0.150	0.150	0.150	3.3	0.495	0.495
	4	MUD10	Duct	1	[10] [15]	0.001	0.050	0.050	1.0	0.050	0.050
	5	MKY10	Rectifier AC/DC, controller	1	[5]	0.000	0.015	0.015	1.0	0.015	0.015
GRID CONNECTION (AA)	6	AAG10 XG001	Subsea connector	1	[5]	0.000	0.009	0.009	1.0	0.009	0.009
	7	AAG10	Umbilical cable, 1.5 kV	1	[5]	0.042	0.111	0.111	1.0	0.111	0.111
	8	CFA10	Umbilical fibre optic cable	1	[6]	0.010	0.016	0.016	1.7	0.027	0.027
CORROSION PROTECTION (AE)	9	AE10	Corrosion control	1	[5]	0.044	0.117	0.117	1.0	0.117	0.117
TURBINE CONTROLLER (CA)	10	CA10	Turbine controller	1	[5]	0.057	0.151	0.151	1.0	0.151	0.151
STRUCTURE (U1)	11	UMD20, UMD10	Support piles, Foundation	1	[15]	0.050	0.050	0.050	1.0	0.050	0.050
ELECTRICAL SYSTEM (MS)	13	MKC10	LV Load brake switch	1	[7]	0.014	0.014	0.014	1.0	0.014	0.014
	14	MKY11	Converter, DC/AC	1	[1][2] [3]	0.120	0.215	0.215	1.0	0.215	0.215
	15	MST10	Transformer (1.5kV/11kV), including cooling	1	[5]	0.008	0.081	0.081	1.0	0.081	0.081
	16	MSC10	HV circuit-breaker	1	[7]	0.017	0.017	0.017	1.0	0.017	0.017
	17	MSC12 QA001	Isolator switch	1	[7]	0.006	0.014	0.014	1.0	0.014	0.014
LOW VOLTAGE DC UNINTERRUPTABLE ELECTRICAL SUPPLY (B)	18	MSA12 QB001	LV load-break switch	1	[7]	0.014	0.014	0.014	1.0	0.014	0.014
	19	BUU10	Converter DC/AC	1	[5]	0.096	0.368	0.368	1.0	0.368	0.368
	20	BUU11	LV Supply 400V circuit breaker	1	[7]	0.002	0.018	0.018	1.0	0.018	0.018
	21	BUV10	Battery	2	[4]	0.032	0.147	0.098	1.0	0.147	0.098
	22	BU	Low-voltage DC cables	1	[4]	0.010	0.010	0.010	1.0	0.010	0.010
ANCILLARY SYSTEM (XA)	23	XAA20	Heat exchanger	1	[4]	0.071	0.120	0.120	1.0	0.120	0.120
ONSHORE CONTROL SYSTEMS (CA)	25	CA10	Programmable controller	1	[5]	0.286	0.754	0.754	1.0	0.754	0.754
	26	XAA30	Environment Controller	1	[5]	0.044	0.117	0.117	1.0	0.117	0.117
	24	CA11	Process automation & SCADA	1	[5]	0.286	0.754	0.754	1.0	0.754	0.754
STRUCTURE (U1)	27	UMD21	House	1	[11]	0.025	0.025	0.025	1.0	0.025	0.025
DEVICE TOTAL FAILURE RATE, λ at 100% (Failures/Unit/year)								3.459			4.160
DEVICE RELIABILITY SURVIVOR FUNCTION, R(1YR), %								3.147%			1.561%

13.5 TSD4

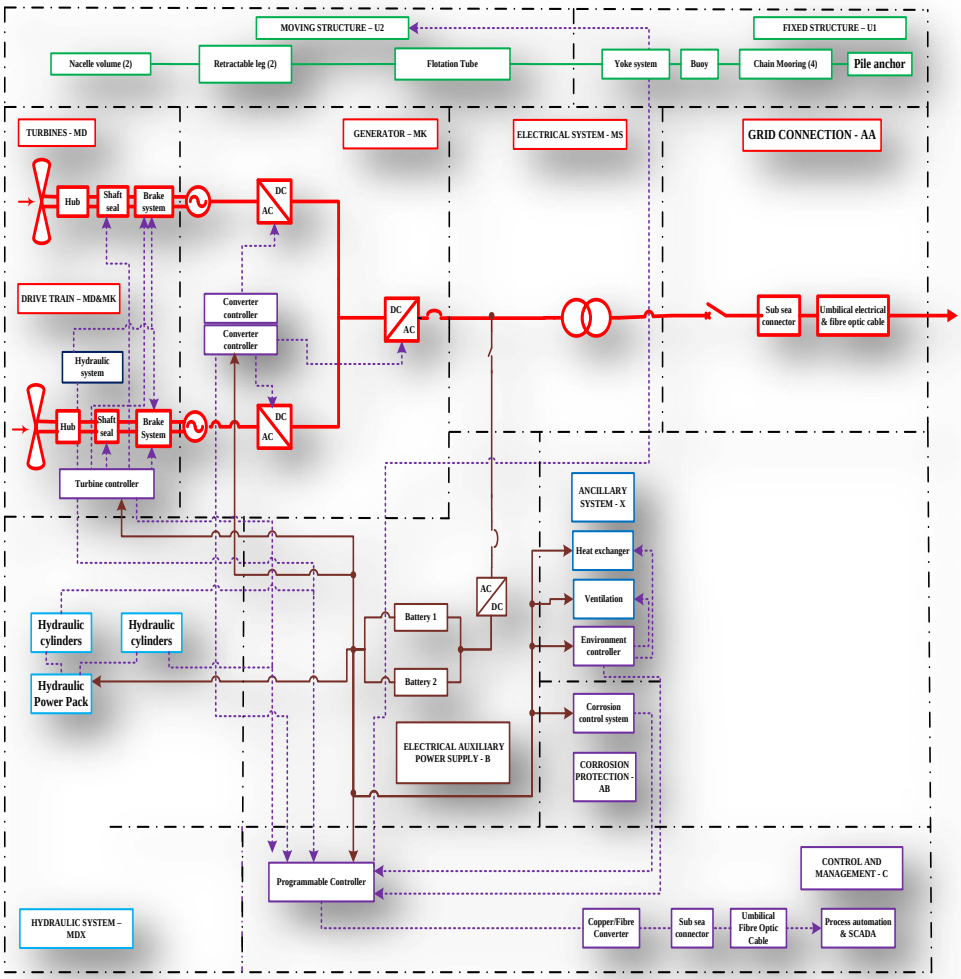

Figure 13.7 TSD4 schematic diagram based on SRTT concept

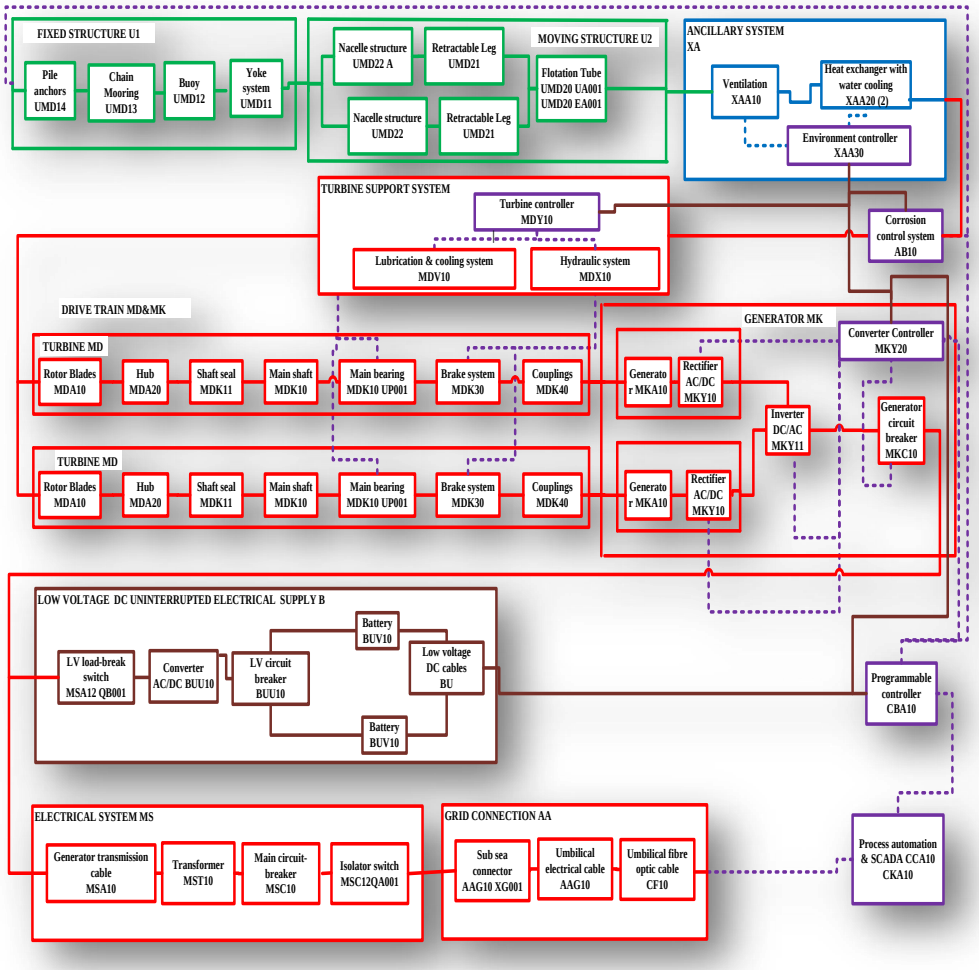

Figure 13.8 TSD4 functional block diagram (FBD) or RBD4 based on SRTT

Table 13.5 TSD4 Parts Structure & Annual Failure Rate Range

RELIABILITY CHARACTERISTICS FOR:					Surrogate data failure rates (Failures/year)			Failure Rate Estimate λt_FREcon (Failures/year)		Failure Rate Estimate λt_FREenv (Failures/year)			
System/Branch	Number of subassembly i = 1 to Ni	VGB Code	Subassemblies	Qt	Data Source Table 12.1	λGi_min	λGi_max	Predicted total failure rate (Failures/year)		Environmental adjustment factor	Adjusted single subassembly failure rate	Predicted total failure rate (Failures/year)	
								$\lambda t\_FREcon100\% = \lambda Gi\_max$	$\lambda t\_FREcon50\% = \lambda Gi\_max$	π_e	$\lambda Gi\_max * \pi Ei$	$\lambda t\_FREenv100\% = \lambda Gi\_max * \pi Ei$	$\lambda t\_FREenv50\% = \lambda Gi\_max * \pi Ei$
DRIVE TRAIN (MDK MK)	1	MDA10	Fixed pitch rotor blades	4	[1][2] [3]	0.115	0.230	0.460	0.595	1.9	0.437	0.874	0.929
	2	MDA20	Hub	2	[1][2] [3]	0.083	0.125	0.250		1.0	0.125	0.250	
	3	MDK11	Shaft seal	2	[4]	0.061	0.061	0.123		1.0	0.061	0.123	
	6	MDK10, MDK10 UP001, MDK40	Main shaft, main bearing, couplings	2	[1][2] [3]	0.031	0.055	0.110		1.0	0.055	0.110	
	8	MDK30	Brake system	2	[1][2] [3]	0.055	0.135	0.270		1.7	0.230	0.459	
	9	MKA10	PM Synchr. Generator	2	[8]	0.271	0.271	0.542		1.7	0.460	0.921	
	10	MKY10	Rectifier AC/DC	2	[1][2] [3]	0.000	0.015	0.030		1.7	0.025	0.051	
	11	MKY11	Inverter DC/AC	1	[1][2] [3]	0.120	0.215	0.215	0.215	1.7	0.366	0.366	0.366
	12	MKY20	Converter Controller	1	[1][2] [3]								
	13	MKC10	Generator circuit breaker	1	[5]	0.020	0.175	0.175	0.175	1.0	0.175	0.175	0.175
ELECTRICAL SYSTEM (MS)	14	MSA10	Generator transmission cable	1	[6]	0.010	0.010	0.010	0.010	1.0	0.010	0.010	0.010
	15	MST10	Transformer, including cooling (400V/11kV)	1	[5]	0.008	0.081	0.081	0.081	1.0	0.081	0.081	0.081
	16	MSC10	Main circuit-breaker	1	[5]	0.020	0.175	0.175	0.175	1.0	0.175	0.175	0.175
	17	MSC10 QA	Isolator switch	1	[5]	0.000	0.037	0.037	0.037	1.0	0.037	0.037	0.037
LOW VOLTAGE DC UNINTERRUPTABLE ELECTRICAL SUPPLY (U)	18	BKA10 QA001	LV load-break switch	1	[5]	0.005	0.010	0.010	0.010	1.0	0.010	0.010	0.010
	19	BUU10	Converter AC/DC	1	[5]	0.000	0.015	0.015	0.015	1.0	0.015	0.015	0.015
	20	BUU11	LV Supply 400V circuit breaker	1	[5]	0.005	0.011	0.011	0.011	1.0	0.011	0.011	0.011
	21	BUV10	Battery	2	[5]	0.032	0.147	0.098	0.098	1.0	0.147	0.098	0.098
	22	BU	Low voltage DC cables	2	[6]	0.010	0.010	0.020	0.007	1.0	0.010	0.020	0.007
GRID CONNECTION (AA)	23	AAG10 XG001	Sub-sea connector	1	[5]	0.000	0.009	0.018	0.006	1.0	0.009	0.018	0.006
	24	AAG10	Umbilical electrical cable	1	[5]	0.042	0.111	0.111	0.111	1.0	0.111	0.222	0.074
	25	CFA10	Umbilical fibre optic cable	1	[6]	0.010	0.016	0.016	0.016	3.3	0.052	0.052	0.052
ANCILLARY SYSTEM (XA)	26	XAA20	Heat exchanger seawater cooled	2	[4]	0.002	0.263	0.070	0.070	1.0	0.105	0.070	0.070
	27	XAA10	Ventilation system	1	[6]	0.105	0.105	0.105	0.105	1.0	0.105	0.105	0.105
CONTROL AND MANAGEMENT SYSTEM (C)	28	CA10	Programmable controller	1	[5]	0.239	0.630	0.630	0.630	1.0	0.630	0.630	0.630
	29	MDY10	Turbine controller	1	[5]	0.124	0.328	0.328	0.328	1.0	0.328	0.328	0.328
	30	XAA30	Environment controller	1	[5]	0.044	0.117	0.117	0.117	1.0	0.117	0.117	0.117
	31	CA11	Process automation & SCADA	1	[5]	0.286	0.754	0.754	0.754	1.0	0.754	0.754	0.754
CORROSION PROTECTION (AB)	32	AB	Corrosion control system	1	[5]	0.044	0.117	0.117	0.117	1.0	0.117	0.117	0.117
HYDRAULIC SYSTEM (MDX)	33	MDX10	Hydraulic cylinders	2	[5]	0.039	0.039	0.079	0.039	1.0	0.039	0.079	0.039
	34	MDX20 GP001	Hydraulic Power Pack	1	[5]	0.039	0.039	0.039	0.039	1.0	0.039	0.039	0.039
MOVING STRUCTURE (U2)	36	UMD22 UA001 UB001 UL001 UP001	Nacelle structure	2	[15]	0.009	0.009	0.018	0.018	1.0	0.009	0.018	0.018
	37	UMD21 UA001 UB001 UL001	Retractable Leg	2	[15]	0.009	0.009	0.018	0.018	1.0	0.009	0.018	0.018
	38	UMD20 UA001 UB001 UL001 UMD20 EA001	Flotation Tube	1	[15]	0.001	0.001	0.001	0.001	1.0	0.001	0.001	0.001
FIXED STRUCTURE (U1)	39	UMD12	Buoyancy support with swivel	1	[15]	0.050	0.050	0.050	0.050	1.0	0.050	0.050	0.050
	40	UMD13	Connecting links	4	[12] [9]	0.100	0.185	0.171	0.171	1.0	0.185	0.171	0.171
	41	UA001 UL001 UP001	Catenary mooring, chain	4	[13]	0.024							
			Catenary mooring, steel wire rope	4	[13]	0.000							
	42	UMD14	Pile anchor	4	[14]	0.007							
	43	UMD11	Yoke system	1	[15]	0.050	0.050	0.050	0.050	1.0	0.050	0.050	0.050
DEVICE TOTAL FAILURE RATE, *$\lambda total$* (Failures/unit/year)								5.322	4.068			6.623	4.552
RELIABILITY SURVIVOR FUNCTION, *R(1 year)*, %								0.488%	1.711%			0.133%	1.055%

13.6 TSD5

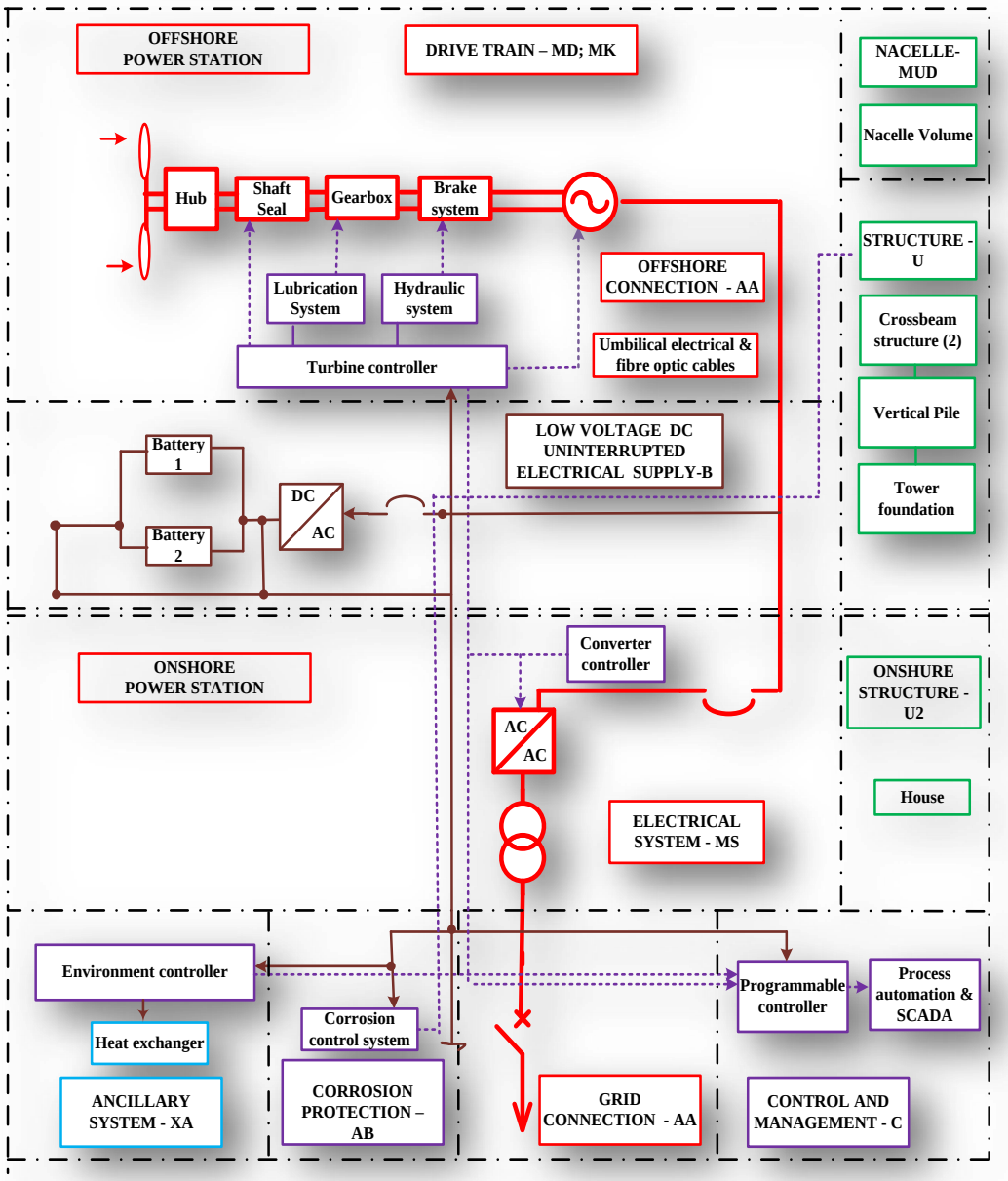

Figure 13.9 TSD5 schematic diagram

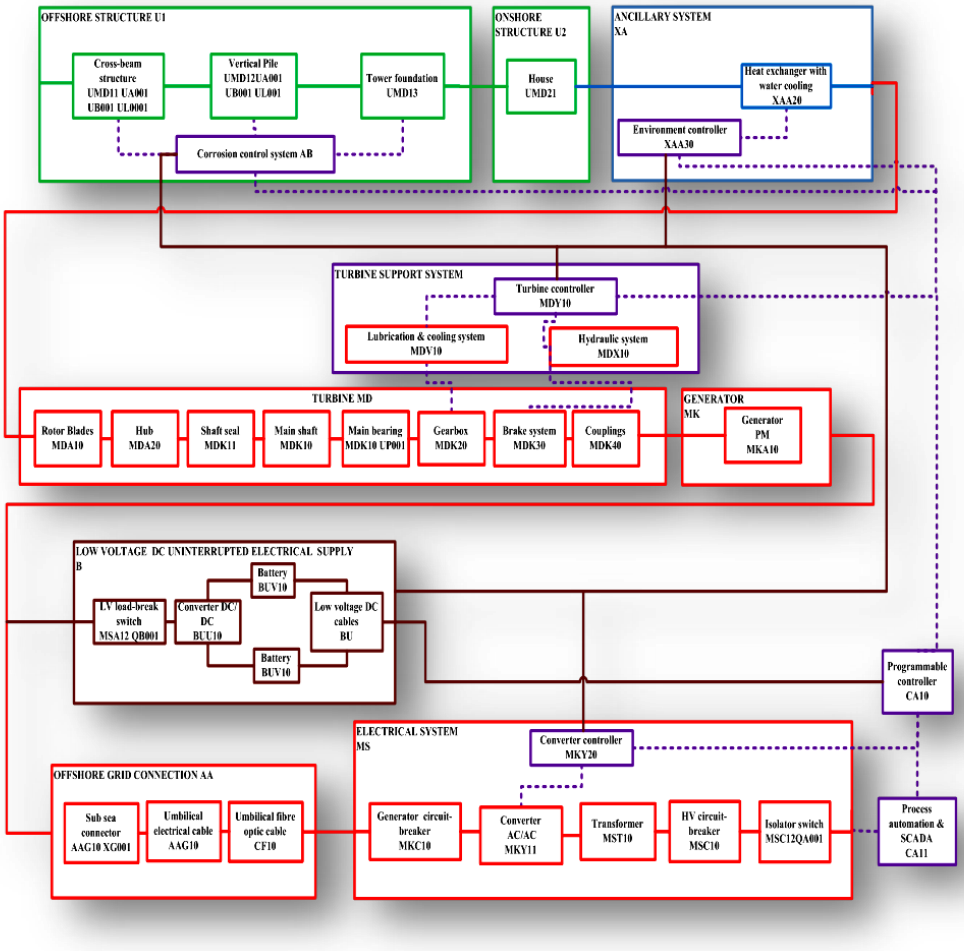

Figure 13.10 TSD5 functional block diagram (FBD) or RBD5

Table 13.6 TSD5 Parts Structure & Annual Failure Rate Range

RELIABILITY CHARACTERISTICS FOR:					Surrogate data failure rates (Failures/year)			Failure Rate Estimate λi_FREcon (Failures/year)	Failure Rate Estimate λi_FREenv		
System/Branch	Number of subassmbly i =1 to Nb	VGB Code	Subassemblies	Qt	Data Source Table 12.1	λGi_min	λGi_max	Predicted Total Failure Rate (Failures/year)	Enviornment adjustment factor	Adjusted single subassembly failure rates	Predicted total failure rate (Failures/year)
								$\lambda i\_FREcon = \lambda Gi\_max$	π_{Ei}	$\lambda Gi\_max * \pi Ei$	$\lambda i\_FREenv = \lambda Gi\_max * \pi Ei$
TURBINE/GENERATOR (MD&MK)	1	MDA10	Fixed Pitch Rotor Blades	2	[1][2] [3]	0.115	0.230	0.230	1.9	0.437	0.437
	2	MDA20	Hub	2	[1][2] [3]	0.083	0.125	0.250	1.0	0.125	0.250
	3	MDK11	Shaft seal	2	[4]	0.061	0.061	0.061	1.0	0.061	0.061
	6	MDK10, MDK10 UP001, MDK40	Main shaft, main bearing, couplings	1	[1][2] [3]	0.031	0.055	0.055	1.0	0.055	0.055
	8	MDK20, MDV10	Gearbox, Lubrication & cooling system	1	[1][2] [3]	0.101	0.134	0.134	1.0	0.134	0.134
	10	MDK30, MDX10	Brake systems, Hydraulic system	1	[1][2] [3]	0.055	0.031	0.031	1.7	0.053	0.053
	11	MKA10	PM Synchronous Generator	1	[8]	0.271	0.271	0.271	1.7	0.460	0.460
	13	MKY10	Rectifier AC/DC, controller	1	[5]	0.000	0.015	0.015	1.7	0.025	0.025
GRID CONNECTION (AA)	14	AAG10 XG001	Sub sea connector	1	[5]	0.000	0.009	0.009	1.0	0.009	0.009
	15	AAG10	Umbilical cable, 4.4 kV	1	[5]	0.042	0.111	0.111	1.0	0.111	0.111
	16	CFA10	Umbilical fibre optic cable	1	[6]	0.010	0.016	0.016	1.7	0.027	0.027
CORROSION PROTECTION (AB)	17	AB10	Corrosion control	1	[5]	0.044	0.117	0.117	1.0	0.117	0.117
TURBINE CONTROLLER (CA)	18	CA10	Turbine controller	1	[5]	0.057	0.151	0.151	1.0	0.151	0.151
Nacelle (MUD)	19	MUD10	Nacelle volume	1	[10]	0.001	0.001	0.001	1.0	0.001	0.001
STRUCTURE (U1)	20	UMD11 UA001 UB001 UL0001	Cross-beam structure	1	[10] [15]	0.001	0.050	0.050	1.0	0.050	0.050
	21	UMD12 UA001 UB001 UL001	Vertical Pile	1	[10] [15]	0.001	0.050	0.050	1.0	0.050	0.050
	22	UMD13	Tower foundation	1	[10] [15]	0.001	0.050	0.050	1.0	0.050	0.050
ELECTRICAL SYSTEM (MS)	23	MKC10	MV Load brake switch	1	[7]	0.015	0.015	0.015	1.0	0.015	0.015
	24	MKY10, MKY20	Converter AC/AC, Converter	1	[1][2] [3]	0.239	0.430	0.430	1.0	0.081	0.081
	25	MST10	Transformer (4.4kV/11kV) , including cooling	1	[5]	0.008	0.081	0.081	1.0	0.081	0.081
	26	MSC10	HV circuit-breaker	1	[7]	0.017	0.017	0.017	1.0	0.017	0.017
	27	MSC12 QA001	Isolator switch	1	[7]	0.000	0.037	0.037	1.0	0.011	0.011
LOW VOLTAGE DC UNINTERRUPTABLE ELECTRICAL SUPPLY (B)	28	MSA12 QB001	LV load-break switch	1	[7]	0.005	0.011	0.011	1.0	0.015	0.015
	29	BUU10	Converter AC/DC	1	[4]	0.000	0.015	0.015	1.0	0.015	0.015
	30	BUU11	LV Supply 400V circuit breaker	1	[7]	0.002	0.018	0.018	1.0	0.018	0.018
	31	BUV10	Battery	2	[4]	0.032	0.147	0.098	1.0	0.147	0.098
	32	BU	Low-voltage DC cables	1	[4]	0.010	0.010	0.010	1.0	0.010	0.010
ANCILLARY SYSTEM (XA)	33	XAA20	Heat exchanger	1	[4]	0.071	0.120	0.120	1.0	0.120	0.120
ONSHORE CONTROL SYSTEMS (CA)	34	CA10	Programmable controller	1	[5]	0.286	0.754	0.754	1.0	0.754	0.754
	35	XAA30	Environment Controller	1	[5]	0.044	0.117	0.117	1.0	0.117	0.117
	36	CA11	Process automation & SCADA	1	[5]	0.286	0.754	0.754	1.0	0.754	0.754
STRUCTURE (U1)	37	UMD21	House	1	[11]	0.025	0.025	0.025	1.0	0.025	0.025
DEVICE TOTAL, $\lambda p\text{-}tot100\%$ (Failures/year)								*4.104*			*4.172*
DEVICE RELIABILITY SURVIVOR FUNCTION, R(1YR), %								*1.651%*			*1.541%*

THE END